Assessing the role of sCYLD and Bcl-3 in immune regulation

Dissertation
Zur Erlangung des Grades
“Doktor der Naturwissenschaften”
am Fachbereich Biologie
der Johannes Gutenberg-Universität
in Mainz

vorgelegt von
Joumana Masri
aus Köln

Mainz 2010

Dekan:

Berichterstatter 1:

Berichterstatter 2:

Tag der mündlichen Prüfung:

Abbreviations

Ab	antibody
APC	antigen presenting cell or allophycocyanin
approx.	approximately
Bio	biotinylated
β-ME	β-mercaptoethanol
bp	base pair
BSA	bovine serum albumin
°C	temperature in degrees Celsius
CD	cluster of differentiation
CFA	Complete Freund's Adjuvant
cDNA	complementary DNA
CNS	central nervous system
Conc	concentration
d	day/s
DC	dendritic cell
DMEM	Dulbecco's modified Eagle medium
DNA	desoxyribonucleic acid
dNTP	desoxynucleotide triphosphate
DTT	dithiothreitol
EAE	experimental autoimmune encephalomyelitis
EDTA	ethylene-diaminetetraacetic acid
ELISA	enzyme-linked immunosorbent assay
ES	embryonic stem
EtOH	ethanol
FACS	fluorescence activated cell sorting
FCS	fetal calf serum
Fig.	Figure
FITC	fluorescein isothiocyanate
Flp	site-specific recombinase, product of yeast *FLP1*- gene
FoxP3	forkhead box protein 3
FRT	Flp recombination target
g	gram
hr/s	hour/s
HEPES	N-2-hydroxyethylpiperazine-N'-2- ethansulfonic acid
i.p.	intraperitoneally
IFNγ	interferon-γ

Ig	immunoglobulin
IL	interleukin
kb	kilobase pair
l	liter
LN	lymph node/s
loxP	recognition sequence for Cre (locus of X-ing over of phage P1)
LPS	lipopolysaccharide
M	molar
MACS	magnetic cell sorting
MFI	mean fluorescence intensity
MHC	major histocompatibility complex
min	minute
ml	milliliter
mM	millimolar
MOG	myelin oligodendrocyte glycoprotein
mRNA	messenger RNA
MS	multiple sclerosis
PBS	phosphate buffered saline
PCR	polymerase chain reaction
PE	phycoerythrine
Ptx	Pertussis toxin
RAG	recombinase activating gene
RNA	ribonucleic acid
rpm	revolutions per minute
RT	room temperature
sec	seconds
SA	streptavidine
s.c.	subcutaneously
SN	supernatant
Taq	polymerase from *Thermus aquaticus*
TCR	T cell receptor
U	units
w/v	weight per volume
WT	wild type
µl	microliter
µM	micromolar
3’	three prime end of DNA sequences
5’	five prime end of DNA sequences

1 Introduction

1.1 The NF-κB signaling pathway

The family of Rel/NF-κB transcription factors, which comprises RelA (p65), c-Rel, RelB, NF-κB1 (p50 and its precursor p105), and NF-κB2 (p52 and its precursor p100), plays a central role in the mammalian immune system. It does not only regulate processes such as the development and survival of immune cells, lymphocytes and lymphoid organs but also controls immune responses (Vallabhapurapu and Karin, 2009).

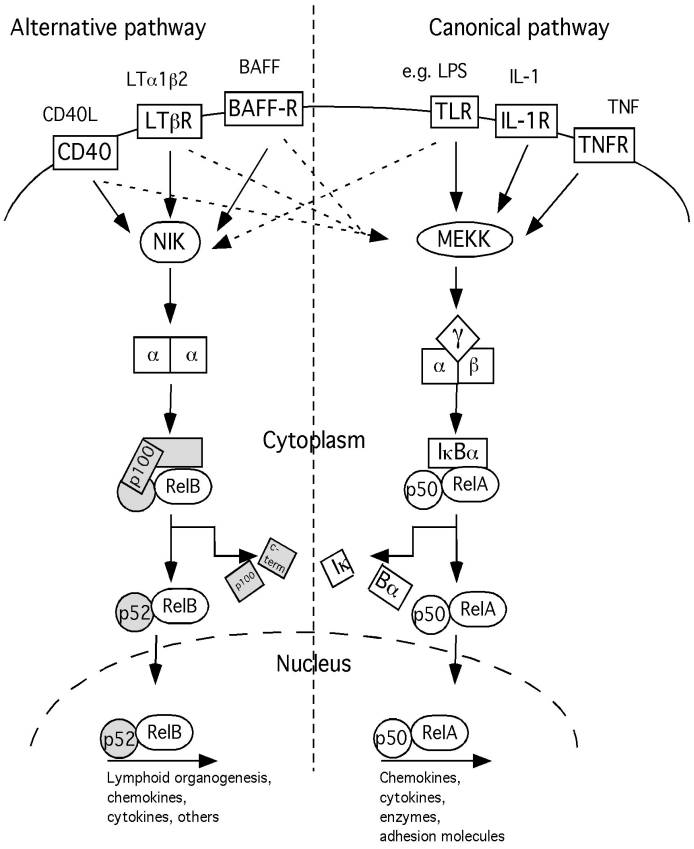

Figure 1 Schematic of alternative and canonical NF-κB signaling
(left) The alternative pathway for NF-κB results in nuclear translocation of p52–RelB dimers, is strictly dependent on IKKα homodimers and is activated by LTβR, BAFF and CD40L via NIK. Many studies strongly suggest that the alternative pathway plays a central role in the expression of genes involved in development and maintenance of secondary lymphoid organs. (right) The canonical NF-κB pathway is activated by a variety of inflammatory signals, resulting in coordinated expression of multiple inflammatory and innate immune genes. The proinflammatory cytokines IL-1β and TNFα activate NF-κB, and their expression is induced in response to NF-κB activation, thus forming an amplifying feed-forward loop. Abbreviations: BAFF, B-cell-activating factor belonging to the TNF family; CD40L, CD40 ligand; IKK, IκB kinase complex (α, β, γ); IL-1, interleukin-1; LT, lymphotoxin; NIK, NF-κB-inducing kinase; TLRs, Toll-like receptors; TNFα, tumor necrosis factor α; MEKK, mitogen ERK kinase kinase.

Therefore, it is not surprising that dysregulation of the NF-κB pathway, caused either by mutation or epigenetic mechanisms, is involved in many diseases, especially ones associated with chronic inflammation, immunodeficiency or cancer (Courtois and Gilmore, 2006).

The major activation pathway is the canonical NF-κB pathway, which encompasses the nuclear translocation of RelA:p50 and c-Rel:p50 heterodimers. These heterodimers are retained in the cytoplasm in complex with IκB family members, which mask the dimers' nuclear localization signal (NLS). Receptor engagement, e.g. TLR (Toll-like receptor) or TNFR (tumor necrosis factor receptor), results in the activation of the trimeric IκB kinase complex (IKK= IKKα, IKKβ, IKKγ=NEMO). It leads to the phosphorylation, subsequent ubiquitination and finally degradation of the inhibitory IκBs. After that the NF-κB heterodimers' NLS are unmasked and they can translocate to the nucleus where they regulate gene transcription.

The alternative NF-κB signaling pathway is activated in response to a small subset of TNF family members, including CD40L, LTαβ (lymphotoxin), BAFF (B cell-activating factor), RANKL (receptor activator of NF-κB ligand) and TWEAK (TNF-related weak inducer of apoptosis). Upon ligand binding, NIK (NF-κB inducing kinase) activates IKKα dimers, which then phosphorylate p100 resulting in its polyubiquitination and partial degradation. The processed form of p100, namely p52 can then translocate to the nucleus together with its binding partner RelB. The alternative pathway has been implicated in lymphoid organogenesis as well as B cell development and survival (Senftleben et al., 2001; Weih and Caamano, 2003)

1.2 Regulation of the NF-κB pathway by ubiquitin signaling

Ubiquitin is a highly conserved 76-amino acid polypeptide, which functions as a versatile signaling tag. It is attached to one or more lysine residues of cellular proteins through an enzymatic cascade involving three classes of enzymes termed E1 (ubiquitin-activating enzyme), E2 (ubiquitin-conjugating enzyme) and E3 (ubiquitin ligase). Ubiquitin itself contains seven lysines, each of which can be further conjugated to the carboxyl terminus of another ubiquitin to form a polyubquitin chain. It has been shown that polyubiquitin chains linked through lysine at position 48 (Lys48) target proteins for proteasomal degradation, whereas alternative linkage through lysine 63 (Lys63) has several non-degradative functions (Fig.2).

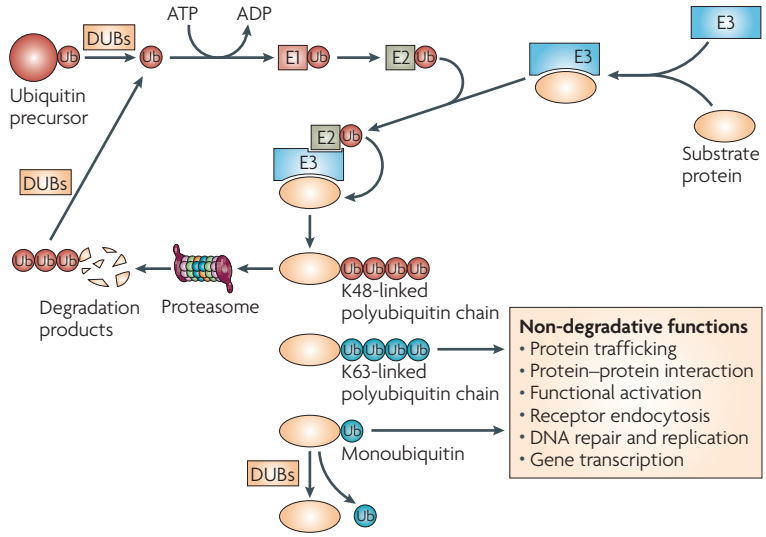

Figure 2 Protein ubiquitination from (Sun, 2008)
Ubiquitination is an energy-consuming process, which involves covalent tagging of a substrate protein with one (monoUb) or a chain of ubiquitins (polyUb). Ubiquitins are linked between their carboxy-terminal glycine residue and an internal lysine residue. The most commonly used internal lysines are K48 and K63. Generally K48 linkages target the substrate for degradation whereas K63 linkages mediate different non-degrading functions. E1: Ubiquitin (Ub) activating enzyme, E2: Ub-conjugating enzyme, E3: Ub ligase, DUB: Deubiquitinating enzyme.

During NF-κB canonical signaling, receptor engagement leads to ubiquitination of IκB (Lys48), which results in its proteasomal degradation, and unveiling of the p50/RelA NLS and nuclear translocation. Alternative activation of RelB/p100, however, can only occur if p100 is ubiquitinated (Lys48) and partially degraded to yield p52. The RelB/p52 dimer then regulates gene transcription.
Polyubiquitin chains of the Lys63 type also play a major role in NF-κB signaling regulation. Lys63-ubiquitin chains mediate protein-protein interaction serving as scaffolds for the assembly of active protein complexes and are generally regarded as important regulators of cell signaling. In fact many molecules in the NF-κB signaling pathway are linked to Lys63-ubiquitin chains, which confer activating potential to their binding partners. These molecules will be addressed in the next section, in which an enzyme that regulates their ubiquitination status will be discussed.

1.3 CYLD

Cylindromatosis is a rare, recessive genetic disease characterized by the formation of benign tumors on parts of the body that are exposed to sunlight (UV light), mostly the scalp. The mutated gene, *cyld*, encodes a tumor

suppressor protein (Bignell et al., 2000) that negatively regulates NF-κB activation (Brummelkamp et al., 2003; Kovalenko et al., 2003; Regamey et al., 2003; Trompouki et al., 2003). CYLD is a deubiquitinase and a member of the USP (ubiquitin-specific protease) family of enzymes that can specifically cleave poly-ubiquitin chains of the 'Lys63' type. There is strong evidence suggesting that IKK activation by different receptor signals involves conjugation of Lys63-linked ubiquitin chains to its signaling components, including NEMO and upstream regulatory factors, such as Tak1 (transforming growth factor–β-activated kinase 1), TRAF2 (tumor necrosis factor receptor-associated factor 2), TRAF6, and RIP1 (receptor-interacting protein 1) (Chen, 2005; Sun, 2008). Table 1 summarizes some of CYLD's substrates and their reported functions.

More recently, CYLD has been shown to bind to and deubiquitinate Bcl-3, preventing its nuclear accumulation (Massoumi et al., 2006). The role of Bcl-3 and the consequences of its localization will be subject of further analysis and discussion in this thesis. In all cases described so far, CYLD's deubiquitinating activity exerts a negative regulatory effect on NF-κB signaling.

Table 1 Confirmed and published interaction partners of the deubiquitinase CYLD and the processes they are involved in

Substrate	Publication	Reported function
RIP1	(Wright et al., 2007)	Spermatogenesis
TRAF2	(Kovalenko et al., 2003)	Survival and apoptosis
NEMO	(Brummelkamp et al., 2003)	Survival and apoptosis
Lck	(Reiley et al., 2004)	T cell development and activation
Bcl-3	(Massoumi et al., 2006)	Proliferation and cell cycle
TRIP	(Regamey et al., 2003)	Survival and apoptosis
TRAF6/7	(Yoshida et al., 2005)	Inflammation and apoptosis
TAK1	(Koga et al., 2008)	T cell development and activation
Plk1	(Stegmeier et al., 2007)	Proliferation and cell cycle

The CYLD protein encompasses 956 residues harboring a NEMO binding site located between residues 570 and 674 and a TRAF2 binding site located between CYLD residues 394 and 470 (Fig.3). Massoumi et al. could show that full length Bcl-3 interacted with CYLD and that the binding site for Bcl-3 on

CYLD corresponded to the C-terminal part of the protein (Massoumi et al., 2006). Furthermore, the *cyld* gene encodes three cytoskeletal-associated protein-glycine (CAP-Gly) conserved domains found in other proteins to coordinate the attachment of organelles to microtubules indicating a role for CYLD in cytoskeletal formation (Gao et al., 2008). The third CAP-Gly domain was reported to specifically interact with one of the two proline-rich sequences of NEMO/IKKα (Saito et al., 2004). In addition to CYLD truncations caused by genetic abnormalities also naturally occurring splice variants exist. Our lab could recently show that a splice variant of CYLD missing exons 7 and 8 (sCYLD) is naturally found in murine cells in addition to full length CYLD (FL-CYLD) (Hovelmeyer et al., 2007).

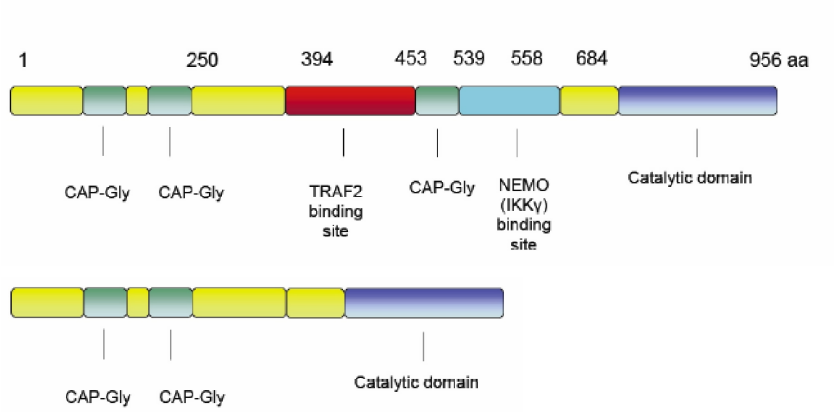

Figure 3 Protein domain structure of the two CYLD variants
FL-CYLD (top) and sCYLD (bottom). CAP-Gly: cytoskeleton-associated protein-glycine conserved domain (see text).

1.4 The IκB-like molecule Bcl-3

The proto-oncogene Bcl-3 (B cell leukemia-3) was first identified as a gene involved in the recurring chromosomal translocation t (14;19), which is found in a subset of patients with chronic lymphocytic leukemia (B-CLL) (Crossen, 1989; Hatada et al., 1992; Ohno et al., 1990; Wulczyn et al., 1992). Unlike other IκB proteins, Bcl-3 does not sequester NF-κB complexes in the cytoplasm. Instead, Bcl-3 is predominantly a nuclear protein and is involved in regulating nuclear NF-κB activity. Bcl-3 seems to have two divergent functions. First, it delays the turnover of DNA-bound repressive p50 homodimers, creating a stable DNA-bound complex thereby repressing transcription (Bours et al., 1993; Caamano et al., 1996; Fujita et al., 1993; Kuwata et al., 2003; Muhlbauer et al., 2008; Watanabe et al., 1997). Second, in the absence of CYLD, nuclear Bcl-3 activates transcription of cyclin D1 via p50 and p52 (Massoumi et al., 2006). Bcl-3- deficient mice are more

susceptible to infectious diseases due to severe defects in the microarchitecture of their secondary lymphoid organs including reduced germinal centers, follicular dendritic cell networks, and splenic B cell zones (Franzoso et al., 1997; Schwarz et al., 1997). Bcl-3 is thus a critical regulator of lymphoid organogenesis and immune function. Inconsistent and contradicting published results about Bcl-3 using different systems (prokaryotic/eukaryotic) raise the question, if it will be possible to confine one single function to Bcl-3. Part of this thesis will be dedicated to elucidating the function of Bcl-3 by over-expressing it in a cell-specific manner using the Cre/loxP system (Sternberg and Hamilton, 1981).

1.5 The role of NF-κB signaling in cells of the immune system

Many of the receptors, which activate either the classical or the alternative NF-κB pathways, are expressed on hematopoietic cell types, suggesting an important role for NF-κB in their development and activation. Indeed, NF-κB signaling plays pivotal roles in hematopoietic cell development and function (Vallabhapurapu and Karin, 2009).

1.5.1 B lymphocytes

B cells are the basis for a humoral immune response. Upon activation, which mostly involves antigen and T helper cells, B cells start producing antigen specific immunoglobulins. These immunoglobulins also known as antibodies protect the host against pathogens that multiply outside cells mainly by facilitating uptake of the pathogen by phagocytic cells that are specialized to destroy ingested bacteria.
In B cells, the non-canonical pathway of NF-κB activation is the main pathway, which is activated in response to stimulation of a subset of the TNF-receptor (TNFR) superfamily, including receptors for BAFF, lymphotoxin-β (LTβ) and CD40 ligand. Stimulation of these receptors activates the protein kinase NIK, which in turn activates IKKα. IKKα then phosphorylates p100 at two C-terminal serine residues, leading to the selective degradation of its IκB-like domain by the proteasome (Senftleben et al., 2001; Xiao et al., 2001). The mature p52 subunit and its binding partner, RelB, translocate to the nucleus to regulate gene expression.

1.5.2 T lymphocytes

T cells play a central role in cell-mediated immunity and can be divided into several subsets as shown in Figure 4. Upon encounter of their specific

antigen on an antigen-presenting cell (APC) naïve $CD4^+$ T cells differentiate into a specific T helper cell line, depending on environmental (e.g. cytokines) conditions.

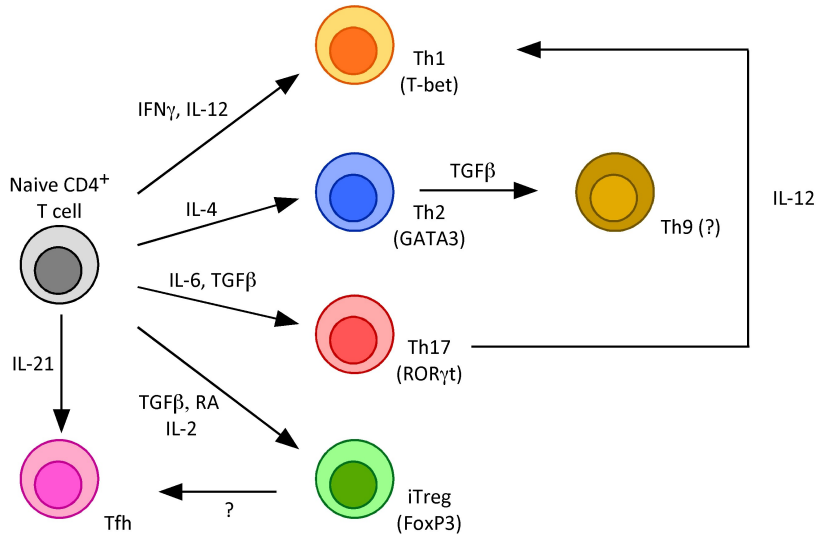

Figure 4 T cell differentiation and conversion (adapted from (Zhou et al., 2009))
Naïve $CD4^+$ T cells, which encounter antigen presented in the context of MHC class II on APCs, can differentiate into Th1, Th2, Th17, iTreg (induced regulatory) and Tfh (T follicular helper) cells. Differentiation programs are controlled by cytokines produced by cells of the innate immune system.

Th1 cells develop in the presence of IL-12 produced by dendritic cells and macrophages and IFNγ produced by NK cells and $CD8^+$ T cells- a milieu, which predominates in the early phase of the response to viruses and some intracellular bacteria. Th2 cells, on the other hand, develop in response to IL-4 and are mainly involved in the defense against extracellular pathogens. Th1 and Th2 differentiation require the expression of specific ‘‘master regulator’’ transcription factors, called T-bet and GATA3 respectively. Th17 cells produce the cytokines IL-17A and IL-17F, which regulate immune responses adapted to clearing extracellular bacteria, such as *Klebsiella pneumoniae* or *Bacteroides fragilis* (Chung et al., 2003; Happel et al., 2005) and fungi such as *Candida albicans* (Huang et al., 2004). T follicular helper (Tfh) cells represent a recently defined $CD4^+$ T cell subset characterized by the expression of the chemokine receptor CXCR5 and an enhanced ability to support B cells to mount antibody responses.

In T lymphocytes, T cell receptor (TCR) activation leads to phosphorylation of IκB by the IκB kinase (IKK) complex, which then results in its ubiquitination and degradation. This allows the nuclear translocation of NF-κB, where it activates genes involved in the function, survival, and homeostasis of T cells (Schulze-Luehrmann and Ghosh, 2006). But NF-κB signaling has been shown to be essential for more then TCR signaling. *nemo*$^{-/-}$ mice are embryonic

lethal, but fetal livers from these knock-outs embryos could not reconstitute either B or T lymphopoiesis in irradiated host mice (Kim et al., 2003). The T cell specific knock-out of *nemo* (which is a known target of CYLD) resulted in the complete absence of NK and regulatory $CD4^+$ $CD25^+$ T cells (Schmidt-Supprian et al., 2004). *nf-κb1*$^{-/-}$ (*p50/p105*$^{-/-}$) mice had impaired Th2 differentiation due to the failure to induce the transcription factor GATA3 expression (Das et al., 2001). *c-rel*$^{-/-}$ mice showed defects in Th1 development as well as in cytokine production (IL-2, GM-CSF) in $CD4^+$ T cell responses (Gerondakis et al., 1996; Hilliard et al., 2002). Knock-out mice for different IκBs also displayed strong phenotypes, including reduced proliferative capacity in *iκbα*$^{-/-}$ T cells (Chen et al., 2000) and defective Th1 and Th2 differentiation in *relB*$^{-/-}$ and *bcl-3*$^{-/-}$ mice respectively (Corn et al., 2005; Franzoso et al., 1997).

1.5.3 Dendritic cells (DCs)

DCs are generated from either myeloid or lymphoid bone marrow progenitors through intermediate precursors that home to sites of potential antigen entry, where they differentiate into immature DCs. After antigen capture in the presence of maturation signals associated with inflammation or infection, immature DCs are activated by Toll-like receptors (TLRs), interferons (IFNs), or members of tumor necrosis factor receptor (TNF-R) family and undergo a complex maturation process. *In vivo* this process is accompanied by migration of DCs to T cell-rich areas of lymphoid organs, where they present antigen-derived peptides to antigen-specific T cells and direct their differentiation into T effector or memory cells. In addition, mature DCs can induce NK cell activation and B cell differentiation into plasma cells. In contrast, antigen capture in the absence of activation stimuli may lead to the induction of T cell tolerance, as a result of antigen presentation by immature DCs in the absence of co-stimulatory signals such as CD80 and CD86 (Steinman et al., 2003).
NF-κB signaling is involved not only in the development of DCs but also in the process of activation and maturation. Kobayashi et al. (Kobayashi et al., 2003) could demonstrate that TRAF6, which is negatively regulated by CYLD (Trompouki et al., 2003), is a necessary factor for maturation of dendritic cells. Hilliard et al. showed that there was no significant differences between normal and c-Rel–deficient APCs in their expression of B7-1, B7-2, MHC class I, and MHC class II molecules, but demonstrated that c-Rel–deficient cells produced significantly smaller amounts of IL-12 p40, a cytokine essential for Th1 cell differentiation (Hilliard et al., 2002). NF-κB2 (p52/p100) was found to

negatively regulate RelB activity, which in turn is associated with increased MHC class II and co-stimulatory expression and enhanced ability to induce $CD4^+$ T cell responses (Zanetti et al., 2003). Dendritic cells from *nf-κb2*$^{-/-}$ mice therefore displayed enhanced function (Speirs et al., 2004). But RelB does not only seem to be necessary for dendritic cell activation, but also for their development. Wu et al. showed that *relb*$^{-/-}$ mice lacked certain thymic and splenic DC populations (Wu et al., 1998). Carmody et al. reported, that dendritic cells form *bcl-3*$^{-/-}$ mice produced significantly more cytokines than WT DCs upon stimulation with several TLR ligands (Carmody et al., 2007).

1.5.4 Macrophages

Macrophages are mononuclear phagocytes that are widely distributed throughout the body. These cells can contribute to development and homeostasis and participate in innate and adaptive immune responses. The physiology of macrophages can vary tremendously depending on the environment in which they reside and the local stimuli to which they are exposed. Macrophages are secretory cells, and in that role can promote and regulate immune responses and contribute to autoimmune pathologies. Although dendritic cells are important in presenting antigens, particularly to initiate primary immune responses, macrophages are the professional APC type most prominent in inflammatory sites and specialized for clearing necrotic and apoptotic material. Macrophages can act not only as professional APCs, but can also perform either pro- or anti-inflammatory roles, dependent on the means by which they are activated (DiPietro et al., 1998) (Adams DO, New York: Raven Press, 1998, pp. 471-9). IFNγ is the classical macrophage-activating factor leading to synthesis and release of inflammatory mediators, enhanced phagocytosis together with up-regulation of MHC class II and co-stimulatory molecules (Murray, 1988; North, 1978). However, other stimuli such as IL-4 can initiate a state of ‘alternative activation’ with the development of anti-inflammatory characteristics (Goerdt and Orfanos, 1999).
Macrophage development and function are dependent on NF-κB signaling, as was shown in various knock-out mouse models. Li et al. could show, that macrophages deficient in *IKKα* displayed enhanced phagocytic clearance of bacteria, more efficient antigen-presenting capacity and elevated secretion of several key pro-inflammatory cytokines and chemokines (Li et al., 2005). *NF-κB1*$^{-/-}$-derived macrophages showed impaired ERK mitogen-activated protein kinase pathway activation in response to TLR signals, which led to a reduced

expression of IL-6, IL-10 and Cox-2 (Banerjee et al., 2006; Waterfield et al., 2003).

2 Specific aims of this thesis

NF-κB signaling plays a major role in the immune system by regulating a wide variety of processes ranging from the development and survival of lymphocytes and lymphoid organs to the control of immune responses and malignant transformation. CYLD is a deubiquitinating enzyme and a negative regulator of NF-κB signaling. There are two known splice forms of CYLD in the murine system with different functions as was shown for B cells (Hovelmeyer et al., 2007).

Objective 1: Analyzing the impact of sCYLD overexpression on dendritic cells and macrophages

A previous publication from our lab demonstrated that sCYLD overexpression affected B cell function. Therefore, we used bone marrow-derived dendritic cells from WT, CYLD knock out ($CYLD^{ko}$) and $CYLD^{ex7/8}$ mice (which overexpress the short splice variant of CYLD in the absence of the full length transcript) and compared the expression of surface markers, cytokine secretion, *in vivo* capacity to stimulate T cells, and the ability to phagocytose, process and present antigen. This project was done in collaboration with Dr. Cathy Srokowski from the laboratory of Prof. Dr. Hansjörg Schild.

Another set of antigen presenting cells besides dendritic cells are the versatile macrophages. Crossing LysMcre mice (Clausen et al., 1999) to $Cyld^{floxed/floxed}$ ($Cyld^{FL/FL}$) mice (N. Hövelmeyer) allowed the specific overexpression of sCYLD in cells of the myeloid lineage. Deletion efficiency of this Cre in macrophages reached 83-98% according to (Clausen et al., 1999). We used the LysMcre $Cyld^{FL/FL}$ mice to investigate if sCYLD overexpression influenced macrophage function.

Objective 2: Understanding the role of the IκB-like molecule Bcl-3 in dendritic cell function using CD11c-Cre Bcl-3 mice

Results obtained from analysis of dendritic cell function upon overexpression of sCYLD pointed to the importance of expression levels of the transcription factor Bcl-3. Having the opportunity to analyze the impact of cell-type specific overexpression of Bcl-3 in dendritic cells by crossing the CD11c-Cre strain (Caton et al., 2007) to a conditional Bcl-3 overexpressing strain (made by M. Wörns), this project was pursued to further understand the role of Bcl-3 in DC biology.

Objective 3: Analyzing T cell development and function upon Bcl-3 overexpression

Various publications have shown the involvement of Bcl-3 in T cell development and function (Bassetti et al., 2009; Franzoso et al., 1997; Ge et al., 2003). Crossing the conditional Bcl-3 overexpressing mice to the CD4-Cre transgene (Lee et al., 2001; Sawada et al., 1994) allowed T cell specific Bcl-3 overexpression, causing an impressive colitis phenotype. T cell populations and differentiation capacities were analyzed, as well as their proliferative capacity.

3 Materials and Methods

3.1 Chemicals and biological material

Chemicals were purchased from Sigma (Steinheim), Fluka Chemie (Switzerland), Merck (Darmstadt) or AppliChem (Darmstadt) unless stated otherwise. Solutions were prepared with double distilled water (ddH2O). Bacterial media were autoclaved prior to use. Sterility of solutions and chemicals used in cell culture was maintained by working under a sterile hood (Heraeus, Germany).

Table 2 List of chemical substances

Name of Chemical	**Supplier**
Agar	Gibco GmbH, Karlsruhe
Agarose, electrophoresis grade	AppliChem, Darmstadt
Ampicillin	Sigma-Aldrich, Steinheim
Bovine serum albumine (BSA)	Sigma-Aldrich, Steinheim
Chloroform	Merck, Darmstadt
Dimethylsulfoxide (DMSO)	Merck, Darmstadt
Dithiothreitol (DTT)	Boehringer GmbH, Mannheim
dNTPs	Pharmacia Biotech, USA
Ethanol, abs.	AppliChem, Darmstadt
Ethidium bromide	Sigma-Aldrich, Steinheim
Ethylendiamine tetraacetate (EDTA)	Fluka Chemie GmbH, Switzerland
Fetal calf serum (FCS)	Boehringer GmbH, Mannheim
Ficoll 400	Amersham Pharmacia, Freiburg
Glacial acetic acid	Fluka Chemie GmbH, Switzerland
Hydrochloric acid (37%)	Merck, Darmstadt
Isopropanol	AppliChem, Darmstadt
Magnesium chloride	Sigma-Aldrich, Steinheim
β-Mercaptoethanol (β-ME)	Fluka Chemie GmbH, Switzerland
Mineral oil	Sigma-Aldrich, Steinheim
Phenol	Sigma-Aldrich, Steinheim
Potassium chloride	Merck, Darmstadt
Potassium hydrogenphosphate	Merck, Darmstadt
Proteinase K	Roche, Switzerland

Sodium azide	Fluka Chemie GmbH, Switzerland
Sodium carbonate	Fluka Chemie GmbH, Switzerland
Sodium chloride	AppliChem, Darmstadt
Sodium citrate	Fluka Chemie GmbH, Switzerland
Sodium dodecyl sulfate	AppliChem, Darmstadt
Sodium hydrogencarbonate	Fluka Chemie GmbH, Switzerland
Sodium hydrogenphosphate	Fluka Chemie GmbH, Switzerland
Sodium hydroxide	Fluka Chemie GmbH, Switzerland
Tris base	Fluka Chemie GmbH, Switzerland
Tween 20	Sigma-Aldrich, Steinheim

3.2 Molecular biology

3.2.1 Preparation of genomic DNA

Cells or tail biopsy were lysed over night (o/n) at 56°C in lysis buffer (10 mM Tris- HCl, pH 8; 10 mM EDTA; 150 mM NaCl; 0.2% (w/v) SDS; 400 mg/ml proteinase K). Undigested tissue was pelleted by centrifugation and the supernatant was mixed with an equal volume of isopropanol for genomic DNA precipitation. Finally, DNA was retrieved by centrifugation, washed in 70% (v/v) EtOH, dried at RT, and resuspended in Tris buffer (10 mM Tris-HCl, pH 7.5).

3.2.2 Polymerase chain reaction (PCR)

PCR (Mullis and Faloona, 1987; Saiki et al., 1985) was used for genotyping i.e. to screen mice for the presence of targeted alleles or transgenes from tail tip DNA (primers are shown in table 4 and 5). PCRs were also performed for the amplification of DNA segments required for further cloning. The QuikChange® Site-Directed Mutagenesis Kit (Stratagene) was used to incorporate base pair exchanges and thus amino acid exchanges in sequences of interest. Reactions were performed in Bio-Rad myCycler, Bio-Rad iCycler and Corbett Research machines.

Table 3 Sequences of oligonucleotides

Primer	Sequence (5'-3')	T_{ann} [°C]
RosaFA	AAAGTCGCTCTGAGTTGTTAT	58
RosaRA	GGAGCGGGAGAAATGGATATG	58
SpliAcB	CATCAAGGAAACCCTGGACTACTG	58
Cre8	CCCAGAAATGCCAGATTACG	63

MLys1	CTTGGGCTGCCAGAATTTCTC	63
MLys2	TTACAGTCGGCCAGGCTGAC	63
Cyld 1	CCTATGTGGTACTGACCAGA	58
Cyld 2	GTGAATGAAGCTAGGCCATAC	58
Cyld wt	CATGGAAGGAGGCTGCGGTGGAGGAGAT	58
CD4cre fw	CCCAACCAACAAGAGCTC	60
CD4cre rv	CCCAGAAATGCCAGATTACG	60
CD11c cre fw	ACTTGGCAGCTGTCTCCAAG	60
CD11c cre rv	GCGAACATCTTCAGGTTCTG	60
LacZ-fw	GCATCGAGCTGGGTAATAAGCGTTGGCAAT	58
LacZ-rv	GACACCAGACCAACTGGTAATGGTAGCGAC	58
F4 CYLD	ACAACATGGATGCCAGGTTG	58
R4 CYLD	CCGCTAATAAAGGTCCTCTG	58

3.2.3 RNA isolation and Quantitative Real-Time PCR

RNA from murine cells was prepared using the RNeasy Mini kit (Qiagen, Hilden, Germany). DNA was removed by DNaseI digestion (Qiagen, Hilden, Germany). RNA was subsequently used for Quantitative Real-Time PCR in a LightCycler ® 480(Roche) using the QuantiTect SYBR Green RT-PCR Kit (Qiagen, Hilden, Germany). All procedures were carried out according to the manufacturer's instructions. Primers for Quantitative Real-Time PCR were purchased from Qiagen using the company's website https://www1.qiagen.com/GeneGlobe/Default.aspx. Expression of all genes was normalized to that of HPRT.

Table 4 List of primers used for qRT-PCR

Name	Sequence (5' – 3')
Bcl-3 fw	TGCCCATTTACTCTACCCCGACGA
Bcl-3 rv	CAGCGATGTGGAGAGGCGTGTC
sCYLD fw	CTATTGGCAACTGGGATGGAAGG
sCYLD rv	CACTTAAATAGCCCCCAAATGCTTC
FL-CYLD fw	AGTCCACCCTTGCCCATCTCTT
FL-CYLD rv	CATTCATCTTCCAGTTCCAGTCCA
iNOS fw	TGGTCCGCAAGAGAGTGCT
iNOS rv	CCTCATTGGCCAGCTGCTT
HPRT fw	TTAAGCAGTACAGCCCCAAAATG
HPRT rv	CAAACTTGTCTGGAACAAATCC

3.2.4 Amplification and isolation of plasmid DNA

Competent *Escherichia coli* DH5α cells were prepared according to the protocol of Inoue *et al*. (Inoue et al., 1990) and used in heat shock transformations of plasmid DNA. Plasmid DNA was isolated from transformed *Escherichia coli* DH5α bacteria with an alkaline lysis method (Qiagen, Hilden, Germany). Plasmid DNA of higher purity was obtained with QIAGEN columns (Qiagen, Hilden, Germany) following the supplier's instructions.

3.2.5 Agarose gel electrophoresis and DNA gel extraction

Separation of DNA fragments by size was achieved by electrophoresis in agarose gels (0.8% - 2% (w/v); 1x TAE (Sambrook, 1989); 0.5 mg/ml ethidium bromide. DNA fragments were recovered from agarose gel slices using the peqGOLD Gel Extraction Kit (Peqlab, Germany) according to the manufacturer's instructions.

3.2.6 Quantification of DNA and RNA

The concentration of nucleic acids was determined by measuring the absorption of the sample at 260 nm and 280 nm, respectively, in a spectrometer (Eppendorf GmbH, Germany). An OD_{260} of 1 corresponds to approximately 50 µg/ml for double-stranded DNA or 40 µg/ml for RNA and single-stranded DNA. Purity of nucleic acids was estimated by the ratio OD_{260}/OD_{280}, with 1.8 and 2.0 optimal for DNA and RNA, respectively. Alternatively, DNA was separated by electrophoresis in an agarose gel, and the concentration was evaluated from the band intensity in comparison to a standard. Another method for quantification was the usage of the NanoDrop ND-2000 (Peqlab, Germany).

3.2.7 Cloning and sequencing

For molecular cloning of plasmids restriction enzymes and CIP phosphatase from New England Biolabs and T4 DNA Ligase from Invitrogen were used according to manufacturers' instructions. Cloning techniques were applied according to Sambrook, 1989. Sequencing was performed by Genterprise (Mainz) with commercial primers (e.g. T7, M13, etc).

Table 5 Primer sequences used for cloning

Name	Sequence (5'- 3')
Myc-CYLDfw	CGCGGGATCCATGGAGCAGAAACTCATCTCTGAAGAAG

	ATCTGGCTATGAGTTCAGGCCTGTGGAGCCAAG
CYLDrv	TTATTTGTACAGGCTCATGGTTGG
IL-6 fw	ATATGGCGCGCCACCATGAAGTTCCTCTCTGCAAG
IL-6 rv	ATATGGCGCGCCGATCCAAACGGCTCATC

3.3 Biochemistry

3.3.1 Preparation of protein extracts

Cells were lysed on ice in buffer A by gently mixing up and down. After spinning down at 13000 rpm for 10 sec at 4°C, supernatants (cytosolic fraction) are transferred to a fresh tube. The pellet is washed in buffer A and again centrifuged at 13000 rpm for 10 sec at 4°C. The pellet is then lysed in an equal amount of buffer B and frozen at -80°C for 30 min. Samples are then thawed on ice for 30 min. After spinning samples down at 13000 rpm for 10 min at 4°C, the supernatant (nuclear fraction) can be collected.

Buffer A
20 mM HEPES pH 7.9
10 mM KCl
1 mM EDTA
10 % glycerol
0.2 % NP-40
1 mM DTT

Buffer B
20 mM HEPES pH 7.9
10 mM KCl
1 mM EDTA
20 % glycerol
420 mM NaCl
1 mM DTT

0.1 mM Na3VO4, 0.5mM PMSF, 1µg/ml aprotinin, 1µg/ml pepstatin are freshly added to these buffers.

For preparation of whole cell lysates cell pellets or organs were lysed for 10 min on ice in appropriate amounts of RIPA buffer to which protease inhibitor cocktail (Roche) and Phosphatase inhibitor (Roche) was added.

RIPA buffer
20 mM Tris pH 7.5
150 mM NaCl
1% Nonidet P-40
0.5% Sodium Deoxycholate
1 mM EDTA
0.1% SDS

The concentration of protein lysates was determined by Bio-Rad protein assay.

3.3.2 Western Blot

Lysates were run on 4-12% (gradient) SDS-PAGE gels from NUPAGE® Novex Gel Systems (Invitrogen) in Bio-Rad gel electrophoresis chambers (Bio-Rad, Germany) and subsequently blotted with a semi-dry blot system (Bio-Rad, Germany). Primary antibodies used are stated in table 6. Secondary HRP conjugated anti-rabbit, anti-mouse, anti- donkey antibodies were purchased from eBiosciences and Sigma Aldrich. ECL Plus reagent from GE Healthcare (formerly Amersham) was used as a substrate for the HRP reaction. Sensitive films (Kodak) were used for detection and developing occurred in an automatic developer.

Table 6 List of antibodies used for detection of proteins after western blotting

Antibody	Host	Supplier
anti-Bcl-3 (C-14) #sc-185	Rabbit polyclonal	Santa Cruz
anti-Tubulin	Rabbit polyclonal IgG	Cell Signaling
anti-p65/RelA #3034	Rabbit polyclonal IgG	Cell Signaling
anti-HDAC	Rabbit polyclonal IgG	Cell Signaling
anti-p105/p50 (H-119) #sc-7178	Rabbit polyclonal IgG	AbCam
anti-CYLD (E-4)	Mouse monoclonal IgG_{2b}	Santa Cruz
anti-Actin (I-19) HRP	Goat polyclonal IgG	Sigma
anti-Lamin A/C #2032	Rabbit polyclonal IgG	Cell Signaling
anti-RelB (C-19) #sc-226	Rabbit polyclonal IgG	Santa Cruz
cRel I #sc-71	Rabbit polyclonal IgG	Santa Cruz
P100/p52 #4882	Rabbit polyclonal IgG	Cell Signaling
anti-Multi-Ubiquitin, clone FK2	Mouse IgG	StressGen
Anti-Bcl-3, #sc-185	Rabbit polyclonal IgG	Santa Cruz

3.3.3 Electromobility shift assay

Binding of proteins with DNA-binding domains such as transcription factors to DNA causes a decrease of electrophoretic mobility in a polyacrylamide gel. This can be visualised by incubation of radiolabelled target DNA with putative DNA binding proteins. DNA with bound protein yields a retarded band compared to DNA only when the gel is exposed on to an autoradiographic film after electrophoresis.

Buffers:

10 x BRB (binding reaction buffer)

	Stock	added	Final conc.
Tris pH 7.5	1 M	50 µl	100 mM
NaCl	5 M	50 µl	0.5 M
DTT	1 M	25 µl	50 mM
EDTA	0.5 M	10 µl	10 mM
Glycerol	100 %	200 µl	40 %
BSA (nuclease free)	10 mg/ml	50 µl	1 mg/ml

Make up to 500 µl with autoclaved water.

Aliquot in portions of 20 µl in 0.5 ml Eppendorf tubes and store at – 20 °C.

10 x TBE

	Added	Final conc. of 1x
Tris-HCl	108 g	0.089 M
Boric Acid	55 g	0.089 M
EDTA	40 ml of 0.5 M	0.002 M

Make up to 1 l with distilled water and store at RT.

Tracking dye:

0.25 % w/v Bromophenol blue (0.025 g = a grain in 10 ml)

0.25 % w/v Xylene cyanol (0.025 g = a grain in 10 ml)

30 % v/v glycerol = 3 ml glycerol in 10 ml

Make up to 10 ml with water.

Polyacrylamide gel

For one non-denaturing gel mix in a 50 ml conical tube:

0.8 ml	10 % APS
4 ml	10 x TBE
6.6 ml	30 % Acrylamide:Bisacrylamide solution
28.5 ml	distilled water
8 ml	1 M DTT

Mix by inversion, add 24 ml of TEMED, mix again and pour the gel quickly.

The shift was performed using the Gel Shift Assay System and the NF-κB oligo (Promega, USA) according to the manufacturer's instructions. For supershift the nuclear lysates were incubated with an antibody against p50 (Assay Designs, Ann Arbor, MI) for 30 min at RT after the binding reaction occurred.

Probes were loaded and gels were run over night at 40V until the two tracking dye bands were separated using 0.5x TBE as running buffer. Gel was placed on Whatman paper (Millipore) and dried on a gel dryer at 80°C. Gel was subsequently placed in a developing cassette and exposed at -80°C for 4 to 8 hrs. Films were developed using an automatic developer.

3.3.4 Luciferase assay

BMDC were transfected with 10µg of the pTATA-Luc+ using the Mouse Dendritic Cell Nucleofector Kit™ (VPA-1011; Amaxa, Cologne, Germany) according to the manufacturer's instructions. To exclude differences in transfection efficiency, cells were co-transfected with 300 ng of pRL-TK (Promega), which contains the thymidine kinase promoter region upstream of the *Renilla reniformis* luciferase. Cells were lysed after 24 hrs, and luciferase activity was measured by a luminometer (Berthold, Germany) using the dual luciferase reporter assay system from Promega. Data were standardized according to the *Renilla* luciferase activity.

3.4 Cell biology

3.4.1 Preparation of single cell suspensions from lymphoid organs

Murine organs were taken and placed into ice-cold PBS/2%FCS. Spleen, lymph nodes (LN), and thymus were passed through a nylon cell strainer (40 µm, BD Falcon, Germany) to obtain single cell suspensions. Erythrocytes were lysed from spleen and thymus preparations in 140 mM NH_4Cl, 17 mM Tris-HCl pH 7.65 for 2 min at RT. To stop lysis, cells were washed with PBS/2%FCS, centrifuged (5 min, 1200 rpm, 4°C), resuspended in the appropriate amount of PBS/2%FCS and kept on ice. For isolation of dendritic cells (DCs), LN or spleens were subjected to mild collagenase D digestion (2 mg/ml; Roche) in the presence of DNAse (2mg/ml; Sigma, Germany) for 30-45 min at 37°C. Then, normal preparation of single cell suspensions by passing digested tissues through nylon cell strainers followed. Blood from the tail vein was collected in a tube with heparin (Ratiopharm GmbH, Ulm) and then layered on top of 7% (w/v) Ficoll 400 (Pharmacia, Freiburg, Germany). After 1400x g centrifugation at RT for 15 min, lymphocytes were recovered from the interphase of the gradient, resuspended in PBS/2% FCS and kept on ice.

3.4.2 Cell counting

Viable cells were assessed using the trypan blue dye exclusion test and counted using a Neubauer chamber (Assistent, Sondheim, Germany). Afterwards, an aliquot of the cell suspension was diluted with physiological trypan blue solution (Gibco, Long Island, NY, USA), which stains dead cells blue but cannot be taken up by live cells. After counting 16 single quadrants, the counted cell number (N) was multiplied by the dilution factor (V) and the 'chamber factor' (10^4) resulting in the number of live cells per ml ($NxVx10^4$ =cell number/ml).

3.4.3 Flow cytometry

After preparing single cell suspensions from organs and determining the cell numbers, red blood cell lysis was performed – if necessary – as described above. An appropriate amount of cells (0.2-10 x 10^6 per sample) was surface-stained in 25-100 µl PBS/2%FCS with combinations of fluoresceine isothiocyanate (FITC), phycoerythrine (PE), CychromeTM (Cyc), allophycocyanin (APC), Peridinin-chlorophyll protein complex (PerCP), biotin-conjugated monoclonal antibodies or tandem conjugated systems that combine PE/APC with cyanine dyes for 15 min at 4°C. Stainings with biotinylated mAbs were followed by a secondary staining step with Streptavidin (SA)-Cychrome, SA-PE, SA-APC or SA-PE-Cy7. After staining, the samples were washed and resuspended in FACS buffer (PBS, 2% BSA, 0.1% NaN_3). Stained cells were analyzed on a FACSCanto, FACSCantoII or a FACSScan (BD, Heidelberg, Germany) and events in a live gate were analyzed with CellQuest Software (BD, Heidelberg, Germany) or FlowJo ® software (Treestar).

Table 7 List of antibodies used for FACS stainings

Specificity	Clone	Supplier
CD4	GK1.5, L3T4	BD Bioscience
CD8α	5H10, YTS 169,4	eBioscience/Immunotools
CD11b	M1/70	eBioscience
CD11c	HL3	BD Bioscience
CD19	1D3	BD Bioscience
CD25	PC61/7D4	BD Bioscience
CD44	IM7	BD Bioscience
CD45.2	104	eBioscience

CD62L	MEL-14	Immunotools
CD69	H1.2F3	BD Bioscience
CD86	GL1	BD Bioscience
CD90.2	53-2.1	eBioscience
F4/80	BM8	eBioscience
Ly6c	AL-21	BD Bioscience
Ox40L	RM134L	eBioscience
IFNγ	XMG1.2	BD Bioscience
Vβ11 TCR	RR3-15	BD Bioscience
IL-17A	TC11-18H10	BD Bioscience
B7H4	9	eBioscience
FoxP3	FJK-16s	eBioscience
Gr-1 (Ly6G)	RB6-8C5	BD Bioscience
TCRβ	H57-597	BD Bioscience
MHCII(I-A and I-E)	M5/114.15.2	abcam
B220	RA3-6B2	BD Bioscience

Intracellular stainings for Foxp3 were done using the Foxp3 Staining Set from Natutec (Frankfurt, Germany) according to the manufacturer's instructions. Intracellular stainings for IFNγ and IL-17A were performed using the Cytofix/Cytoperm kit from BD Biosciences according to the manufacturer's instructions.

3.4.4 Magnetic cell sorting

Specific cell populations were either sorted or cells were depleted from a heterogeneous cell suspension by magnetic cell sorting (MACS; Miltenyi Biotec, Bergisch Gladbach, Germany). Cell populations were labeled with antibody-coupled microbeads (10 µl beads, 90 µl PBA per 10^7 cells) and separated on LS, MS or LD MACS columns in a magnetic field (Miltenyi et al., 1990). The purity of isolated populations was subsequently tested by FACS analysis: MACS-isolated T cells reached > 90% purity.

3.4.5 CFSE labeling

CFSE (carboxyfluorescein diacetate succinimidyl ester) is a membrane-permeable fluorescent dye, which is non-fluorescent in its native form, but is rendered highly fluorescent after diffusion into the cell. The dye is then unable to diffuse out of the cell and upon one cycle of cell division the stain is halved in each of the daughter cells, which can be detected by flow cytometry. For

proliferation analysis freshly isolated $CD4^+$ T cells were labeled with CFSE (0.5 mM; Molecular probes, Eugene, Oregon, USA). After washing the cells twice in 10 ml PBS, pH 7.4, they were incubated with 0.5 mM CFSE in 1 ml PBS per 10^7 cells at RT for 8 min (Lyons and Parish, 1994). To stop the staining reaction 8 ml of RPMI 1640 (Gibco, Long Island, NY, USA) plus 10% FCS were added. The cells were then washed twice in 10 ml RPMI, and resuspended in the appropriate volume of PBS or medium.

3.4.6 Culture of *ex vivo* lymphocytes

Spleen and LN were aseptically removed from mice and then passed through a sterile sieve. Erythrocytes were lysed for 2 min using NH_4Cl (140 mM NH_4Cl, 17 mM Tris-HCl pH 7.65). Lymphocytes were kept in RPMI 1640 (supplemented with 10% (v/v) FCS), 1 mM sodium pyruvate, 2 mM L-glutamine, 1x non-essential amino acids, 0.1 mM 2-β-mercaptoethanol, and 10 mM HEPES (Gibco), supplemented with the indicated compounds, e.g. MOG_{35-55}, in the indicated concentration for 3-5 days at 37°C.

3.4.7 T cell proliferation assay

To extract bone-marrow (BM), bones (femurs and tibiae) were flushed with PBA, erythrocytes lysed as described above, and cells cultured in DMEM (Gibco), supplemented with 20 ng/ml of GM- CSF (PeproTech Inc., USA). On day 6, DCs were matured with LPS (100 ng/ml; Sigma-Aldrich, Steinheim, Germany), harvested, counted, and cultured with 0.5 x 10^5 CFSE-labeled 2D2 $CD4^+$ T cells in 96-well plates for four days at 37°C with or without MOG_{35-55} (1 to 10 µg/ml). At harvest, the purity of DCs was evaluated by flow cytometry for murine DC surface markers, CD11c and MHCII, and was 80-90%.

3.4.8 Mouse bone marrow derived dendritic cells

Mouse immature DCs were generated according to standard protocols. Bone marrow was extracted from the tibia and femur of mice using 2%FCS in PBS with a 22 gauge needle. Bone marrow was resuspended into single cell suspension by gentle pipetting. Blood cells were lysed with red blood cell lysis buffer (140 mM NH_4Cl, 17 mM Tris-HCl pH 7.65) and remaining cells were cultured in 6 well plates (Greiner Bio One) at $3.0x10^6$/well. On day 2 and 4 culture medium containing GM-CSF (200 U/ml) was replaced along with the removal of non-adherent cells. Culture media RPMI was supplemented with 10% FCS, glutamine, penicillin/streptomycin, and 50µM 2-β-mercaptoethanol. On day 6 the immature DCs were activated with TLR ligands or TNFR agonist

or left untreated. The following TLR stimuli were used: TLR3 agonist Poly-I:C (Amersham, Freiburg, Germany). TLR4 was stimulated with LPS (Salmonella typhimurium: Sigma, Deisenhofen, Germany). TLR9 was stimulated with CpG.

3.4.9 Peritoneal and bone marrow derived macrophages (BMDMs)

For elicitation of peritoneal macrophages mice were injected with 1 ml of 2% w/v Bio-Gel P-100 (Bio-Rad) 4 days prior to sacrifice. After that, macrophages were retrieved by peritoneal lavage with 10 ml of ice-cold PBS using a 20-G needle. Cell suspension was kept on ice for 5 minutes to allow for Bio-Gel beads to settle. Supernatants containing the cells were transferred to a new tube.
For BMDMs bone marrow cells were harvested and cultured in medium containing macrophage colony-stimulating factor (M-CSF) (Stanley, 1985). After 7 days in culture, contaminating non-adherent cells are eliminated and adherent cells were harvested for assays.

3.4.10 Cytokine release measurement with ELISA or CBA-Flex

After 12 to 72 hrs of incubation cell culture supernatants were collected and frozen at -80 °C for subsequent analysis. Cytokines were analyzed by standard enzyme-linked immunosorbent assay (ELISA) protocols. All ELISA antibodies and recombinant standards were purchased from BD Pharmingen (Heidelberg, Germany) and used according to the manufacturer's instructions. For detection, 3.3', 5,5' TMB liquid substrate (Sigma) was used. The optical density at 450 nm after adding 2M H_2SO_4 was analyzed using a Lambda E reader from MWG Biotech (Ebersberg, Germany). Where indicated, cytokine detection in BMDC culture supernatants was detected also with anti-IL-6, IL-10 and TNF-α antibodies from BD Cytometric Bead Array Flex system (CBA-Flex) and analyzed with FCAP Array SoftwareTM according to manufacturer's instructions.

3.4.11 Preparation of mouse embryonic fibroblasts (MEFs)

Females of the desired genotype were mated with males of the desired genotype. Mating was detected by a daily plug check. Thirteen to fourteen days after mating, the pregnant mice were sacrificed by cervical dislocation. The embryos and uterine horns were separated from the abdomen, carefully detached from the animal, and placed in a dish with PBS where the brain, liver and as many red blood cells as possible were removed. The tissue was passed through nylon cell strainers (40µm) and pelleted by centrifugation at

RT at 1200 rpm for 5 min. Cells obtained from one embryo were subsequently plated in 10 cm plates in EF medium. After 24 hrs, the medium was changed to remove cellular debris. Confluent plates were either expanded or frozen.

3.5 Mouse experiments

Tail bleeding as well as the general handling of mice was performed according to Hogan (Hogan, 1987) and Silver (Silver, 1995)

3.5.1 Mice

C57BL/6 mice were obtained from Charles River or Jackson Laboratories, C57BL/6 Thy1.1 mice were taken from breedings in our animal facility. Other strains used were: $Cyld^{FL/FL}$ and $Cyld^{ex7/8}$ mice (Hovelmeyer et al., 2007), ROSA-CAGs-STOP-Bcl-3-EGFP mice (M. Woerns), LysMcre mice (Clausen et al., 1999), CD11c-Cre mice (Caton et al., 2007), CD4-Cre mice (Lee et al., 2001; Sawada et al., 1994) and 2D2 mice (Bettelli et al., 2006).

3.5.2 Induction and assessment of EAE

MOG_{35-55} peptide (amino acid sequence: MEVGWYRSPFSRVVHLYRNGK) was obtained from Research Genetics (Huntsville, Alabama, USA). Active EAE was induced by immunization with 50 µg of $MOG_{35–55}$ peptide emulsified in CFA (Difco Laboratories, Detroit, Michigan, USA) supplemented with 8 mg/ml of heat-inactivated *Mycobacterium tuberculosis* H37RA (Difco Laboratories, Detroit, Michigan, USA). The emulsion was administered as a 100 µl subcutaneous (s.c.) injection into the tail base. Mice also received 200 ng of Pertussis toxin (Sigma Aldrich, Steinheim, Germany) i.p. on the day of immunization and two days later. Clinical assessment of EAE was performed daily according to the following criteria: 0, no disease; 1, decreased tail tone; 2, abnormal gait (ataxia) and/or impaired righting reflex (hind limb weakness or partial paralysis); 3, partial hind limb paralysis; 4, complete hind limb paralysis; 5, hind limb paralysis with partial fore limb paralysis; 6, moribund or dead.

3.5.3 Colitis induction and/or scoring

In brief, $CD4^+CD62L^+$ cells were isolated from splenocytes of syngeneic C57BL/6 mice and 1 x 10^6 $CD4^+CD62L^+$ cells were transferred into $RAG1^{-/-}$ mice by intraperitoneal injection. Mice were weighed and scored weekly. The endoscopic score of colitis severity (MEICS: range 0–15 points) was based on evaluation of colon translucency (0–3 points), presence of fibrin attached to

the bowel wall (0–3 points), granular aspect of the mucosa (0–3 points), morphology of the vascular pattern (0–3 points), and the presence of loose stools (0–3 points). Endoscopy was performed using a miniaturized colonoscope (Colowiew, Storz, Germany).

3.6 Software

For molecular cloning, Gene Construction Kit (Textco BioSoftware Inc.) and Vector NTI (Invitrogen) were used. For analyzing FACS data CellQuest (BD) and FlowJo® were used. For statistics, Prism® (GraphPad Software Inc.) and Microsoft Excel were used. Values are typically represented as mean ±SD or ± SEM (standard error of mean). Statistical significance was assessed using 2-tailed Student's *t*-test. P-values < 0.05 were regarded significant, displayed by '*' in the figures (** = p-value < 0.05; *** = p-value < 0.005)

4 Results

4.1 Impact of sCYLD overexpression on dendritic cell and macrophage function

Hövelmeyer et al. (Hovelmeyer et al., 2007) could demonstrate that over-expression of the short splice variant of CYLD (sCYLD), in the absence of its full-length form, causes major changes in B cell homeostasis. Not only did the over-expression lead to prolonged survival of B cells but also to an impressive enlargement of lymphatic organs, caused by excessive activation of the NF-κB signaling pathway. Knowing that deregulation of CYLD expression in these mice (henceforth termed $CYLD^{ex7/8}$ mice) has a strong impact on NF-κB signaling we sought to analyze the role of sCYLD in dendritic cell and macrophage function.

4.1.1 Analysis of dendritic cell function in $CYLD^{ex7/8}$ and $CYLD^{ko}$ mice

Dendritic cells (DC) are the most potent antigen-presenting cells (APC) of the immune system. Derived from bone marrow progenitor stem cells, DCs migrate to the tissues where they become keepers of the immune system. They possess the unique competence to initiate primary T cell responses. They can also stimulate both B and T cells during an ongoing immune response (Banchereau et al., 2000; Banchereau and Steinman, 1998; Steinman and Inaba, 1999). Located in most tissues, DCs are capable of efficiently capturing and processing a large variety of antigens. In response to microbial products they upregulate the surface expression of co-stimulatory molecules (such as CD80 and CD86) as well as MHC class II, which is required for antigen presentation. DCs then migrate to secondary lymphoid organs where they encounter antigen-specific T cells and activate them (Banchereau and Steinman, 1998). The capacity of DCs to activate naïve as well as memory T cells, is not shared by any other antigen-presenting cell.
Until recently, the scarceness of DCs in most tissues has hindered the study of DC phenotype, morphology, function and ontogeny. Purification methods to obtain these cells from tissues are time consuming and can induce alterations in the DCs recovered. The ability to derive DCs from progenitors *in vitro* has allowed to overcome many of these obstacles (Lardon et al., 1997), especially since preparations from bone marrow progenitors allow the generation of

large amounts of dendritic cells (Lutz et al., 1999). In this work, bone marrow from CYLD$^{ex7/8}$, CYLD knock-out (henceforth termed CYLD^{ko}) and wild type (WT) mice were obtained and BMDCs from the different mouse strains were grown in the presence of GM-CSF as described in materials and methods. On day 6 of the differentiation process, BMDCs were subjected to stimulation with a variety of different TLR ligands including LPS, CpG and Poly I:C.

4.1.1.1 Over-expression of sCYLD enhances the expression of co-stimulatory molecules on BMDCs

Prior to analyzing BMDCs from CYLD$^{ex7/8}$ mice it was important to show that these cells overexpress the short transcript of CYLD in the absence of the full-length version. Western Blotting with an antibody against CYLD showed the expected result, i.e. WT BMDCs expressed the full-length as well as the short form, whereas CYLD$^{ex7/8}$ BMDCs overexpressed the short in absence of the full-length protein and finally the CYLD^{ko} BMDCs expressed none.

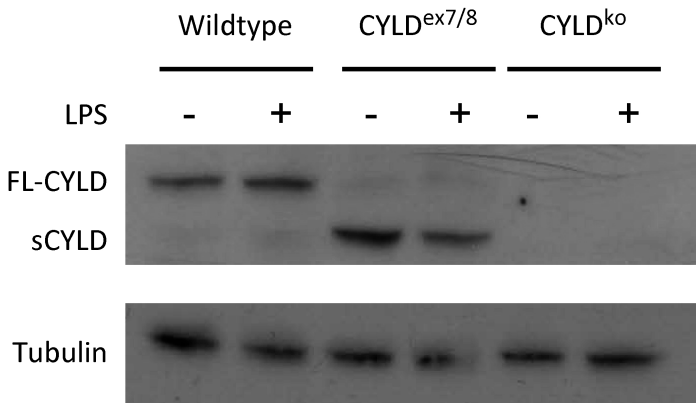

Figure 5 Expression of the CYLD variants in WT, CYLD$^{ex7/8}$ and CYLD^{ko} BMDCs
BMDCs were cultured for 6 days in the presence of GM-CSF and stimulated 12 hrs with 100 ng/ml LPS. 50 µg of whole cell lysates of BMDCs of indicated genotypes were subjected to western blotting. The two CYLD variants (sCYLD – 86kDa and FL-CYLD -107kDa) were both detected by the same antibody. Tubulin (55 kDa) was used as a loading control.

Considering that DCs are the most important APCs of the immune system we commenced to analyze cell surface expression of CD86 (also known as B7-2), OX40L and MHC class II. CD86 is a glycoprotein, which binds CD28 on T cells and provides a co-stimulatory signal, which is necessary for their clonal expansion. Its transcription is upregulated by LIGHT (Lymphotoxin-related Inducible ligand that competes for Glycoprotein D binding to Herpes virus entry mediator on T cells) through activation of NF-κB (Zou and Hu, 2005). OX40L is the ligand for OX40 (also known as CD134), which is a receptor expressed on activated CD4$^+$ and some of the CD8$^+$ T cells and also serves

as a co-stimulatory molecule. The OX40/OX40L interaction enhances the proliferation and activation of $CD4^+$ cells of both Th1 and Th2 subtypes (De Smedt et al., 2002). MHC class II, on the other hand, is a molecule, which is expressed on all APCs and is required for the presentation of extracellular antigens on the cell surface. It is increased and stabilized on the surface of mature activated dendritic cells. Yoshimura et al. could show that the expression of MHC class II, CD86 and other co-stimulatory molecules on DCs is NF-κB dependent (Yoshimura et al., 2001). By analyzing the surface expression of aforementioned markers on BMDCs of the different CYLD genotypes by FACS analysis, we could clearly observe an upregulation of these markers on the surface of BMDCs derived from the $CYLD^{ex7/8}$ mice. Expression levels of the $CYLD^{ko}$ BMDCs resembled the WT.

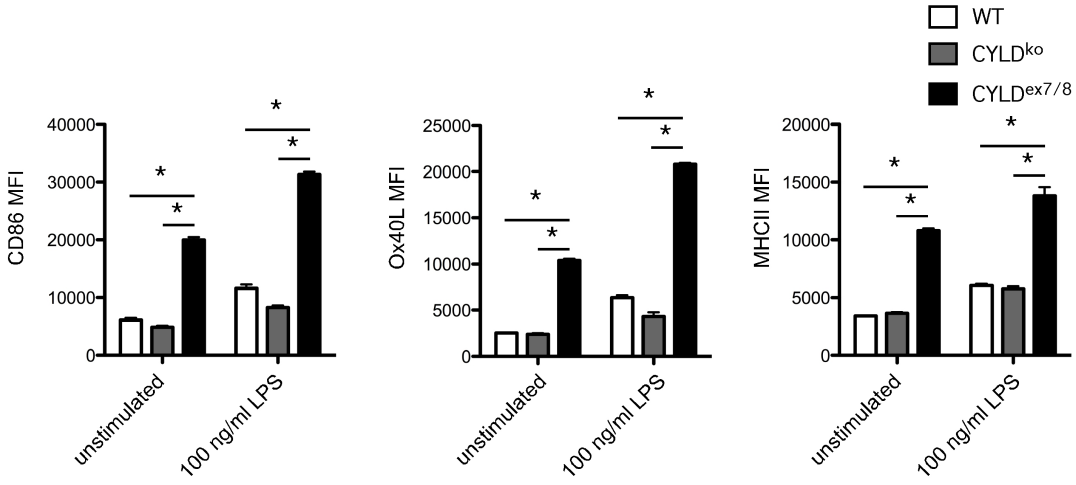

Figure 6 Expression levels of activation markers on WT, $CYLD^{ex7/8}$ and $CYLD^{ko}$ BMDCs
BMDCs from WT, $CYLD^{ko}$, and $CYLD^{ex7/8}$ mice were differentiated with GM-CSF for 6 days in culture and stimulated (100 ng/ml LPS, 12 hours) and submitted to fluorescence-activated cell sorting (FACS) analysis of the $CD11c^+$ population and cell surface expression of CD86, MHC II, and Ox40L. Mean fluorescence intensity (MFI) values of indicated cell surface expression markers shown are means of triplicates and SEM shown as error bars. *p < .05 using t test for $CYLD^{ex7/8}$ compared with WT and $CYLD^{ko}$ stimulated BMDCs.‡ (‡: Experiments marked with this symbol were part of a collaborative project with Dr. Cathy Srokowski).

4.1.1.2 Increase of inflammatory cytokine secretion in $CYLD^{ex7/8}$ BMDCs

Another hallmark of DC activation is the secretion of cytokines after activation of TLR signaling by LPS. Cytokine secretion by DCs after stimulation by bacterial antigens is necessary for elicitation of an immune response, since it is required for the differentiation of naïve T cells into effector cells (Moser and Murphy, 2000). Exposure of DCs to conserved bacterial structures, results in the activation of the NF-κB and/or the MAP kinase (MAPK) signaling

pathways and mounts in a specific cytokine response depending on the nature of the upstream trigger. To investigate whether cytokine expression profiles of DCs from mice of different CYLD genotypes diverge, BMDCs were isolated from WT, CYLD$^{ex7/8}$ and CYLD^{ko} mice and cultured with either basal DC medium or DC medium supplemented with 100 ng/ml LPS for 12 hours.
Secretion levels of the pro-inflammatory cytokines IL-6 and TNFα were significantly increased in BMDCs from CYLD$^{ex7/8}$ mice compared to WT or even CYLD^{ko}. This observation was not only true for stimulatory conditions (i.e. LPS treatment) but also for the steady state. This result is in line with publications showing that these cytokines are induced by NF-κB transcription factors in DCs (Jones, 2005; Preischl et al., 1996). Additionally, levels of the anti-inflammatory cytokine IL-10 were markedly reduced in CYLD$^{ex7/8}$ BMDCs, whereas they were normal in both WT and CYLD^{ko} cells, emphasizing the pro-inflammatory phenotype of the CYLD$^{ex7/8}$ BMDCs.

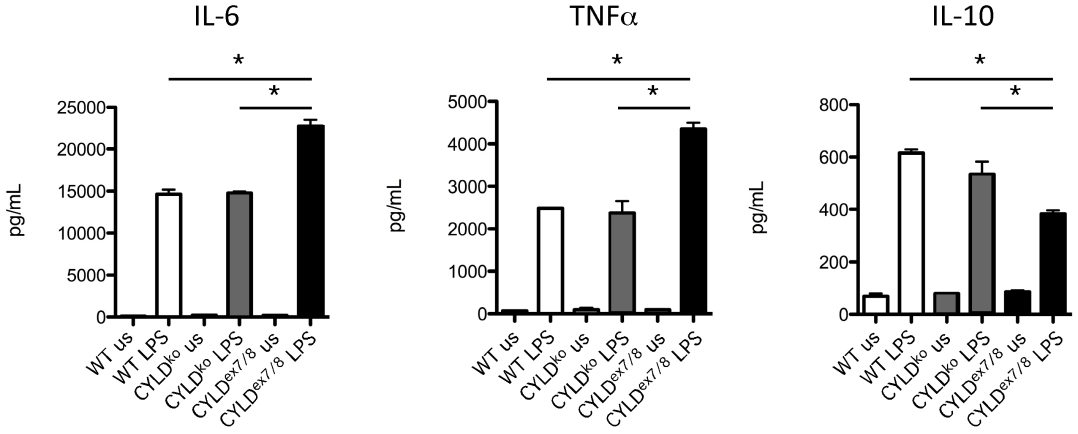

Figure 7 Secretion of inflammatory and anti-inflammatory cytokines by WT, CYLD$^{ex7/8}$ and CYLD^{ko} BMDCs
Supernatants from stimulated BMDCs cultures measured for IL-10, TNF-α, and IL-6 cytokines with Becton Dickinson CBA Flex Set System. *p < .05 using *t* test for WT compared with CYLD$^{ex7/8}$ and for CYLD^{ko} compared with CYLD$^{ex7/8}$ stimulated BMDCs. Values shown are means of triplicates with SEMs. ‡

4.1.1.3 BMDCs from CYLD$^{ex7/8}$ mice induce an increased clonal T cell expansion

Depending on the conditions, DCs can stimulate the differentiation and activation of a variety of T cells, which affect the immune response differently. They can stimulate cytotoxic T cells (CTLs), which express the co-receptor CD8 and hence interact with MHC class I bearing cells, to proliferate vigorously, which is unusual for CD8$^+$ T cells (Bender et al., 1995; Bhardwaj et al., 1994). CD4-expressing T helper cells, on the other hand, need cells that

express MHC class II molecules. In the presence of mature DCs and IL-12 secretion (Cella et al., 1996; Koch et al., 1996; Reis e Sousa et al., 1997), these T cells turn into interferon-γ (IFNγ)-producing Th1 cells. IFNγ activates the antimicrobial activities of macrophages and together with IL-12 promotes either the differentiation of Th1 or $CD8^+$ cytotoxic T cells.

In order to investigate how overexpression of sCYLD affects the interplay between dendritic cells and T cells *in vivo*, naïve St42 TCR specific T cells were adoptively transferred into WT recipients. St42 mice express a transgenic TCR recognizing the peptide SGP from Ad5E1a protein presented on $H2\text{-}D^b$. Two days later, the same mice were injected i.p. with BMDCs from mice of one of the three genotypes (i.e. WT, $CYLD^{ko}$ and $CYLD^{ex7/8}$), which were stimulated beforehand with 100 ng/ml LPS for 12 hrs and loaded with SGP peptide. Since the St42 specific T cells carried a different congenic marker (Thy1.1) than the endogenous WT T cells (Thy1.2), it was possible to follow the expansion of transferred cells.

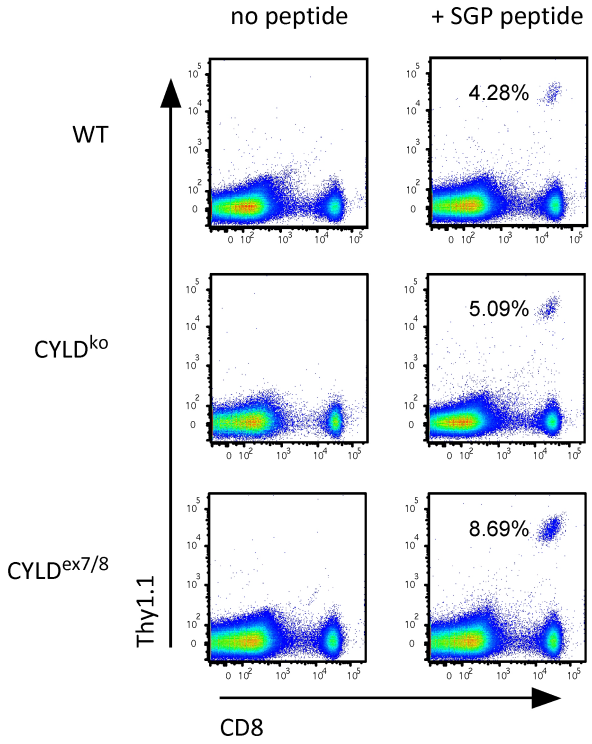

Figure 8 sCYLD confers a stimulatory phenotype in BMDCs that leads to T-cell expansion
Day 3 analysis of blood T-cell expansion of adoptively transferred TCR tg (St42) donor splenocytes into WT recipient mice immunized with day 6–differentiated and 12 hrs LPS-stimulated WT, $CYLD^{ko}$, or $CYLD^{ex7/8}$ BMDCs SGP peptide loaded and injected intraperitoneally to recipient WT mice. Percentages indicate $Thy1.1^+$ $CD8^+$ cells. Values are representative of more than 4 mice per group and repeated 3 times. ‡

Peripheral blood from recipient mice was analyzed by FACS on day three after BMDC transfer, T cell expansion was almost twofold higher in WT recipients that had received the BMDCs from the $CYLD^{ex7/8}$ mice, than in mice receiving $CYLD^{ko}$ BMDCs (Fig. 8). A finding which again demonstrated the enhanced stimulatory capacity of the $CYLD^{ex7/8}$ BMDCs.

4.1.1.4 BMDCs from CYLD$^{ex7/8}$ fail to induce peripheral tolerance

Dendritic cells serve as “nature’s adjuvants” for immunity (Inaba et al., 1990); they need to mature in response to stimuli inherent to an infection (e.g. TLR ligands) or other settings such as transplantation or contact allergy. In the absence of such co-stimulatory signals, dendritic cells no longer activate an immune response when encountering an antigen, but induce tolerance towards it. This phenomenon is part of an important mechanism termed peripheral tolerance, which protects the organism from an autoimmune response to self- or harmless environmental proteins.

In order to investigate if the tolerogenic capacity of DCs from CYLD$^{ex7/8}$ and/or CYLD^{ko} mice is impaired, a DC-targeting approach utilizing an ovalbumin (OVA)-conjugated anti-DEC-205 antibody was employed. DEC205 (CD205) is mainly expressed by CD8α^{+} DCs in the T-cell rich areas of the lymphoid organs and mediates the efficient uptake, processing and presentation of antigens on MHC class II products *in vivo* (Hawiger et al., 2001). The presentation of OVA mediated by anti-DEC-205 occurs on MHC class I through a TAP-dependent pathway. One valuable feature of OVA as a model protein is that CD8^{+} MHC class I-restricted TCR transgenic OT-I cells are available.

To study T cell tolerance mediated by anti-DEC-205:OVA and the role of sCYLD in this mechanism, WT controls along with CYLD$^{ex7/8}$ and CYLD^{ko} mice received 1 x 10^{6} purified OT-I CD45.1 T cells on day 0 (refer to time schedule and experimental setup in Fig. 9A). On day 1 the same mice were injected subcutaneously with 20 µg of anti-DEC-205:OVA. On day 12 mice were challenged with 50 µg of OVA in complete Freund’s adjuvant (CFA). Subsequently the expansion and disappearance of the adoptively transferred OT-I CD45.1 T cells was monitored.

On days 3, 5 and 7 the expansion of OT-I CD45.1 T cells was followed by FACS analysis of blood samples (data not shown). The experiment was terminated on day 15 and spleens of recipient mice were removed and monitored for the presence of OT-I CD45.1 T cells.

A

Timecourse	Experimental process
Day 0	s.c. 20µg anti-DEC205:OVA or PBS
Day 1	i.v. adoptive transfer of OT-I CD45.1 T cells into recipient mice: WT, CYLD$^{ex7/8}$, CYLD^{ko}
Day 12	s.c. challenge with 50µg OVA in CFA
Day 15	evaluation

B

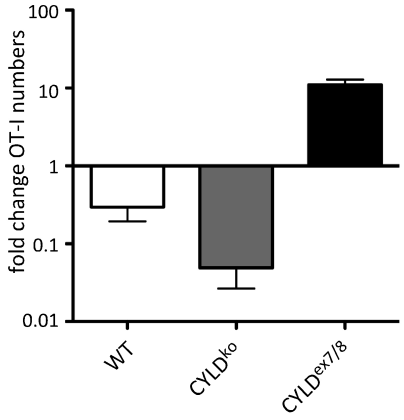

Figure 9 sCYLD overexpression causes a hyperactive phenotype that suppresses the tolerogenic potential of BMDCs
(A) Experimental time course and setup (B) Fold change in OT-I T-cell numbers compared with PBS control in the spleen of recipient mice adoptively transferred with OT-I cells, given 20 µg a-DEC-205:OVA intra footpad and challenged with 50 µg OVA protein in CFA subcutaneously. Cells were analyzed by FACS using CD45.1 and CD8 antibodies to detect OT-I CD45.1 cells gated on CD8. Values represent more than 4 mice per group, with mean values and SEMs. ‡

Recipient mice, which did not receive anti-DEC-205:OVA but were challenged with OVA/CFA on day 12, showed the persistent presence of OT-I CD45.1 T cells in the spleen on day 15 (data not shown), whereas in WT and CYLD^{ko} mice the transgenic T cells appeared to have been completely deleted. CYLD$^{ex7/8}$ mice, however, surprisingly still possessed a well detectable population of the adoptively transferred T cells. As summarized in Figure 9B, these findings suggest, that dendritic cells in CYLD$^{ex7/8}$ mice lack the capacity to induce tolerance towards an exogenous antigen, but rather promote expansion.

4.1.1.5 Analyzing Bcl-3 expression and regulation in CYLD$^{ex7/8}$ BMDCs

To understand the mechanism behind our phenotypic observations (i.e. the hyperactive phenotype in DCs), we focused on NF-κB members involved in CYLD- influenced NF-κB signaling. Bcl-3 has recently been shown to interact with both FL-CYLD and sCYLD and to modulate NF-κB activity (Hovelmeyer et al., 2007; Massoumi et al., 2006). It has also been indicated as an activator of NF-κB signaling when interacting with the NF-κB subunits p50 or p52

(which can be present as homo- or heterodimers). p50 and p52 lack DNA-trans-activation domains and require additional factors like Bcl-3 to induce target gene expression (Franzoso et al., 1993; Franzoso et al., 1992).
To this end, both mRNA as well as protein Bcl-3 expression levels in BMDCs from WT, CYLD$^{ex7/8}$ and CYLD^{ko} mice were analyzed. Quantitative real-time PCR (qRT-PCR) revealed that Bcl-3 transcript expression was significantly increased in CYLD$^{ex7/8}$ BMDCs compared to CYLD^{ko} and WT even in the steady state (i.e. unstimulated). This phenotype was further enhanced when BMDCs were stimulated with LPS (Fig.10).

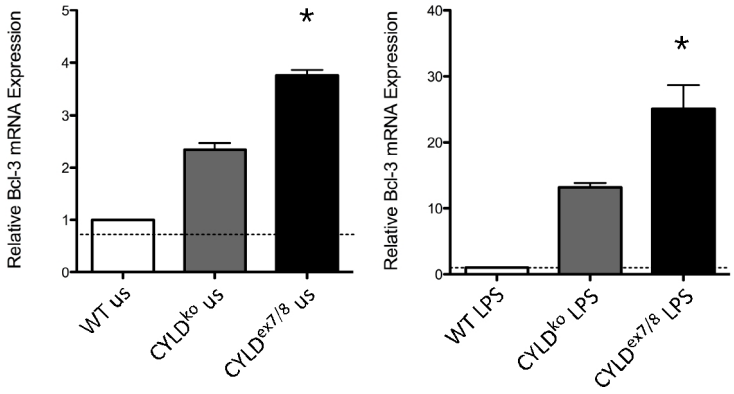

Figure 10 Bcl-3 mRNA expression levels in WT, CYLD^{ko}, or CYLD$^{ex7/8}$ BMDCs
Differentiated day 6 WT BMDCs were stimulated (100 ng/ml LPS, 12 hours) or left untreated, and qRT-PCR was performed to detect mRNA levels of Bcl-3. mRNA levels were normalized by HPRT levels and expressed as fold change. ‡

Knowing that Bcl-3 is mainly located in the cell's nuclear compartment, nuclear extracts from unstimulated and LPS-stimulated WT, CYLD^{ko} and CYLD$^{ex7/8}$ BMDCs were prepared and submitted to immunoblotting. BMDCs from CYLD$^{ex7/8}$ mice showed the highest expression levels of Bcl-3 when compared to CYLD^{ko} and WT BMDCs, whereas CYLD^{ko} BMDCs only showed an intermediate expression level in the unstimulated state. 12 hrs of stimulation with LPS further enhanced the differences in Bcl-3 expression levels (Fig.11).

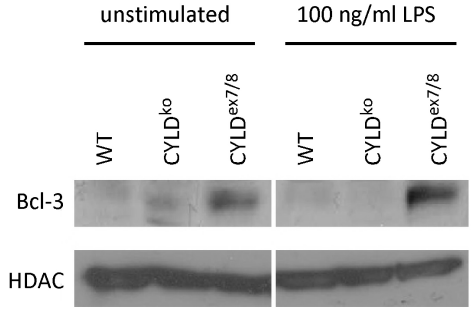

Figure 11 Bcl-3 protein expression in WT, CYLD^{ko}, or CYLD$^{ex7/8}$ BMDCs
Nuclear BMDC extracts from unstimulated and stimulated (100 ng/ml LPS, 12 hours) cells were examined by western blotting using anti–Bcl-3 (~ 55 kDa). Shown are lysates from WT, CYLD^{ko}, and CYLD$^{ex7/8}$ mice. HDAC1 antibody (~ 62 kDa) was used as a loading control. ‡

To clarify the impact of sCYLD overexpression on Bcl-3 expression levels, two expression plasmids (based on the plasmid pcDNA 3.1 from Invitrogen) were designed and cloned. They contained the strong CMV (cytomegalovirus) promoter followed by the PCR-amplified open reading frames (ORFs) of either FL-CYLD or sCYLD fused to a 5 prime myc-tag.

Since transfection of BMDCs is tedious resulting in low transfection efficiencies and often causes activation of treated DCs, murine embryonic fibroblasts (MEFs) from $CYLD^{ko}$ mice were used in this experiment, because they can easily be transfected yielding high transfection efficiencies. The intention behind using fibroblasts from $CYLD^{ko}$ embryos was that the experiment was not to be influenced by endogenous CYLD expression. To investigate the role of sCYLD on Bcl-3 expression $CYLD^{ko}$ MEFs were transfected either with the aforementioned pcDNA3.1-myc-sCYLD plasmid, or with an empty mock plasmid. Total mRNA was isolated, cDNA synthesized and subjected to qRT-PCR using primers to detect Bcl-3 expression. A clear-cut result showing the induction of Bcl-3 expression by sCYLD overexpression could be obtained (Fig. 12A).

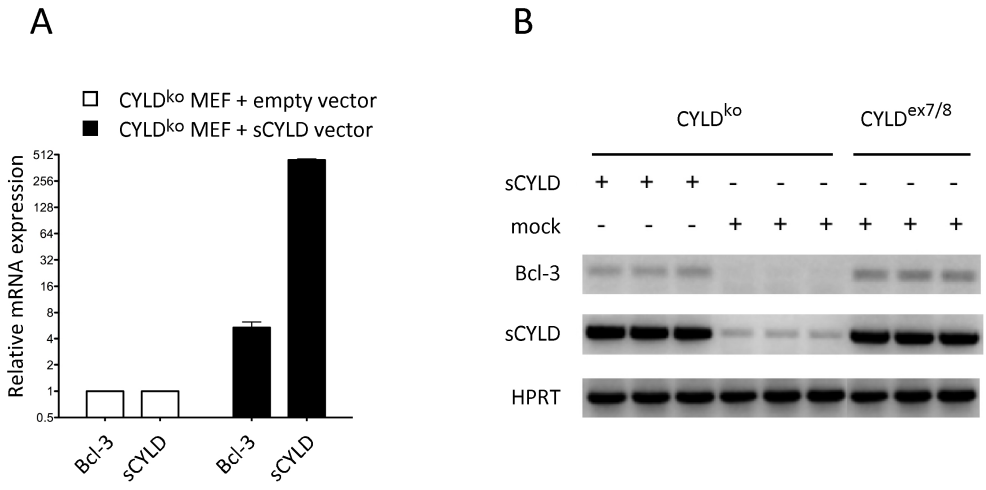

Figure 12 sCYLD induces Bcl-3 expression
$CYLD^{ko}$ mouse embryonic fibroblasts (MEFs) cells were transfected with empty vector or with sCYLD vector. (A) Comparison of Bcl-3 upregulation when sCYLD is expressed in $CYLD^{ko}$ MEFs compared with mock-transfected $CYLD^{ko}$. (B) Gel represents the qRT-PCR products obtained after performance of qRT-PCR on sCYLD-transfected or mock-transfected MEFs as indicated in (A). HPRT served as a control. ‡

These results are also visualized in Figure 12B, in which PCR products have been loaded on an agarose gel next to equal amounts of qRT-PCR products obtained from untransfected or mock-transfected $CYLD^{ex7/8}$ MEFs as a positive control. Faint bands were detectable in mock-transfected $CYLD^{ko}$ MEFs using sCYLD primers, which must be subtracted as background, since $CYLD^{ko}$ MEFs should express no CYLD transcript at all. This result clearly

demonstrates that expression of sCYLD in the absence of the full-length transcript is sufficient to induce Bcl-3 transcription. This leads us to the causal conclusion that the overexpression of sCYLD in the CYLD$^{ex7/8}$ BMDCs is causing the significantly enhanced expression levels of Bcl-3. This phenomenon could not be observed in the CYLD^{ko} BMDCs.

4.1.1.6 Elevated Bcl-3 expression in CYLD$^{ex7/8}$ BMDCs is accompanied by increased NF-κB signaling

Bcl-3 is a regulator of NF-κB signaling, which according to some reports has a negative effect on NF-κB signaling (Hatada et al., 1992; Nolan et al., 1993; Wulczyn et al., 1992), whereas others claim, that it actually has positive, activating effects (Bours et al., 1993; Fujita et al., 1993).
In a more recent report (Hovelmeyer et al., 2007) it was shown that B cells, which overexpress sCYLD had elevated levels of nuclear Bcl-3 accompanied by drastic activation of NF-κB signaling. Therefore, we sought to analyze the activation status of NF-κB signaling in CYLD$^{ex7/8}$ BMDCs compared to WT and CYLD^{ko}, given that augmented NF-κB signaling is often accompanied by an increase in proliferation, activation and/or survival.

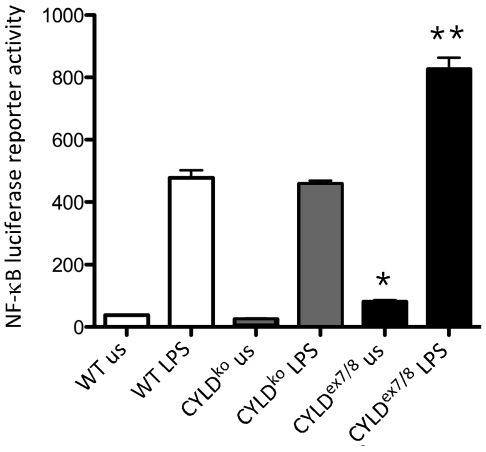

Figure 13 Overexpression of sCYLD causes elevated NF-κB activity
NF-κB luciferase reporter activity of BMDCs transfected with a NF-κB luciferase reporter construct untreated or stimulated (LPS 100 ng/ml, 12 hours). Cells were lysed after 24 hrs, and luciferase activity was measured with a luminometer (Berthold Technologies, Bad Wildbad, Germany) using the dual luciferase reporter assay system from Promega. Data were standardized according to the *Renilla* luciferase activity and normalized to represent fold differences. *p < .05 using 1-way ANOVA between unstimulated samples; **p <.05 using 1-way ANOVA between LPS-stimulated samples. Data represent mean values with standard mean error bars. ‡

Figure 13 shows the result of a luciferase assay, in which BMDCs from the three different genotypes (i.e. WT, CYLD^{ko} and CYLD$^{ex7/8}$) were transfected

with a NF-κB reporter plasmid and an internal control (see materials and methods) for later standardization. Upon transfection BMDCs were either left untreated or stimulated with LPS for 12 hrs. NF-κB activity was 2-fold higher in unstimulated CYLD$^{ex7/8}$ BMDCs compared to control counterparts (Fig.13). This was also the case for stimulated BMDCs. NF-κB activity in CYLD^{ko} BMDCs was comparable to that in WT BMDCs.

Expression analysis of the NF-κB subunits RelB, c-Rel, p65 and p50 in WT, CYLD$^{ex7/8}$ and CYLD^{ko} BMDCs by western blotting confirmed the results retrieved from the luciferase assay, showing that expression levels of these subunits –except for c-Rel- were drastically increased (Fig.14). Western blots were performed with nuclear lysates, so that one can assume that subunits, which have been actively transported to the nuclear department, influence and regulate the expression of NF-κB target genes in these cells.

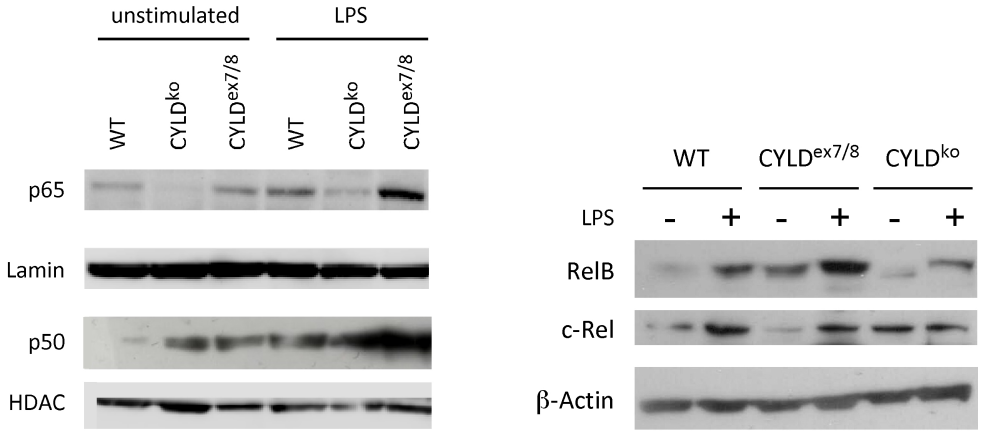

Figure 14 Western blot analysis of NF-κB subunits in WT, CYLD^{ko}, or CYLD$^{ex7/8}$ BMDCs
Nuclear BMDC extracts from unstimulated and stimulated (100 ng/ml LPS, 12 hours) were examined by Western blotting using anti-p50 and anti-p65. Shown are lysates from WT, CYLD^{ko}, and CYLD$^{ex7/8}$ mice. HDAC (62 kDa) and β-Actin (42 kDa) were used as a loading controls. ‡

Bcl-3 was shown to bind p50 homodimers in mammalian systems, where this complex bound to NF-κB target sites and activated gene expression (Bours et al., 1993; Fujita et al., 1993). To investigate whether Bcl-3-:p50:p50 complexes also played a role in the NF-κB activation in the CYLD$^{ex7/8}$ BMDCs, an electromobility shift assay (EMSA) was performed, using nuclear lysates from WT, CYLD^{ko} and CYLD$^{ex7/8}$ BMDCs which were either left untreated or were incubated with anti-p50 to cause a supershift in case of binding.

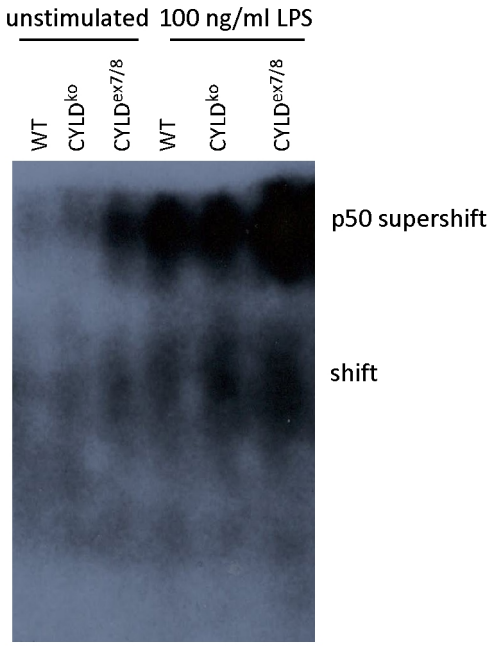

Figure 15 Increased NF-κB target gene expression in CYLD$^{ex7/8}$ BMDCs induced by p50
EMSA was performed with nuclear extracts from BMDCs that were unstimulated or stimulated with 100 ng/ml LPS for 12 hrs and subsequently incubated with NF-κB–specific labeled probe and p50 antibody to perform supershift, and separated by native polyacrylamide gel electrophoresis (PAGE). ‡

In this EMSA ^{32}P end-labeled consensus NF-κB oligos were incubated with nuclear lysates from BMDCs, which were then analyzed on a nondenaturing polyacrylamide gel. Transcription factors, which bound the NF-κB consensus oligo, moved slower through the gel than unbound oligonucleotides, causing a shift (Fig.15). Addition of anti-p50 antibody, which bound to p50 subunits that were associated with NF-κB consensus oligo, resulted in the observed supershift. This EMSA demonstrated that NF-κB activity in CYLD$^{ex7/8}$ BMDCs is significantly higher than in CYLD^{ko} and WT BMDCs and that p50 homodimers seem to play a major role in this activation.

4.1.2 Analysis of the LysMcre Cyld$^{floxed/floxed}$ strain

In CYLD$^{floxed/floxed}$ (Cyld$^{FL/FL}$) mice (generated by Nadine Hövelmeyer) exon 7 is flanked by loxP sites. Cre-mediated excision results in an out-of-frame transcript of the full-length isoform and the overexpression of the short isoform termed sCYLD. Consequently, the mating of these animals to the LysMcre strain (Clausen et al., 1999) results in a strain in which cells of myeloid origin (mainly granulocytes and macrophages, but also microglia in the CNS) express the sCYLD isoform in the absence of the full-length version.
Macrophages are mononuclear phagocytes that are widely distributed throughout the body. These cells contribute to development and homeostasis and participate in innate and adaptive immune responses. The physiology of macrophages can vary depending on the environment in which they reside

and the local stimuli to which they are exposed. Macrophages are secretory cells, and in that role can promote and regulate immune responses and contribute to autoimmune pathologies.

In this work, two types of macrophages were used for experiments:

- Peritoneal macrophages

The peritoneal cavity provides an easily accessible site for the harvesting of moderate numbers of resident, non-manipulated macrophages. Usually, the number of macrophages present in the peritoneum under non-elicited condition is insufficient for extensive biochemical studies. To increase macrophage yield, sterile eliciting agents, such as Bio-Gel, can be injected into the peritoneal cavity prior to cell harvest.

- Bone marrow derived macrophages (BMDMs)

An alternative approach for isolating relatively large numbers of non-elicited macrophages takes advantage of the use of macrophage colony–stimulating factor (M-CSF) to differentiate macrophage progenitor cells from the bone marrow into mature macrophages in culture (Stanley, 1985).

4.1.2.1 Overexpression of sCYLD in elicited peritoneal macrophages does not increase MHC class II expression levels

Peritoneal macrophages from LysMcre CYLD$^{FL/FL}$ and control littermate mice (LysM cre negative) were harvested on day 4 after Bio-Gel injection. Macrophages were stained with F4/80, CD11b and MHC class II antibodies for subsequent FACS analysis. Cells that were positive for the markers F4/80^{+} CD11b^{+} represent the macrophage population, which was then analyzed for MHC class II expression.

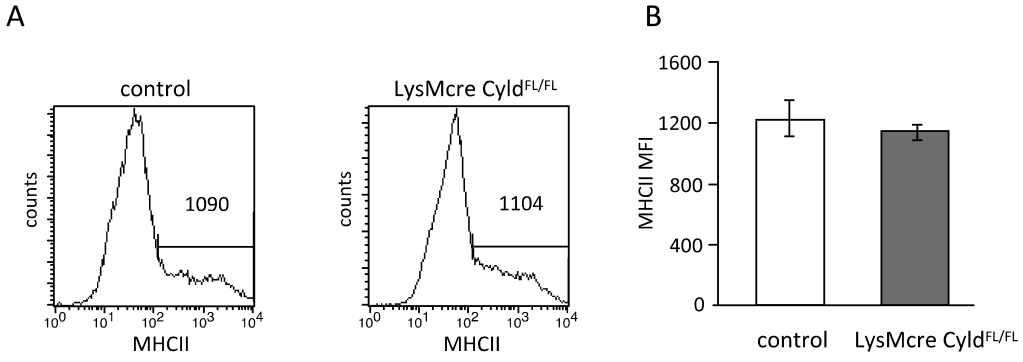

Figure 16 MHC class II mean fluorescence intensity on peritoneal macrophages
(A) MHC class II expression on FACS analyzed peritoneal macrophages from control and LysMcre Cyld$^{FL/FL}$mice pre-gated on CD11b^{+} F4/80^{+}. (B) Average expression levels of surface MHC class II on peritoneal macrophages. Values represent means of n>10 with SDs shown as error bars.

Resting macrophages are known to express low levels of MHC class II

surface molecules, which are induced by ingestion of microorganisms and recognition of their foreign molecular patterns. Once bound, microorganism are engulfed and degraded in endo- and lysosomes, generating peptides that can be presented by MHC class II molecules.

Comparison of peritoneal macrophages from LysMcre Cyld$^{FL/FL}$ and control littermate mice, however, showed no significant difference in expression of MHC class II molecules (Fig.16A and B), even when stimulated with LPS (data not shown).

Macrophage migration into the peritoneal cavity requires protease activity (e.g. MMP-9) for remodeling the extracellular matrix (Gong et al., 2008). In order to assess whether migratory potential of sCYLD overexpressing macrophages was impaired, we also analyzed whether there was a difference in macrophage influx into the peritoneal cavity upon Bio-Gel injection. Since peritoneal lavage often results in very different yields, infiltrating macrophages were quantified by comparison to a population that is assumed to remain constant after Bio-Gel injection, i.e. peritoneum resident B-1 cells. Although a difference in numbers of infiltrating macrophages was detectable, the result was not significant (Fig.17).

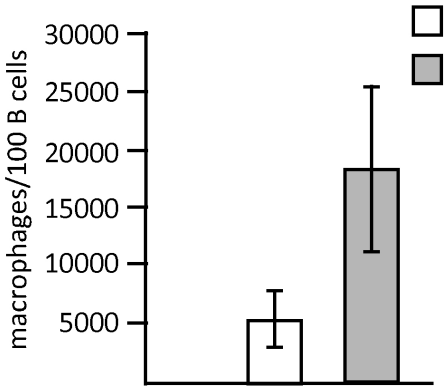

Figure 17 LysMcre Cyld$^{FL/FL}$ macrophages exhibit no migratory defect
Bio-Gel elicited peritoneal macrophages from control and LysMcre Cyld$^{FL/FL}$ mice were quantified relatively to the number of B cells in the peritoneal cavity. Values represent means of triplicates with SDs shown as error bars.

4.1.2.2 Analysis of bone marrow derived macrophages (BMDMs)

Another method to examine the functional capacity of macrophages under different external stimulation conditions is the generation of BMDMs (Zhang 2008 Current protocols in Immunology). Virtually all of the cells in this population of macrophages have the ability to respond to exogenous stimuli, and, therefore, relatively uniform populations of macrophages can be generated and harvested for analysis.

4.1.2.3 MHC class II and CD86 surface expression on LysMcre Cyld$^{FL/FL}$ BMDMs

MHC class II and CD86 are two prominent surface markers which are upregulated after macrophage activation. To assess whether there was a difference in expression levels, BMDMs from control and LysMcre Cyld$^{FL/FL}$ mice were prepared as described in the materials and methods section. They were then either left unstimulated or were stimulated with 100 ng/ml LPS for 12 hours.

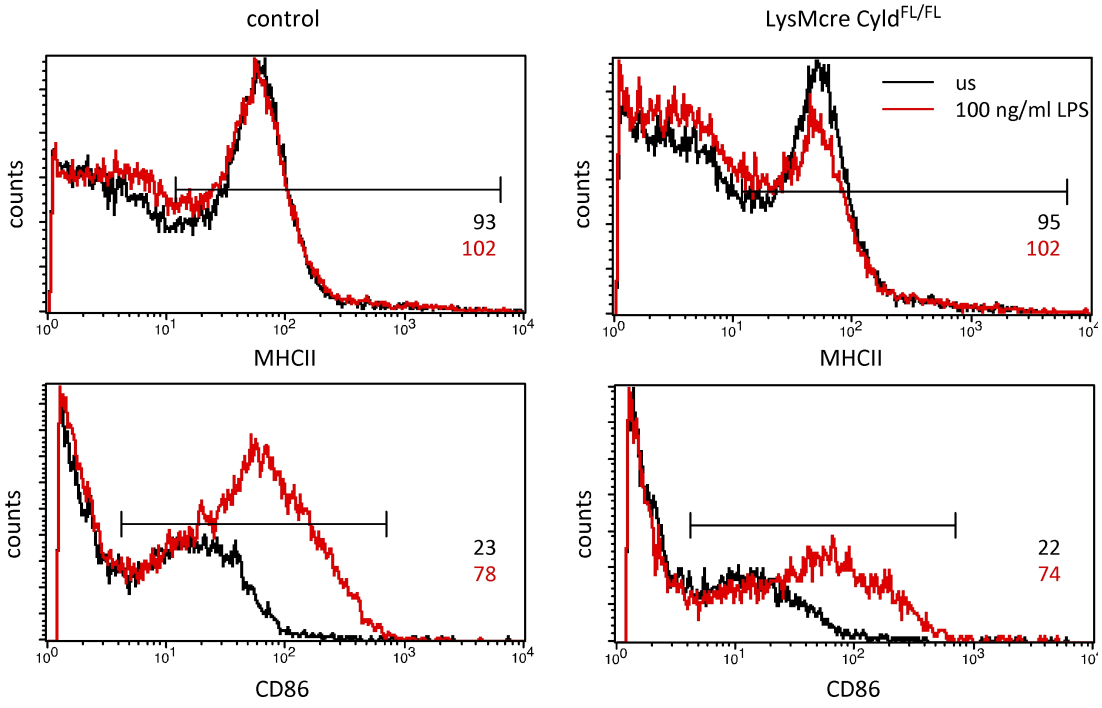

Figure 18 FACS analysis of MHC II and CD86 surface expression on BMDMs
BMDMs from control and LysMcre Cyld$^{FL/FL}$ mice were either left untreated or were stimulated with 100 ng/ml LPS. F4/80^{+} CD11b^{+} cells were analyzed for MHC class II expression.

Stimulating TLR4 on macrophages with LPS was not sufficient for proper upregulation of MHC class II expression. Although a minor enhancement of expression could be detected, there was no difference between LysMcre Cyld$^{FL/FL}$ mice and their respective control littermates (Fig.18 top). As to the expression of the co-stimulatory molecule CD86, the stimulation with LPS led to a clear upregulation. But also for this marker there was no detectable difference in expression (Fig.18 bottom). It could have been advantageous to stimulate the macrophages with a combination of LPS and IFNγ to evoke full activation.

4.1.2.4 Measurement of IL-6 secretion in LysMcre Cyld$^{FL/FL}$ macrophages

Macrophages release a variety of cytokines and chemokines upon interaction with pathogens. These molecules set up a state of inflammation and recruit neutrophils and plasma proteins to the site of an infection. Among the cytokines secreted by macrophages are: IL-1β, IL-6, TNFα and IL-12. IL-6 is known to be quickly upregulated upon macrophage activation. Therefore, IL-6 secretion of macrophages from LysMcre Cyld$^{FL/FL}$ mice was measured and compared to that of control macrophages.

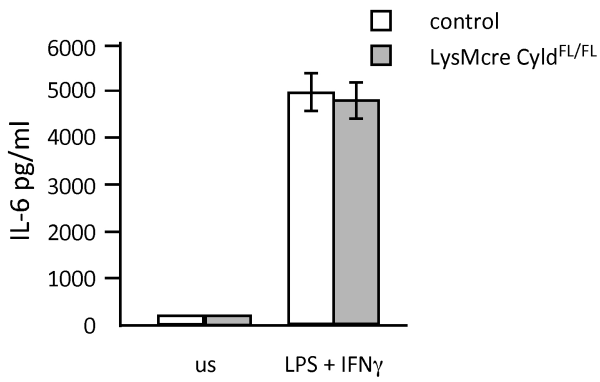

Figure 19 IL-6 ELISA from LysMcre Cyld$^{FL/FL}$ and control macrophages
BMDMs of the two different genotypes were differentiated in the presence of M-CSF (see materials and methods section) and stimulated with 150U/ml IFNγ for 6 hrs and then with 100 ng/ml LPS for another 12 hrs. Cytokine secretion was measured by ELISA (BD Bioscience). Values shown are means of triplicates with SDs.

Upon activation with IFNγ and LPS BMDMs are rendered 'classically activated'. Classically activated macrophages are important immune effector cells that are vital to host defense; they can also propagate inflammatory responses. They are formed in response to a combination of two signals. The first signal is often called a "priming" step, and the best primer of macrophages is IFNγ. IFNγ can be produced by innate immune cells such as natural killer (NK) cells, but a sustained high level of IFNγ usually requires the activation of Th1 cells during cell-mediated immunity. The second stimulus is typically a ligand for one of the Toll-like receptors. These ligands are expressed on microbial organisms and have been termed pattern associated molecular patterns (PAMPs).

Supernatants form classically activated BMDMs from LysMcre Cyld$^{FL/FL}$ and control macrophages were analyzed for IL-6 content by ELISA. Comparing supernatants of unstimulated versus stimulated cells showed, that stimulation was efficient (Fig.19), but there was no difference in IL-6 output between LysMcre Cyld$^{FL/FL}$ and control macrophages.

4.1.2.5 iNOS (inducible nitric oxide synthase) expression in LysMcre Cyld$^{FL/FL}$ macrophages

iNOS is an enzyme which catalyzes the chemical reaction from arginine to citrullin and nitric oxide. Nitric oxide is toxic and helps to kill organisms engulfed by macrophages. It is upregulated upon macrophage activation.

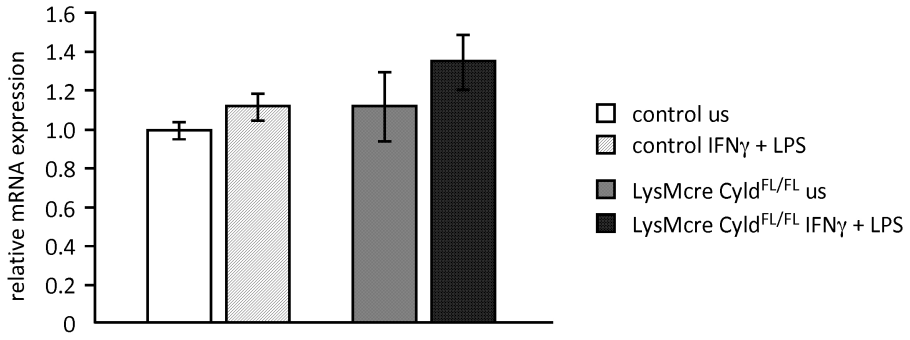

Figure 20 iNOS expression in control and LysMcre Cyld$^{FL/FL}$ macrophages
iNOS levels in macrophages (unstimulated vs. IFNγ [150U/ml]+ LPS [100 ng/ml] stimulation) were assessed by qRT-PCR. mRNA levels were normalized to HPRT expression and expressed as fold change. Values represent means of triplicates with SDs shown as error bars.

Macrophages from control and LysMcre Cyld$^{FL/FL}$ mice were activated with IFNγ [150U/ml] and LPS [100 ng/ml] (see preceding section), total RNA was isolated and reverse transcribed into cDNA, which was then subjected to qRT-PCR using iNOS specific primer and HPRT as a control.
Analysis revealed that there was only a slight increase in iNOS expression after activation and although levels were higher in stimulated LysMcre Cyld$^{FL/FL}$ macrophages compared to their control counterparts, this difference was not significant (Fig.20).

4.1.2.6 Increased EAE severity in LysMcre Cyld$^{FL/FL}$ mice

Experimental autoimmune encephalomyelitis (EAE) is an animal model for multiple sclerosis (MS), which is an autoimmune chronic inflammatory disease of the central nervous system (CNS). Demyelination, perivascular lesions and axonal damage are important factors in MS pathogenesis and disease progression.
Activated macrophages (and microglia cells) are the obvious suspects responsible for mediating this pathology, as macrophages are the dominant effector cell population responsible for acute clinical disease in EAE.

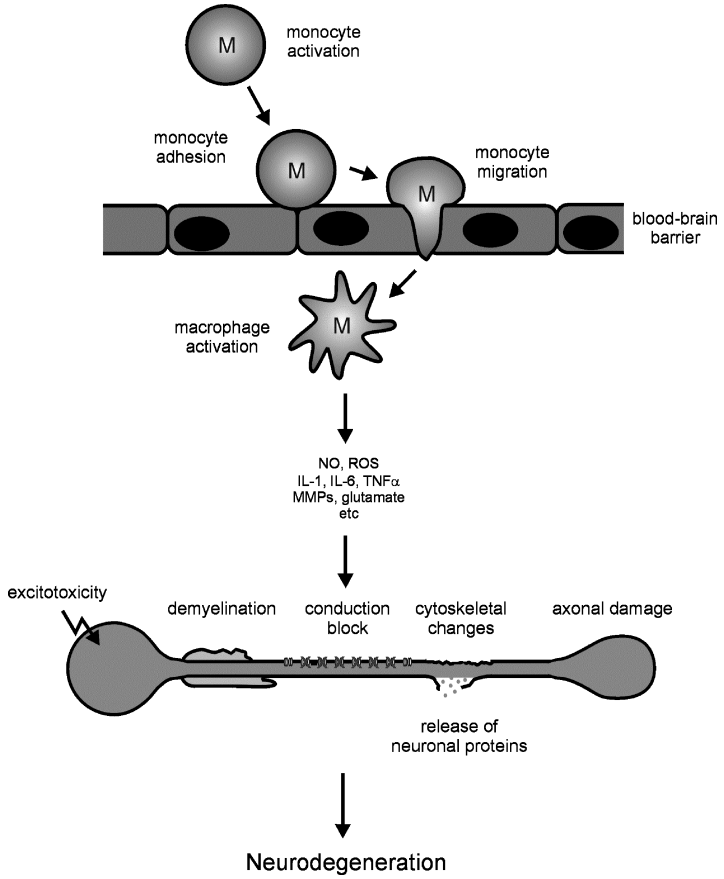

Figure 21 Schematic model of various stages of monocyte/macrophage contribution to the inflammatory process and to neuronal damage in MS and EAE (from (Hendriks et al., 2005))
Activated monocytes migrate through the blood-brain barrier and transform into activated macrophages which secrete free radicals such as NO (nitric oxide) and ROS (reactive oxygen species), inflammatory cytokines like IL-1, IL-6 and TNFα as well as MMPs (matrix metalloproteases) and glutamate, which in excess causes excitotoxicity in neurons resulting in cell death. All the mentioned factors cause damage to neurons and finally lead to neurodegeneration.

The number of macrophages infiltrating the CNS correlates broadly with disease severity (Berger et al., 1997; Heppner et al., 2005; McQualter et al., 2001). Macrophages also associate with dystrophic axons in both EAE and MS (Ferguson et al., 1997; Kornek et al., 2001). Activated macrophages and microglia both produce a large number of deleterious soluble factors, which can induce functional blockade and/or structural damage in axons *in vitro*. Nitric oxide, possibly in combination with reactive oxygen species, is one important candidate (Redford et al., 1997). The role of macrophages in EAE is shortly depicted in Figure 21. Because of this prominent role of macrophages and microglia in disease development and progression, EAE was induced in LysMcre Cyld$^{FL/FL}$ and respective control mice.

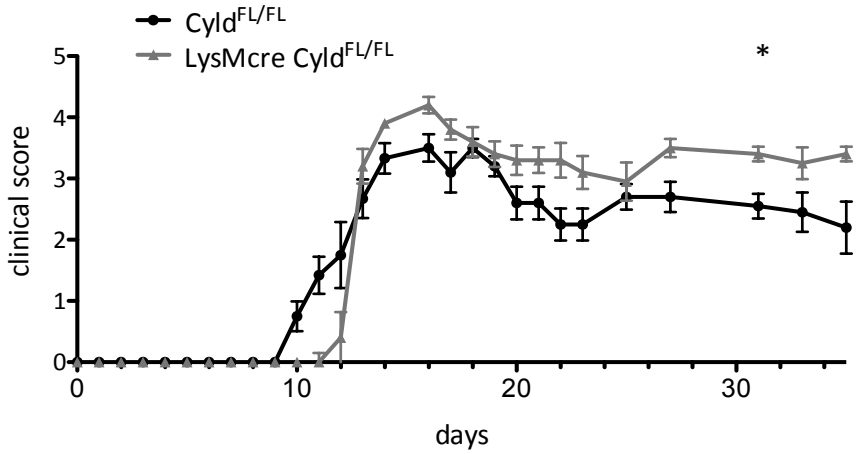

Figure 22 EAE progression and score
LysMcre Cyld$^{FL/FL}$ (grey line) mice suffer form more severe EAE than control littermates (black line). Values represent mean (± SD) clinical scores. Shown is one representative of three individual experiments (n ≥ 6 mice/group).

Figure 22 is representative of three individual EAE experiments, which all showed the same result, i.e. the course of disease (looking at the clinical score) was always more severe in LysMcre Cyld$^{FL/FL}$ than in control mice. In addition LysMcre Cyld$^{FL/FL}$ mice did neither recover as fast nor as much as control littermates.

This led us to analyze CNS infiltrating cells (specifically lymphocytes and macrophages) and CNS resident cells (microglia). To this end, EAE was induced in LysMcre Cyld$^{FL/FL}$ mice and control littermates as described in the materials and methods section. On the peak of disease (around day 12 post induction) mice were sacrificed and brains and spinal cords were isolated. Cells were extracted after homogenization and gradient purification and subjected to FACS analysis after staining for the markers CD11b and CD45.2.

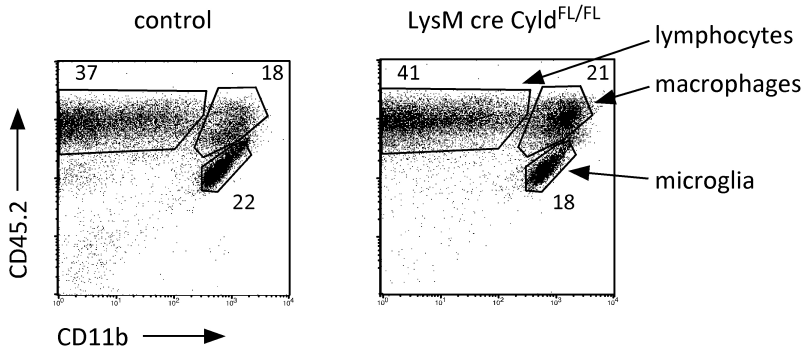

Figure 23 FACS analysis of CNS infiltrating and resident cells on day 12 post EAE induction from LysMcre Cyld$^{FL/FL}$ and control littermates
Homogenized CNS (brain and spinal cord) was subjected to Percoll gradient purification and cells were stained with antibodies against the markers CD11b and CD45.2 which allow the separation of the three distinct populations: lymphocytes (CD45.2^{+}CD11b^{-}), macrophages (CD45.2^{+}CD11b^{hi}) and microglia (CD45.2^{low} CD11b^{+}). Shown dot plots are representative of 4 individual mice per group.

Since disease severity is reflected in increased number of infiltrating lymphocytes and macrophages, it was anticipated that LysMcre Cyld$^{FL/FL}$ mice would show higher numbers of CNS-infiltrating cells.
Surprisingly, percentage values of cellular infiltrates between LysMcre Cyld$^{FL/FL}$ mice and control littermates were comparable (Fig.23). Looking at absolute numbers of infiltrating cells further supported this observation (Fig.24A). Experimental setup (n>4 mice/group) allowed the conclusion that there was no significant difference in numbers of CNS-infiltrating cells.

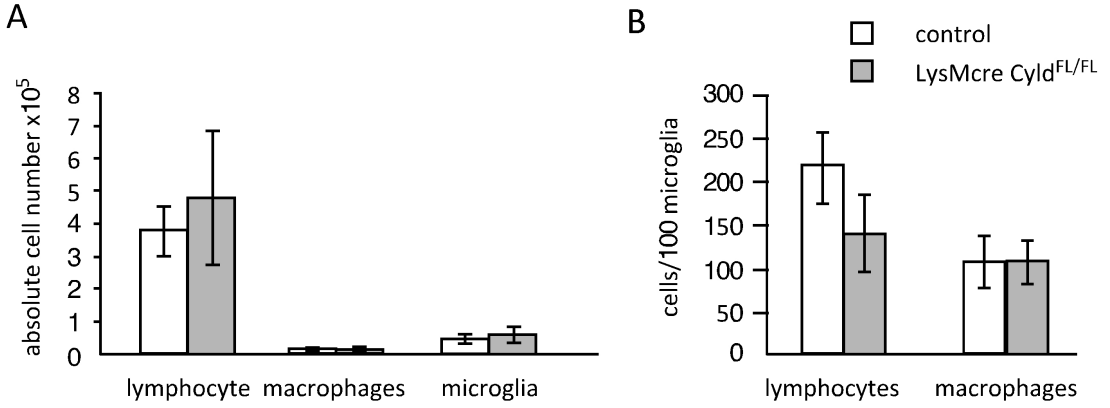

Figure 24 Graphical quantification of CNS resident cells after EAE induction
(A) Graph showing absolute numbers of CNS-infiltrating and resident cells on day 12 post EAE induction from LysMcre Cyld$^{FL/FL}$ and control littermates. Values represent means of quadruplicates with SDs. (B) Comparison of cellular infiltrates into the CNS from LysMcre Cyld$^{FL/FL}$ and control littermate mice. Numbers of infiltrating cells were calculated per 100 microglia. Values represent means of quadruplicates with SDs.

Assuming that the total number of microglia in the CNS is constant data was re-evaluated accordingly, so that numbers of infiltrating lymphocytes and macrophages were normalized to microglia numbers (Fig.24B).
At that point, MHC class II expression levels were compared, since MHC class II is upregulated on activated macrophages and microglia (Hayes et al., 1987; Matsumoto et al., 1986). A difference in terms of expression levels could be part of an explanation for the observed difference in EAE progression between control and LysMcre Cyld$^{FL/FL}$ mice.

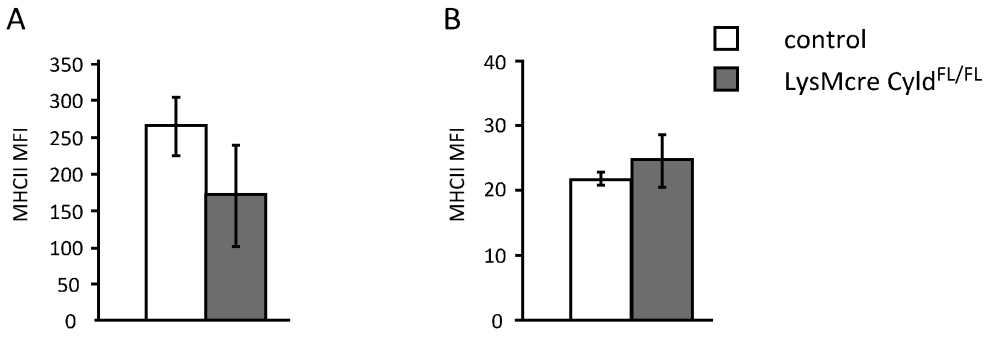

Figure 25 MHC class II expression on macrophages and microglia of control and LysMcre Cyld$^{FL/FL}$ mice
(A) MHC class II expression on CNS-infiltrating macrophages (B) MHC class II expression on CNS resident microglia. Values are representative of n=5 (±SD).

As expected microglia only expressed very low levels of MHC class II compared to infiltrating macrophages, but the analysis of MHC class II expression on macrophages and microglia revealed no difference (Fig.25A and B respectively) between control and LysMcre Cyld$^{FL/FL}$ mice.

4.2 Impact of cell-type specific Bcl-3 overexpression on dendritic cells

After Bcl-3 was identified as a target of CYLD and major regulator of NF-κB activity in B cells and dendritic cells (Hovelmeyer et al., 2007; Srokowski et al., 2009), we sought to investigate whether cell type-specific overexpression of Bcl-3 would be sufficient to cause a phenotype that resembled that of CYLD$^{ex7/8}$ DCs. To achieve this, the ROSA-CAGs-STOP-Bcl-3-EGFP strain (kindly provided by Dr. Marcus Wörns) was crossed to the CD11c-Cre strain (Caton et al., 2007), to obtain mice that specifically overexpressed Bcl-3 in CD11c^{+} cells, i.e. mainly dendritic cells.

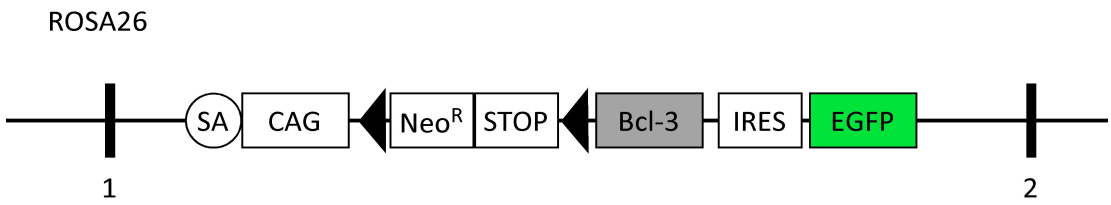

Figure 26 ROSA-CAGs-STOP-Bcl-3 EGFP schematic
Cre-mediated excision of the loxP (black rectangles) flanked Neo^{R}-STOP cassette, which is located between exon 1 and 2 of the genomic ROSA locus, leads to the CAG promoter-driven co-expression of Bcl-3 and EGFP. CAG: CMV early enhancer/chicken β actin promoter, Neo^{R}: Neomycin resistance, IRES: internal ribosome entry site, EGFP: enhanced green fluorescence protein.

Using the ROSA-CAGs-STOP-EGFP plasmid into which a PCR-amplified Bcl-3 open reading frame (ORF) had been inserted allowed the generation of the ROSA-CAGs-STOP-Bcl-3-EGFP strain. In these mice, the Bcl-3 ORF is located downstream of the CAG promoter and a loxP-flanked STOP cassette and upstream of an IRES-EGFP element, so that Cre-mediated excision leads to the cell type-specific co-expression of Bcl-3 and EGFP (Fig. 26).

4.2.1 BMDCs from CD11c-Cre Bcl-3 mice overexpress Bcl-3

Since it is widely accepted that Bcl-3 is subject to quick degradation depending on cell type and cell activation status, the overexpression was to be determined on protein levels. Analysis of mRNA expression levels in this case could have been misleading, because an observed difference must not necessarily translate to comparable changes in protein expression. BMDCs were generated and cultured as previously described and nuclear lysates were prepared. BMDCs from CD11c-Cre Bcl-3 mice showed a weak yet significant increase in Bcl-3 expression when compared to control (CD11c-Cre negative) littermates.

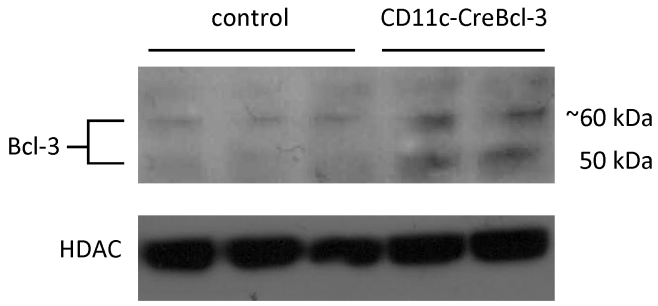

Figure 27 BMDCs from CD11c-Cre Bcl-3 mice overexpress Bcl-3
BMDCs nuclear cell lysates from CD11c-Cre Bcl-3 mice and control littermates were subjected to western blotting and Bcl-3 (~ 50-60 kDa) was detected by using an anti-Bcl-3 antibody. HDAC (62 kDa) was used as a loading control.

The protein Bcl-3 is also a target of post-translational modifications such as phosphorylation and ubiquitination, which explains the double band apparent in the western blot in Figure 27. The upper band most likely represents the multi-phosphorylated form of Bcl-3, whereas the lower band is the unmodified Bcl-3. To assess whether this overexpression of Bcl-3 caused changes in NF-κB activity similar to that observed in the BMDCs from CYLD$^{ex7/8}$ mice, lysates from CD11c-Cre Bcl-3 BMDCs were submitted to western blotting. The NF-κB subunit p105 and its active processed form p50 were detected by an appropriate antibody.

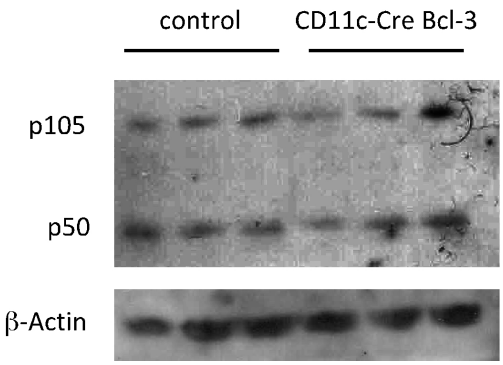

Figure 28 Expression of the NF-κB subunit p105 and its processed form p50
BMDCs whole cell lysates from CD11c-Cre Bcl-3 mice and control littermates were subjected to western blotting and p105 (105 kDa) and p50 (50 kDa) were detected by using an anti-p105/p50 antibody. β-Actin (42 kDa) was used as a loading control.

Unlike the BMDCs from CYLD$^{ex7/8}$ mice, the BMDCs from CD11c-Cre Bcl-3 mice did neither overexpress the subunit p105 (Fig. 28) nor its processed form p50. This phenotype was not influenced by stimulation with LPS (data not shown).

4.2.2 Expression of activation markers on CD11c-Cre Bcl-3 BMDCs

Even though BMDCs from CD11c-Cre Bcl-3 mice did not show an increase in p50 expression levels (as observed in the CYLD$^{ex7/8}$ BMDCs), we sought to investigate whether the higher levels of Bcl-3 were sufficient for upregulation of dendritic cell activation markers.
FACS analysis of BMDCs revealed that there was no difference in the expression of MHC class II and CD86 when comparing unstimulated or stimulated CD11c-Cre Bcl-3 BMDCs to control littermate BMDCs (Fig. 29A). Although differences in mean fluorescence intensity (MFI) were detectable, they were never significant (Fig. 29B), when larger groups from different experiments with the same setup were compared.

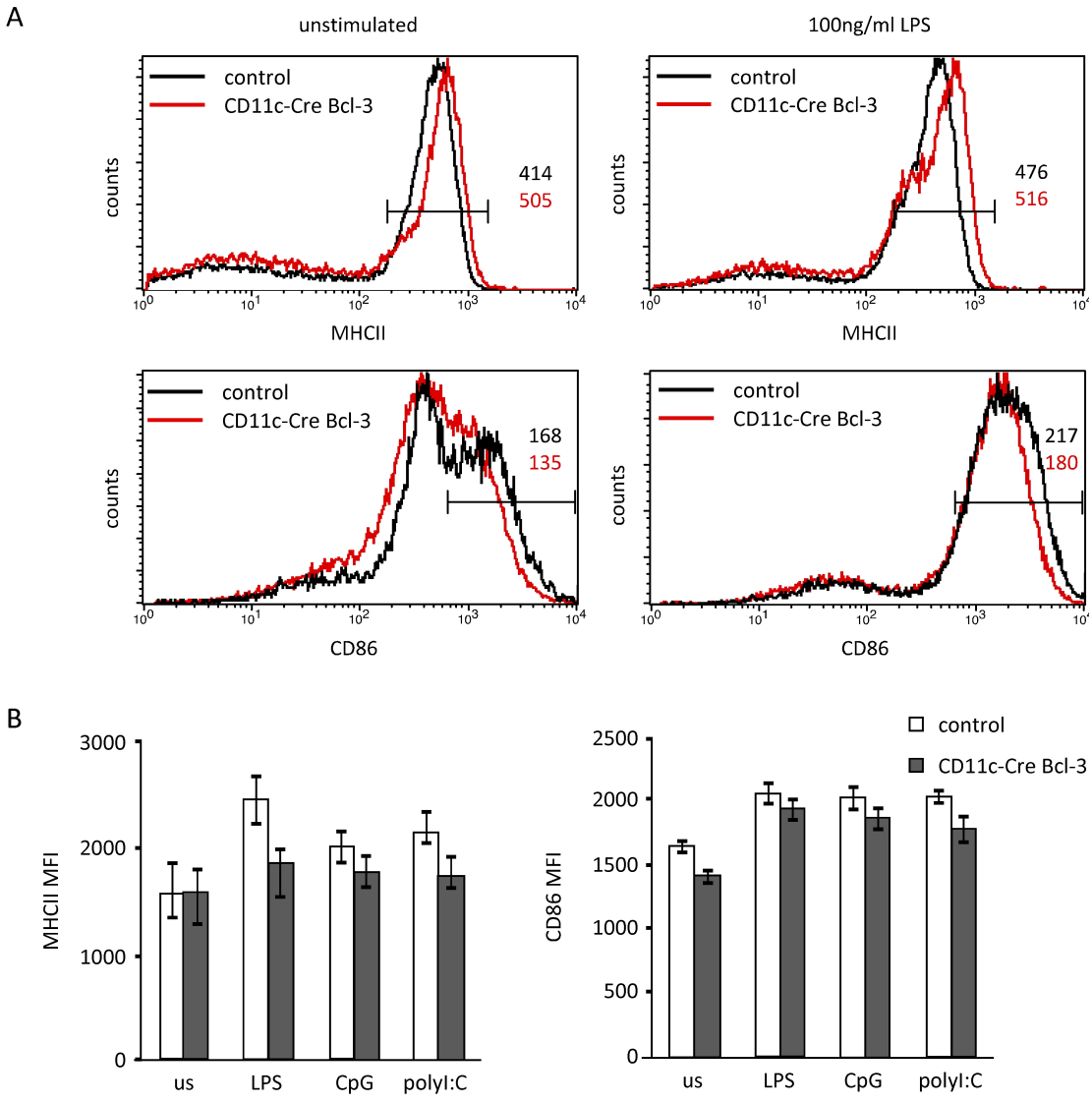

Figure 29 Expression levels of activation markers on WT, CYLD$^{ex7/8}$ and CYLD^{ko} BMDCs
(A) BMDCs from WT, CYLD^{ko}, and CYLD$^{ex7/8}$ mice were differentiated with GM-CSF for 6 days in culture and stimulated (100 ng/ml LPS, 12 hours) and submitted to fluorescence-activated cell sorting. FACS histograms of the CD11c^{+} population show cell surface expression of MHC II (top) and CD86 (bottom). (B) BMDCs from WT, CYLD^{ko}, and CYLD$^{ex7/8}$ mice were differentiated with GM-CSF for 6 days in culture and stimulated (100 ng/ml LPS or 100 nM CpG or 50 µg/ml polyI:C for 12 hours) Graphical representation of mean fluorescence intensity (MFI) values of indicated cell surface expression markers. Values are representative of ten BMDCs preparations with triplicates and SDs shown as error bars.

4.2.3 BMDCs from CD11c-Cre Bcl-3 mice do not show increased levels of inflammatory cytokines

As previously shown for CYLD$^{ex7/8}$ BMDCs, another hallmark of dendritic cell activation is the secretion of inflammatory cytokines. BMDCs were either left untreated or were stimulated with LPS (TLR4 ligand, produced by Gram-negative bacteria), CpG (TLR9 ligand, unmethylated sequence found in

bacterial genomes and viral DNA) or polyI:C (TLR3 ligand, synthetic analog of viral dsRNA) for 12 hrs. Supernatants were collected and cytokine levels of IL-6 and TNFα were assessed by ELISA.

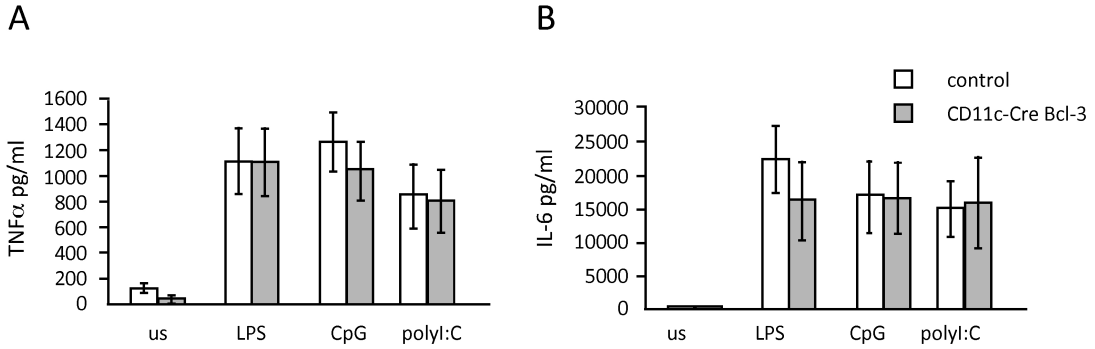

Figure 30 Secretion of inflammatory cytokines by control and CD11c-Cre Bcl-3 BMDCs
Supernatants from unstimulated BMDCs or BMDCs stimulated with 100 ng/ml LPS or 100 nM CpG or 50 µg/ml polyI:C for 12 hrs measured for TNFα (A) and IL-6 (B) cytokines. Values shown are means of triplicates with SDs shown as error bars.

BMDCs from CD11c-Cre Bcl-3 mice did not secrete higher levels of the inflammatory cytokines TNFα or IL-6 than their respective controls (Fig. 30A and B). Stimulation with different TLR ligands i.e. LPS (TLR4 ligand, produced by Gram-negative bacteria), CpG (TLR9 ligand, unmethylated sequence found in bacterial genomes and viral DNA) or polyI:C (TLR3 ligand, synthetic analog of viral dsRNA) for 12 hrs did not cause any changes in cytokine secretion.

4.2.4 Analyzing the stimulatory capacity of CD11c-Cre Bcl-3 BMDCs

After making the observation that the overexpression of Bcl-3 did not cause an upregulation of surface activation markers (CD86, MHCII) or an increase in cytokine secretion (IL-6, TNFα), it was still to be assessed if the stimulatory function of these BMDCs also remained unaltered by the enhanced expression of Bcl-3.
Among the main functions of dendritic cells is the presentation of antigens (either on MHC class I or II, depending on antigen) to T cells and their subsequent activation via the co-stimulatory receptors CD80 and CD86. T lymphocytes, which have the T cell receptor (TCR) that recognizes the antigen presented by the antigen presenting cells, proliferate vigorously to mount a strong immune response.
Since it is an absolute requirement that the TCR recognizes the antigen presented, we utilized the following experimental setup: BMDCs from CD11c-

Cre Bcl-3 or control littermates (CD11c-Cre negative) were cultured for 6 days in medium supplied with GM-CSF (see materials and method section) and stimulated over night (i.e. for 12 hrs) with 100 ng/ml LPS. These APCs were then co-cultured with MACS-purified $CD4^+$ 2D2 TCR transgenic T cells in medium containing various concentrations of MOG_{35-55} peptide (0, 1, 5, 10 µg/ml). The 2D2 TCR tg mice, which were used in this experiment express a TCR specific for MOG_{35-55} in the context of $H2\text{-}A^b$ of the C57BL/6 genetic background (Bettelli et al., 2006). Cells were harvested 4 days later and CFSE-labeled T cells were analyzed by FACS. Cells that have not proliferated should contain more CFSE dye than cells, which have undergone proliferation, since the CFSE is diluted in the cytoplasm with every cell division.

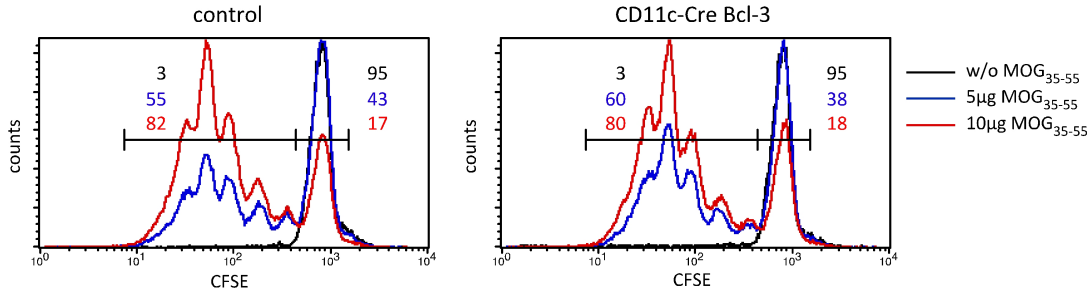

Figure 31 Bcl-3 overexpression of Bcl-3 does not enhance the stimulatory capacity of dendritic cells
FACS analysis of CFSE labeled $CD4^+$ 2D2 TCR transgenic T cells (gated on $CD4^+$ $Vb11^+$) co-cultured with either mature control or CD11c-Cre Bcl-3 BMDCs for 4 days in medium containing various concentrations of MOG_{35-55} peptide.

Analysis of transgenic T cells on day 4 revealed that it did not make a difference whether transgenic T cells were cultured with control or with Bcl-3 overexpressing BMDCs. They proliferated equally in response to presented antigen (Fig.31).

It can be concluded that Bcl-3 overexpression is not sufficient to confer increased stimulatory capacity to dendritic cells. These results are in accordance with the formerly detected normal ‘wild type-like’ levels of MHC class II and CD86 surface expression and the cytokine secretion.

4.3 Investigating the impact of Bcl-3 overexpression on T cell development and function

Due to our interest in the role of the IκB-like molecule Bcl-3 in the development and function in different cells of the murine immune system, the ROSA-CAGs-STOP-Bcl-3-EGFP strain was crossed to the CD4-Cre strain. In this model all T cells should overexpress Bcl-3.

Bcl-3 knockout mice are available and display several T cell phenotypes. It has been shown that Bcl-3 knockout mice show an impaired Th1 response to infection with the intracellular parasite *Toxoplasma gondii* (Franzoso et al., 1997). Others report defects in GATA-3 expression in the absence of Bcl-3, causing abnormal Th2 differentiation (Corn et al., 2005).

Overexpression of Bcl-3, however, has been reported to have no phenotype in thymocytes development when driven by the Lck proximal promoter, which is active in the thymic cortex (Caamano et al., 1996). Transgenic overexpression of Bcl-3, using the human CD2 promoter, slowed down T cell activation in T cell responses to antigen *in vitro* and *in vivo* (Bassetti et al., 2009). McKeithan and colleagues (Ge et al., 2003) could show that Bcl-3 was the gene with the highest transcriptional response in T cells to adjuvant administration *in vivo*. All these findings point to a crucial role of Bcl-3 in T cell development and function. The CD4-Cre ROSA-CAGs-STOP-Bcl-3-EGFP strain (from now on termed CD4-Cre Bcl-3) is a valuable tool, which allows the study of Bcl-3 in the context of T lymphocyte development and function. Bcl-3 overexpression will be confined to T cells, driven by a murine T cell specific promoter. Since Bcl-3 detection after immunoblotting is difficult, due to the lack of good antibodies, Bcl-3 mRNA expression in T cells from CD4-Cre Bcl-3 mice was assessed by quantitative real-time PCR (Fig. 32).

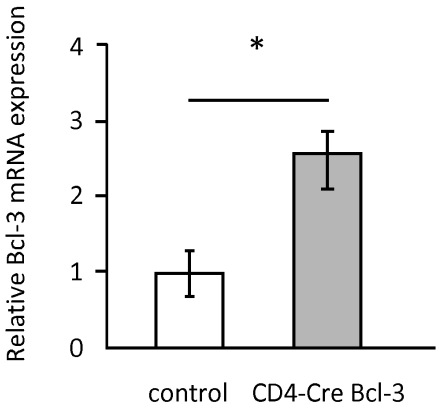

Figure 32 Quantification of Bcl.3 mRNA levels in T cells from CD4-Cre Bcl-3 mice and littermate controls
mRNA levels were normalized by HPRT levels and expressed as fold change. Values represent means of n>3 with SDs.

4.3.1 CD4-Cre Bcl-3 mice develop spontaneous colitis

Shortly after breeding the CD4 transgene to the ROSA-CAGs-STOP-Bcl-3-EGFP mice, we noticed that mice often suffered from severe diarrhea and rectal prolapse. In addition, CD4-Cre Bcl-3 mice that were sacrificed displayed thicker, shorter and very opaque colons compared to control littermates (Fig.33). Mice were endoscopied and found to be suffering from a colitis-like phenotype. Colitis is assessed by scoring mice for five different colitis hallmarks, which are: granularity, translucency and vascularity of the colon as well as the presence of fibrin and the texture of the stool.
Different T cell subsets were shown to play major roles in colitis onset and development (Kaser et al., 2010), which is why we commenced to analyze the different T cell subsets in the CD4-Cre Bcl-3 mice.

Figure 33 CD4-Cre Bcl-3 mice suffer from a colitis-like phenotype
Colons from CD4-Cre Bcl-3 mice and control littermates were removed and cut above the cecum (arrowheads). The control healthy colon (left) is longer, thinner and more translucent than the colon from the CD4-Cre Bcl-3 mouse (right). Blood vessels on the colon of the sick mouse were significantly enlarged.

4.3.2 *Ex vivo* analysis of thymocytes and the peripheral T cell pool

Crossing the ROSA-CAGs-STOP-Bcl-3-EGFP with CD4-Cre–expressing mice generated a T cell repertoire, in which both $CD4^+$ and $CD8^+$ T cells excise the STOP cassette and express the EGFP reporter. Given the early activity of the CD4-Cre transgene, we sought to determine whether early Bcl-3 expression in the thymus would effect thymocyte differentiation. Moreover, $CD4^+$ and $CD8^+$ T cell populations were also looked at in the peripheral lymphoid organs, such as spleen, lymph nodes (LN) and mesenteric lymph nodes (mLN) (Fig. 34).

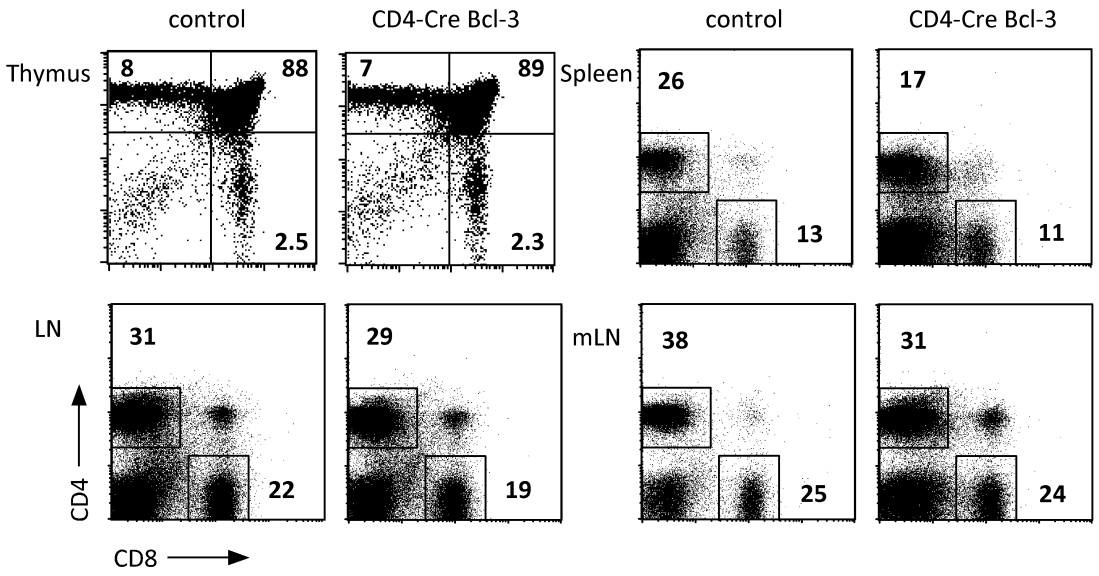

Figure 34 CD4$^+$ and CD8$^+$ T cell populations in the thymus and peripheral lymphoid organs
Organs from CD4-Cre Bcl-3 and control littermates were isolated and single cell suspensions were prepared. All samples were stained for CD4 and CD8 co-receptors. Percentages are depicted in dot plots. LN: lymph nodes, mLN: mesenteric lymph nodes

CD4-Cre Bcl-3 and control littermate mice were sacrificed and cell suspensions from organs were subjected to antibody staining and FACS analysis. Similar to the results of Caamano et al. (Caamano et al., 1996), we could not detect any difference in CD4$^+$ vs. CD8$^+$ thymocytes populations in the thymus (Fig.34). A summary of three separate experiments is shown as a graph in Figure 35A. A phenomenon, which we could observe though and which repeated itself in all performed experiments, was a reduction in CD4$^+$ T cell numbers in the periphery (Fig.35B).

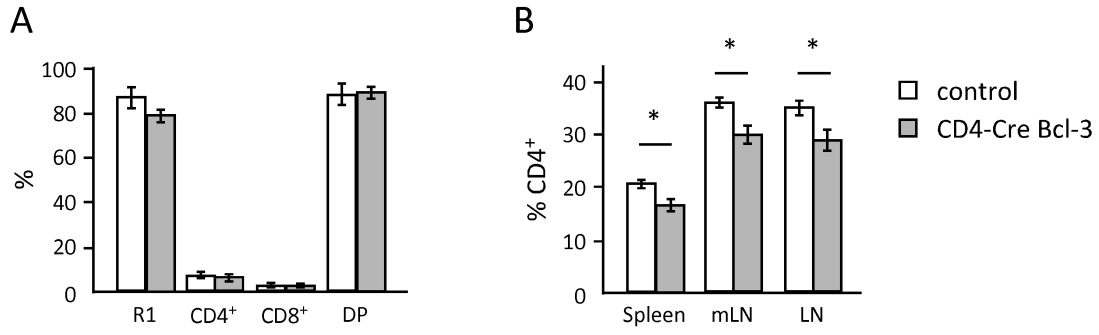

Figure 35 Statistical evaluation of single positive (SP) and double positive (DP) thymocyte percentages and CD4$^+$ T cells in the periphery
(A) R1 corresponds to the number of live cells in the FSC-SSC. Percentages represent mean values from 3 separate experiments (each n>3) with SDs. (B) Graph shows mean percentages of CD4$^+$ T cells in peripheral lymphoid organs (n>8) from CD4-Cre Bcl-3 and control littermate mice with SDs. *p < 0.05 using *t* test.

4.3.3 CD4-Cre Bcl-3 mice have less peripheral effector/memory T cells

Peripheral T lymphocytes can be divided into naïve and effector/memory T cells which can be identified by the differential expression of the two markers CD44 and CD62L. Naïve T cells are $CD44^{low}$ $CD62L^{high}$ whereas effector/memory T cells are $CD44^{high}$ $CD62L^{low}$. Naïve T cells have not encountered antigen and express high levels of CD62L (also known as L-Selectin), which guides their exit from the blood into peripheral lymphoid tissues. Upon antigen encounter they become effector cells, upregulate the activation marker CD44 and proliferate vigorously. The level of effector T cells then falls back to persist at a level significantly (100-1000-fold) above the initial frequency for the rest of the animal's life. These persistent T cells are designated memory T cells. Looking at peripheral CD8 as well as CD4 positive T cells we discovered that there was a significant decrease in $CD4^+$ effector/memory T cells in lymph nodes as well as mesenteric lymph nodes (Fig.36A). CD4-Cre Bcl-3 mice appeared to have more naïve T cells compared to control littermates (Fig.36B), but this increase was not significant.

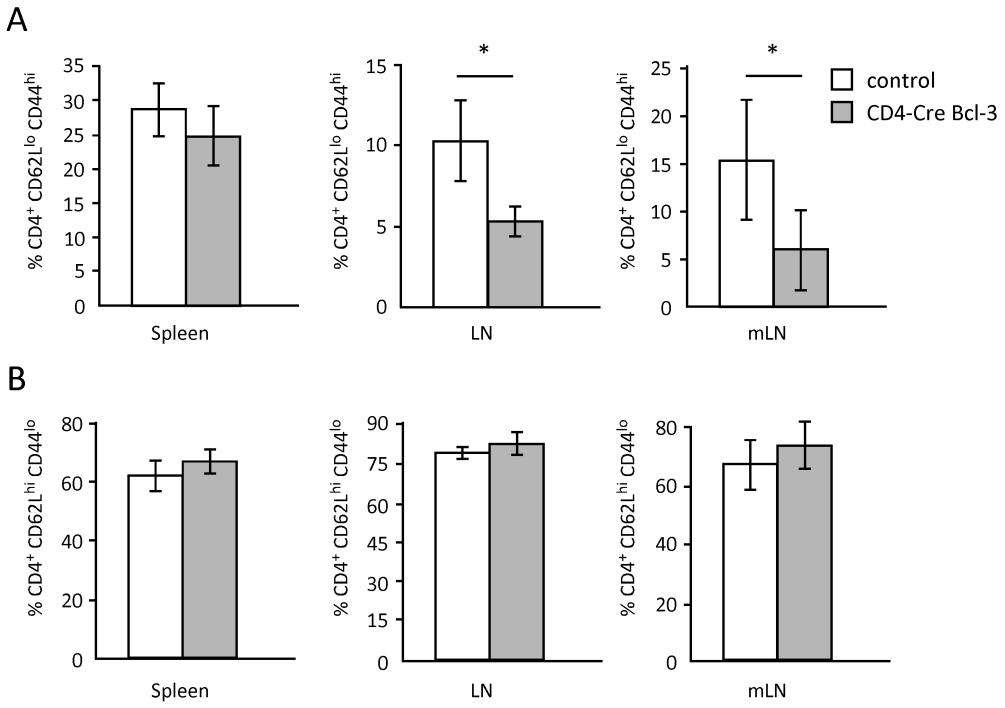

Figure 36 Statistical evaluation of peripheral $CD4^+$ effector/memory, i.e. $CD62L^{low}$ $CD44^{high}$ (A) and naïve, i.e. $CD62L^{high}$ $CD44^{low}$ (B) T cell populations
Spleens, lymph nodes (LN) and mesenteric lymph nodes (mLN) from CD4-Cre Bcl-3 and control littermates were isolated and single cell suspensions were prepared. All samples were stained for CD4, CD44 and CD62L. Values represent means of 4 with SDs *$p < 0.05$ using *t* test.

4.3.4 *Ex vivo* analysis of the Th1, Th17 and Treg subpopulations

Both Th1 and Th17 cells have been implicated in playing important roles in the induction of colitis. Certain types of inflammatory gut diseases are characterized by exaggerated IFNγ responses, as well as IL-23 and IL-17 responses reviewed in (Ahern et al., 2008). To address the question if Th1 and/or Th17 populations were altered in peripheral lymphoid organs of CD4-Cre Bcl-3 mice, single cell suspensions from spleen, lymph nodes and mesenteric lymph nodes were analyzed by FACS.

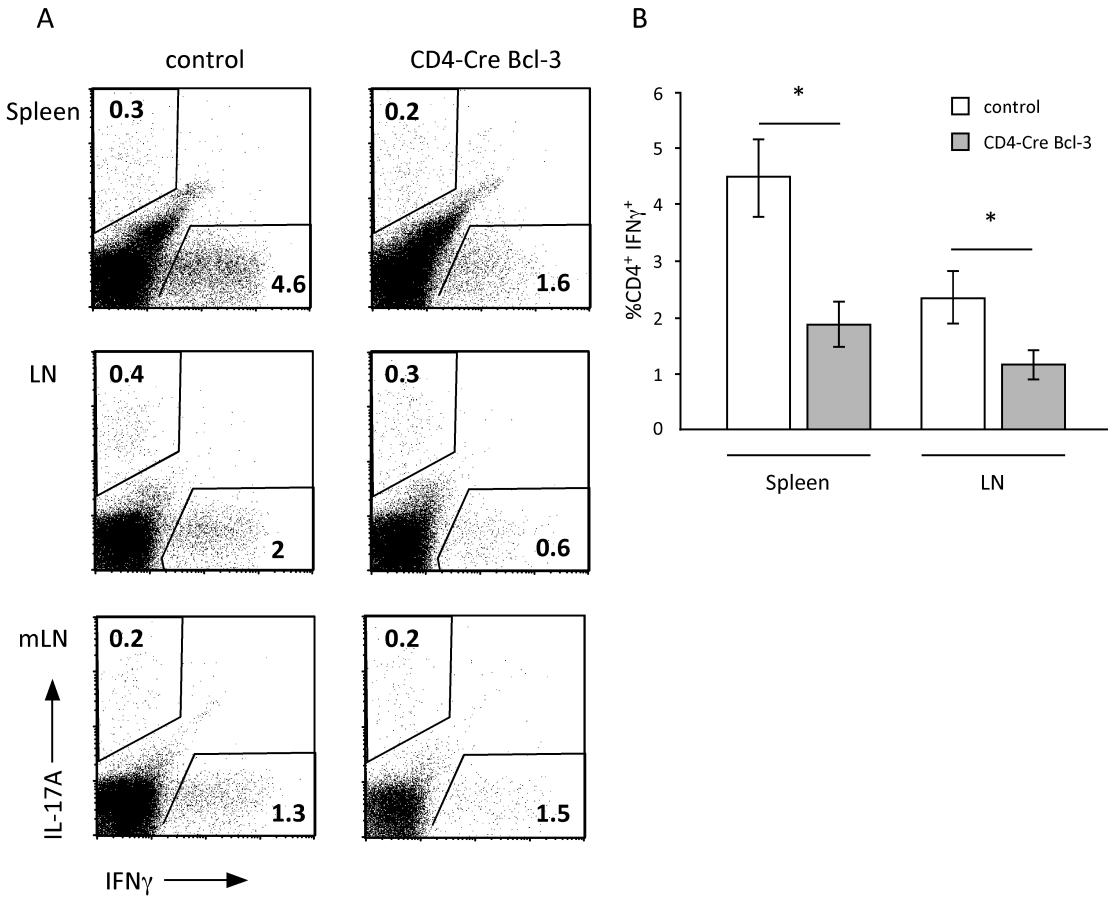

Figure 37 *Ex vivo* Th1 and Th17 T cells
Spleens, lymph nodes (LN) and mesenteric lymph nodes (mLN) from CD4-Cre Bcl-3 and control littermates were isolated and single cell suspensions were prepared. All samples were stained for CD4, IL-17A and IFNg and analyzed by FACS. (A) All shown dot plots have been pre-gated on $CD4^+$ cells. $CD4^+$ $IL\text{-}17A^+$ cells represent the Th17 population whereas $CD4^+$ $IFN\gamma^+$ cells represent the Th1 population. (B) Statistical summary of 4 separate experiments. Spleens and LN of CD4-Cre Bcl-3 mice contained significantly less $CD4^+$ $IFN\gamma^+$ T cells (i.e. Th1 cells) than those of control littermates. Values represent means of 4 with SDs. *$p < 0.05$ using *t* test.

FACS analysis of peripheral T cells revealed that CD4-Cre Bcl-3 mice had significantly reduced numbers of Th1 cells in spleens and lymph nodes (Fig.37 A, B), whereas the Th17 population did not seem to be affected.

Another subset of T cells, which has an ameliorating effect on colitis, is the regulatory T cell population (Tregs). An intimate relationship exists in the intestinal mucosa between pro-inflammatory Th17 cells and $CD4^+$ Tregs, which play an important role in controlling Th17 cell responses (reviewed in (Belkaid and Tarbell, 2009; Weaver and Hatton, 2009)). Tregs are characterized as $CD4^+$ $CD25^+$ cells that express the transcription factor Foxp3 and suppress the proliferation of effector T cells *in vitro* and protect against autoimmune and other inflammatory diseases in several animal models (reviewed in (Barnes and Powrie, 2009)). For example, mice carrying a loss-of-function mutation of Foxp3 completely lack Tregs and develop lethal autoimmune disease (Brunkow et al., 2001). Additionally, mice engineered to lack the expression of specific regulatory cytokines in T cells, including IL- 10 or TGFβ, develop colitis when pathogenic bacteria are present in the intestine (Moro et al., 2008; Podolsky et al., 1993; Xiao et al., 2008). These findings identify Tregs as an important regulatory cell type that contributes to intestinal and systemic immune homeostasis.

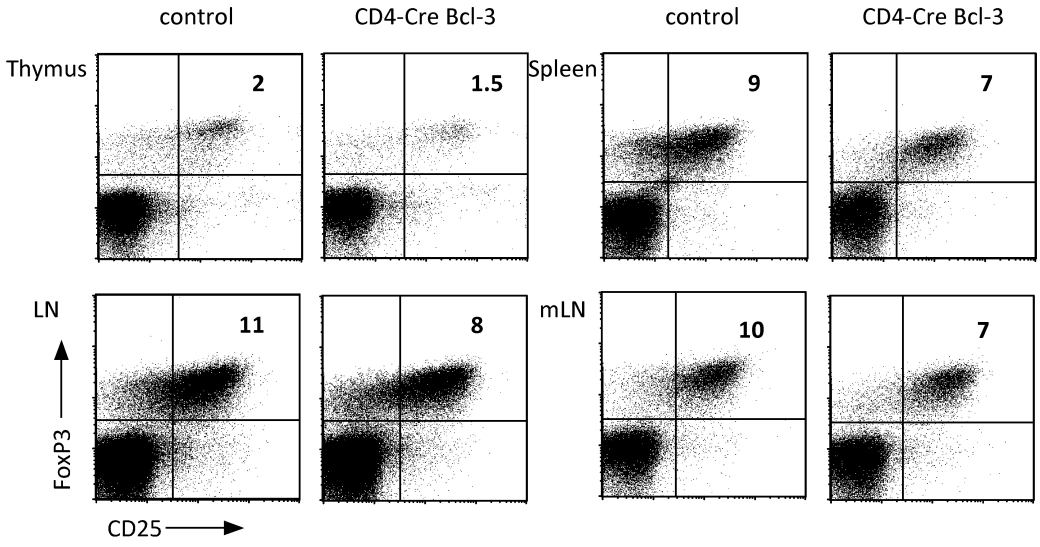

Figure 38 *Ex vivo* Tregs
Thymi, spleens, lymph nodes (LN) and mesenteric lymph nodes (mLN) from CD4-Cre Bcl-3 and control littermates were isolated and single cell suspensions were prepared. All samples were stained for CD4, CD25 and FoxP3 and analyzed by FACS. All shown dot plots have been pre-gated on $CD4^+$ cells. $CD4^+$ $CD25^+$ $FoxP3^+$ cells represent the regulatory T cell population.

Analyzing Treg populations in the thymus as well as the periphery of CD4-Cre Bcl-3 mice, we could conclude that although the population of $CD4^+$ $CD25^+$ $FoxP3^+$ T cells (Tregs) was reduced (Fig.38), this decrease did not reach significance when mice from separate and independent experiments were taken into consideration.

4.3.5 *In vitro* differentiation of naïve CD4$^+$ T cells from CD4-Cre Bcl-3 mice

Upon encountering foreign antigens presented by antigen-presenting cells (APCs), naïve CD4$^+$ T cells can differentiate into Th1, Th2, Th17, iTreg (induced Treg), and Tfh (follicular T helper) cells. These differentiation programs are controlled by cytokines produced by innate immune cells, such as IL-12 and IFNγ, which are important for Th1 cell differentiation, and IL-4, which is crucial for Th2 cell differentiation. TGFβ together with IL-6 induces Th17 cell differentiation, whereas iTreg differentiation is induced by TGFβ and IL-2. Tfh cell differentiation requires IL-21. Specific transcription factors that define the differentiation program of each T helper cell subset have been identified: T-bet for Th1 cells, GATA3 for Th2 cells, RORγt for Th17 cells, and Foxp3 for iTreg cells. Effector T cells had been thought to be terminally differentiated lineages, but it seems like there is a certain plasticity allowing for conversion to other phenotypes. Although Th1 and Th2 cells display more stable phenotypes, iTreg cells and Th17 cells can readily switch to other T helper cell types depending on cytokine conditions. For example, iTregs can become IL-17-producing cells upon stimulation with IL-6 and IL-21. Treg cells can also switch to Tfh cells, a process which requires B cells and CD40-CD40L interaction. Th17 cells may also convert into IFNγ-producing Th1 cells or IL-4-producing Th2 cells when stimulated with IL-12 or IL-4, respectively.

To test whether the capacity of naïve CD4$^+$ T cells to differentiate into a certain T helper cell lineage is influenced in the CD4-Cre Bcl-3 mice, *in vitro* differentiation experiments were conducted (Fig. 39).

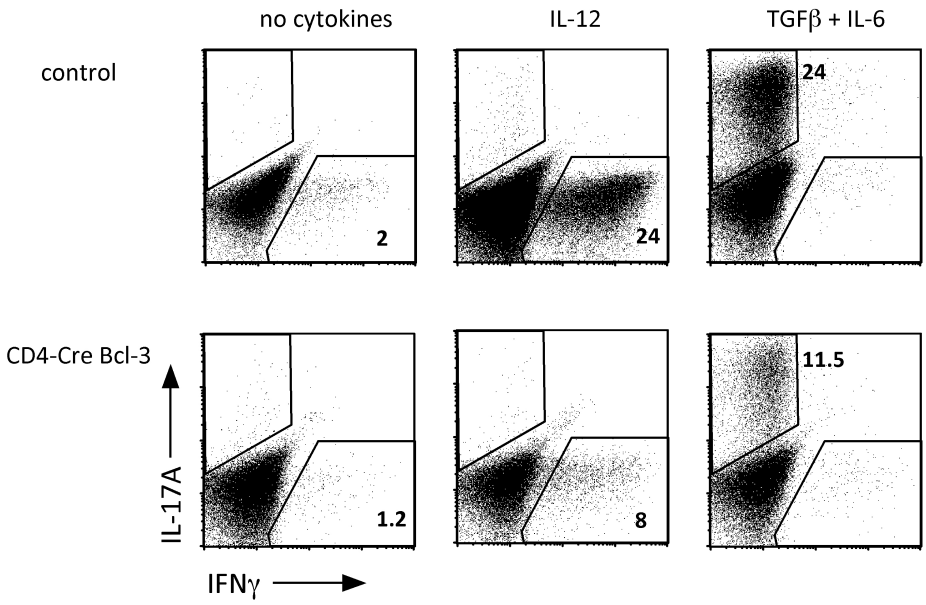

Figure 39 *In vitro* differentiation of naïve CD4$^+$ T cells
MACS-purified CD4$^+$ CD62L$^+$ T cells from spleens and lymph nodes from CD4-Cre Bcl-3 and control littermates were isolated. Cells were subsequently subjected to different stimulations for 4 days in the presence of αCD3 [1µg/ml] and αCD28 [6 ng/ml]. Stimulations were: Th1 conditions IL-12 [10 ng/ml], Th17 conditions IL-6 [30 ng/ml] and TGFβ [3 ng/ml]. Cells were then subjected to intracellular (ic) stainings, using CD4, IL-17A and IFNγ antibodies. FACS analysis was performed. All shown dot plots have been pre-gated on blasting CD4$^+$ cells.

In vitro differentiation experiments can be influenced by many variables and give rise to different results. Therefore, experiments were performed repeatedly under the same conditions and summarized in Table 8. Generally it can be concluded, that naïve CD4 T cells from CD4-Cre Bcl-3 mice show a defect in the differentiation towards the Th1 and Th17 subset.

Table 8 Summary of three independent *in vitro* differentiation experiments. Percentages represent means of n>5 from each experiment. ns: not significant, ***: t < 00.05.

		no cytokines	IL-12	TGFβ + IL6
% CD4$^+$	control	24.85	25.81	31.51
	CD4-Cre Bcl-3	33.56	29.24	36.74
	ttest	ns	ns	ns
% CD4$^+$IL-17$^+$	control	0.82	0.15	24.90
	CD4-Cre Bcl-3	1.047	0.318	17.39
	ttest	ns	ns	**
% CD4$^+$ IFNγ$^+$	control	6.68	56.20	0.93
	CD4-Cre Bcl-3	1.64	26.33	0.37
	ttest	***	***	***

As indicated above, naïve T cells can differentiate in culture to regulatory T cells (Treg) once they are activated in the presence of TGFβ. *In vivo*, Treg cells can be classified into natural Tregs (nTregs), which are generated in the thymus, and induced Treg cells (iTregs), which are derived from naïve T cells

in the peripheral immune organs. Both subsets are dependent on the transcription factor FoxP3 for their differentiation, maintenance and function (Josefowicz and Rudensky, 2009). Presently, it is not clear whether these two types of Treg cells serve different biological purposes or have partially or fully redundant functions and whether mechanistic requirements for Treg cell generation in the thymus and in the periphery are distinct. To analyze if naïve $CD4^+$ T cells from CD4-Cre Bcl-3 mice are able to upregulate FoxP3 expression and become iTregs, spleen and lymph node derived naïve T cells were cultured under iTreg conditions (i.e. TGFβ and IL-2).

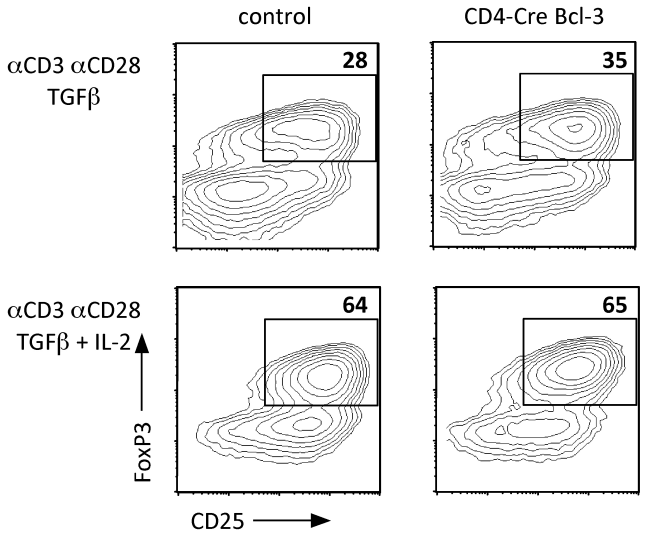

Figure 40 *In vitro* differentiation of naïve $CD4^+$ T cells to iTregs
MACS-purified $CD4^+$ $CD62L^+$ T cells from spleens and lymph nodes from CD4-Cre Bcl-3 and control littermates were isolated. Cells were subsequently subjected to iTreg conditions TGFβ [6 ng/ml] + IL-2 [20 ng/ml] for 4 days in the presence of αCD3 [1µg/ml] and αCD28 [6 ng/ml]. Cells were subsequently stained with antibodies against CD4, CD25 and FoxP3.

Naïve T cells from both CD4-Cre Bcl-3 mice and control littermates were equally capable to differentiate into iTregs *in vitro* (Fig.40). This result could be reproduced in independent experiments.

4.3.6 Naïve $CD4^+$ $CD25^-$ T cells from CD4-Cre Bcl-3 mice fail to induce colitis after transfer to RAG mice

In 1993, two groups (Morrissey et al., 1993; Powrie et al., 1993) independently demonstrated that transfer of a specific subset of $CD4^+$ T cells into immunodeficient mice caused a severe intestinal inflammation. Transfer of all $CD4^+$ T cells did not induce this phenotype. Later studies identified part of the $CD4^+CD25^+$ T cell population (Tregs) as responsible for suppressing the inflammation.

When we noticed the spontaneous colitis-like phenotype in the CD4-Cre Bcl-3 mice, we sought to exclude any possible external influence, so we employed this model to test whether the T cells from CD4-Cre Bcl-3 mice were colitogenic. Therefore, $CD4^+$ T cells were depleted of all $CD25^+$ cells by MACS purification and 1 x 10^6 cells were injected i.p. into $RAG1^{-/-}$ recipient mice. Mice were scored weekly. Three weeks after transfer, recipients of WT naïve $CD4^+$ T cells started to develop colitis, which increased in severity until mice were sacrificed five weeks after transfer (Fig. 41A). As expected, the disease was accompanied by weight loss (Fig. 41B). Mice that received T cells from CD4-Cre Bcl-3 mice, however, did not get sick.

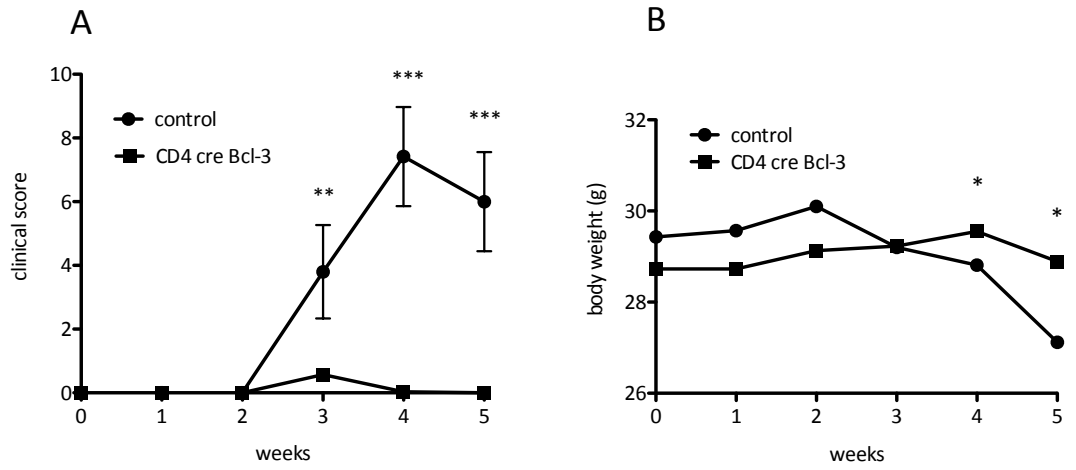

Figure 41 Transfer colitis model
Per mouse, 1 x 10^6 MACS purified naïve $CD4^+$ $CD25^-$ T cells from either CD4-Cre Bcl-3 mice or control littermates were injected i.p. into $RAG1^{-/-}$ recipients (n = 5/group). Mice were scored and weighed weekly. (A) Clinical score of mice, which received naïve $CD4^+$ $CD25^-$ T cells. The endoscopic score of colitis severity was based on evaluation of colon translucency (0–3 points), presence of fibrin attached to the bowel wall (0–3 points), granular aspect of the mucosa (0–3 points), morphology of the vascular pattern (0–3 points), and the presence of loose stools (0–3 points). (B) Body weight curves. (Black circles: $RAG1^{-/-}$ which received control cells, black squares: $RAG1^{-/-}$ which received cells from CD4-Cre Bcl-3 mice).

When mice were sacrificed 5 weeks after transfer to retrieve the transferred cells. WT cells had repopulated the recipients whereas T cells from the CD4-Cre Bcl-3 donors very poorly did so (Fig.42).

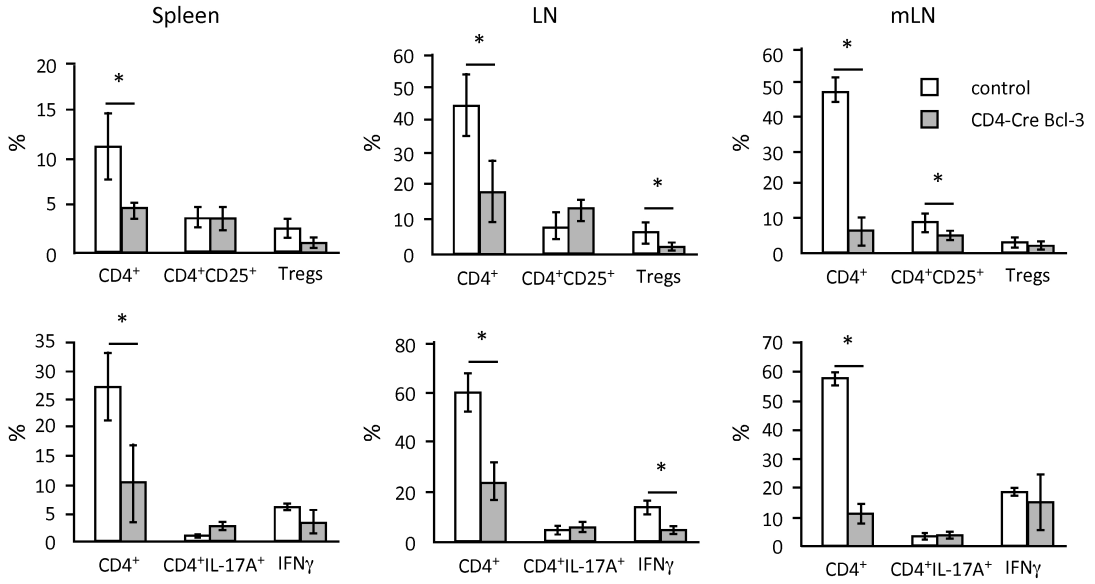

Figure 42 Replenishing of the T cell populations in RAG1$^{-/-}$ mice 5 weeks after cell transfer
Mice were sacrificed and spleens, lymph nodes (LN) and mesenteric lymph nodes (mLN) were retrieved. Single cell suspensions were prepared. All samples were stained for CD4, CD25, IL-17A and IFNγ and analyzed by FACS. Values represent means of n>3 with SDs.

Transferred naïve T cells from CD4-Cre Bcl-3 mice apparently did not expand. Another -very unlikely- reason for their disappearance could be that they did not home to the lymphoid organs. But the experiment shown in the upcoming section favors the first hypothesis.

4.3.7 *In vitro* assay reveals proliferation defect in CD4-Cre Bcl-3 T cells

To assess whether the proliferative capacity of Bcl-3 overexpressing T cells upon antigen encounter was impaired, *in vitro* proliferation studies were performed.

Following appropriate stimulation, T lymphocytes will proliferate extensively *in vitro*. Traditionally, mitogenic lectins such as phytohemagglutinin (PHA) and concanavalin A (Con A) have been used for polyclonal T cell stimulation. A more physiologically relevant approach uses anti-CD3 and anti-CD28 antibodies to stimulate T cells in a manner that partially mimics stimulation by antigen-presenting cells.

Splenic and lymph node derived naïve CD4 T cells from CD4-Cre Bcl-3 and control littermate mice were isolated and cultured in the presence of different (optimal and sub-optimal) concentrations of anti-CD3 or anti-CD3 in combination with anti-CD28.

All stimulations gave the same result, one of which is representatively shown in Figure 43.

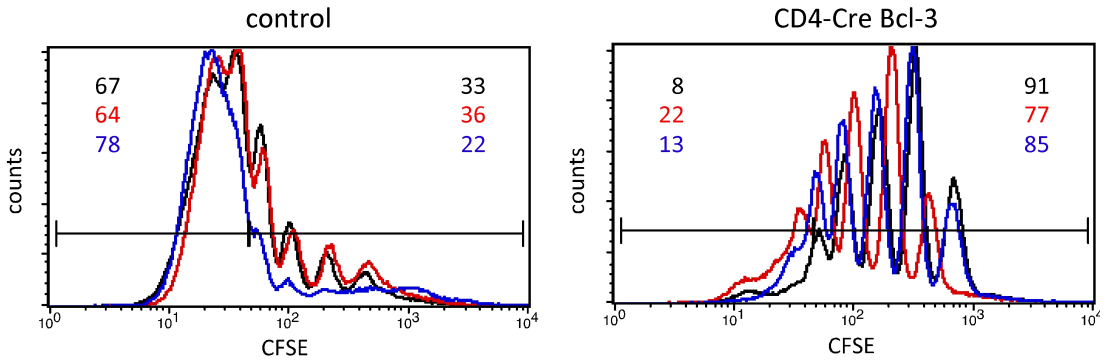

Figure 43 Comparative CFSE dilution in labeled cells after with αCD3 and αCD28 *in vitro*
MACS-purified naïve $CD4^+$ T cells were CFSE labeled and cultured for 4 days in the presence of αCD3 [1 µg/ml] and αCD28 [6 ng/ml]. Subsequently, cells were stained with αCD4 antibody and analyzed by FACS. Differently colored lines in the histograms represent 3 separate cell preparations from three individual mice. Numbers represent percentages.

The *in vitro* proliferation assay revealed that naïve T cells from CD4-Cre Bcl-3 mice failed to respond properly to the stimulus, indicating that these cells have problems proliferating upon antigen encounter. Some of the naïve T cells apparently underwent a few cell divisions (which can be seen as peaks in the histogram), but their proliferation capacity was dramatically decreased compared to cells from control littermates. On the other hand, significantly more Bcl-3-overexpressing CD4 T cells survived *in vitro* culture compared to control cells, as could be observed by FACS analysis (data not shown). It can be concluded that T cells overexpressing Bcl-3 show better survival *in vitro*, but display extremely impaired proliferation capacity upon stimulation.

5 Discussion and Outlook

NF-κB signaling and its components are highly conserved across different species, highlighting the important role of this pathway in cellular development and function. This thesis mainly focuses on two proteins involved in NF-κB signaling -CYLD and Bcl-3- investigating their role and function in antigen-presenting cells (APCs) and T cells.

5.1 Role of CYLD transcripts in dendritic cell and macrophage function

The deubiquitinating enzyme CYLD belongs to the family of ubiquitin-specific proteases (USPs) and negatively regulates NF-κB signaling, by removing Lys63-linked poly-ubiquitin chains from its target signaling molecules. In human, eight different alternative splice forms have been discovered to date. CYLD expression is highest in the human brain, testes, and skeletal muscles, whereas in mouse, the highest expression levels of CYLD are detected in the brain, testes, skin, and thymus. In our group a naturally occurring short splice from of murine CYLD (sCYLD) was identified (Hovelmeyer et al., 2007; Massoumi et al., 2006). A mouse overexpressing sCYLD in the absence of the full-length transcript was generated ($CYLD^{ex7/8}$) and B cell development and function were analyzed and published (Hovelmeyer et al., 2007).

5.1.1 Impact of sCYLD overexpression on dendritic cell function

Dendritic cells (DCs) are known as major regulators of adaptive immunity, but little is known about intracellular mechanisms specifically responsible for regulating DC function and survival. Interestingly, many inducers of DC maturation are also strong activators of NF-κB transcription factors (Baldwin, 1996; Ghosh et al., 1998), suggesting that these factors may play a key role in DC maturation. Several studies (Burkly et al., 1995; Weih et al., 1995; Wu et al., 1998) demonstrated the importance of different NF-κB units for dendritic cell development and function.

In our studies we compared all observed $CYLD^{ex7/8}$ DC phenotypes to the CYLD knock-out ($CYLD^{ko}$) (Massoumi et al., 2006). Thereby, we could show that overexpression of sCYLD in the absence of the full-length transcript (FL-CYLD) caused a much stronger phenotype than the complete absence of *cyld* gene products. DCs from $CYLD^{ex7/8}$ exhibited a hyperactive phenotype, which

was reflected in elevated levels of surface activation markers (CD86, Ox40L, MHC class II), increased secretion of inflammatory cytokines (IL-6 and TNFα), decreased secretion of the anti-inflammatory cytokine IL-10, enhanced capacity to induce clonal T cell expansion (in an adoptive co-transfer model of St42 TCR specific $CD8^+$ T cells and SGP-peptide loaded BMDCs) and the inability to induce tolerance (employing a DC-targeting approach utilizing an ovalbumin (OVA)-conjugated anti-DEC-205 antibody and OT-I TCR transgenic T cells). $CYLD^{ko}$ DCs on the other hand, resembled the WT DCs in all functional assays. Even NF-κB subunit expression seemed to be almost normal, except for a slight increase in total activity, as seen in the electromobility shift assay. Although Massoumi et al. showed that Bcl-3 was upregulated in TPA (12-O-tetra- decanoylphorbol-13 acetate) treated fibroblasts from $CYLD^{ko}$ mice (Massoumi et al., 2006), we could not detect upregulation of Bcl-3 protein levels in unstimulated or LPS-stimulated $CYLD^{ko}$ BMDCs, which might be due to differential expression of Bcl-3 depending on the cell type. Only Bcl-3 mRNA levels in $CYLD^{ko}$ BMDCs seemed to be minimally increased compared to WT. But this difference disappeared, when BMDCs were stimulated with LPS. It is possible, that Bcl-3 is differently regulated in the complete absence of CYLD transcripts.

We could also demonstrate that Bcl-3 transcription is activated by sCYLD expression, by transfecting $CYLD^{ko}$ MEFs with a plasmid coding for sCYLD and looking at Bcl-3 mRNA expression by quantitative real-time PCR. Bcl-3 upregulation is most likely to be mediated by NF-κB, which is upregulated by sCYLD (as we could show for various subunits by immunoblotting), since analysis of the region immediately upstream of the Bcl-3 transcription site, has identified two high affinity NF-κB binding sites (Brasier et al., 2001).

Notably, besides impaired thymocyte development in one of the three available CYLD knock-outs (Reiley et al., 2006), most of the existing CYLD knock-out mice only displayed phenotypes upon treatment with chemicals or infection with bacteria (Lim et al., 2007), which suggests that the loss of CYLD can be compensated by other DUBs such as A20 (Sun, 2008). A20 is dual-function enzyme: it exerts an E3 ligase activity using its C-terminal zinc-finger domains and was also found to be a deubiquitinating enzyme for K63-linked polyubiquitinated substrates (Wertz et al., 2004). It is remarkable that A20 and CYLD target the same set of signaling factors involved in the activation of NF-κB (Sun, 2008). Since both enzymes have been implicated as K63-specific DUBs, the question is raised as to why NF-κB signaling requires two similar enzymes with apparently redundant functions. One answer could be that they act in different phases of NF-κB activation, since it has been shown that

CYLD is almost constitutively active whereas A20 exerts its function only upon induction. A20 seems to be required for the termination of NF-κB signaling whereas CYLD is responsible for controlling the same pathway when spontaneously activated (Beyaert et al., 2000; Boone et al., 2004; Hutti et al., 2007; Lee et al., 2000). This leads to our hypothesis, that sCYLD acts as a dominant negative. In this case, its abundant presence in the cell would block the access of other (deubiquitinating) enzymes to target substrates, causing uncontrolled NF-κB pathway activation. A fact, which supports this hypothesis, is that DCs that have attenuated A20 expression show a phenotype, which is similar to that of $CYLD^{ex7/8}$ DCs. A20-silenced DCs showed spontaneous and enhanced expression of co-stimulatory molecules and pro-inflammatory cytokines and had different effects on T cell subsets: they inhibited Treg cells and hyperactivated tumor-infiltrating cytotoxic T lymphocytes and T helper cells that produced IL-6 and TNFα and were refractory to Treg cell–mediated suppression (Breckpot et al., 2009; Song et al., 2008).

Another hypothesis, which is so far without evidence, is that overexpression of sCYLD leads to a 'gain-of-function' phenotype. In $CYLD^{ex7/8}$ mice the inhibitory function of FL-CYLD is lost, whereas the activating function of sCYLD is strongly enhanced.

So far, strong phenotypes of the $CYLD^{ex7/8}$ mice have been observed in B cells (Hovelmeyer et al., 2007), dendritic cells (Srokowski et al., 2009), and T cells (Sonja Reissig, unpublished results), but we could not yet assign a function to sCYLD. A labor-intensive approach to achieve this would be the generation of a mouse, which solely expresses FL-CYLD in the absence of the short splice variant. The targeting construct would have to contain mutant splice acceptor sites, which prevent splicing and thereby the formation of sCYLD splice product. Performing genome-wide scale proteome and/or transcriptome analyses, comparing changes between WT and $CYLD^{ex7/8}$ mice, would also allow us to draw conclusions about the function of sCYLD.

So far, what can be concluded is that sCYLD overexpression leads to increased NF-κB activity in dendritic cells. NF-κB subunits of both the canonical and the alternative (non-canonical) pathway were upregulated in their expression. We found elevated expression levels of RelB, p65 and p50 and could show that significantly increased p50 binding to NF-κB consensus sites occurred in $CYLD^{ex7/8}$ DCs. This went together with high nuclear Bcl-3 expression in $CYLD^{ex7/8}$ DCs, which led to the assumption that p50 homodimers interact with Bcl-3 (as previously shown by Fujita et al. (Fujita et al., 1993)) to result in target gene expression. This hypothesis does not exclude the possibility that the upregulation of other NF-κB members

contributes to the phenotype. It has been demonstrated that MHC class II expression, cytokine secretion as well as upregulation of co-stimulatory surface molecules is impaired, when NF-κB signaling is inhibited (Yoshimura et al., 2001).
Finally, it has to be mentioned, that CYLD$^{ex7/8}$ mice overexpress sCYLD in all body cells and tissues, meaning that the observed phenotype is not entirely DC-intrinsic. A similar phenotype could be observed in CD11c-Cre Cyld$^{FL/FL}$ mice (which overexpress sCYLD only in dendritic cells), but it was far less pronounced than the CYLD$^{ex7/8}$ phenotype (personal communication, C. Srokowski). Therefore, DCs from CYLD$^{ex7/8}$ mice are likely to be influenced by their environment *in situ*, which could contribute to their hyperactive status.

5.1.2 Analyzing the impact of sCYLD overexpression in macrophages

After observing the strong phenotype caused by overexpression of sCYLD in dendritic cells, we decided to investigate whether the overexpression of sCYLD would also lead to a phenotype in another set of antigen presenting cells, namely macrophages. For this purpose, Cyld$^{FL/FL}$ mice were crossed to the LysMcre strain (Clausen et al., 1999), which leads to recombination in cells of myeloid origin and subsequently to overexpression of sCYLD in macrophages and granulocytes.
Neither peritoneal nor bone marrow-derived macrophages showed any significant phenotypes concerning changes in the: expression of the surface activation markers CD86 and MHC class II, secretion levels of the pro-inflammatory cytokine IL-6, iNOS mRNA levels or infiltration into the peritoneal cavity after Bio-Gel injection. Contrary to our expectations, all of these analyzed criteria remained unaltered indicating that upregulation of sCYLD in macrophages does not cause a hyperactive phenotype like in DCs overexpressing sCYLD. Using CYLD knock-out mice, Reiley et al. showed that CYLD (in contrast to A20) does not seem to play a role in regulating NF-κB signaling in macrophages (Reiley et al., 2007). So maybe macrophages are simply not affected by alterations in CYLD transcript expression. It is a common observation, that a protein can exert an important function in one cell type and be completely superfluous in another.
One phenotype, which could be observed in the LysMcre Cyld$^{FL/FL}$ mice, was the enhanced severity and prolonged duration of EAE. Unexpectedly, this phenotype was not accompanied by an increased lymphocyte or macrophage infiltration into the CNS compared to control group mice. There was also no

detectable change in MHC class II expression on CNS-resident macrophages and microglia. Activated macrophages and microglia both produce a large number of soluble factors, which can induce functional blockade and/or structural damage in axons *in vitro*. Amongst these are nitric oxide, possibly in combination with reactive oxygen species (Redford et al., 1997), matrix metalloproteinases and other molecules including excitotoxins (Smith et al., 2000a) and proteases ((Anthony et al., 1998) for review (Gold et al., 2006)). Trying to explain the obtained results, it has to be taken into consideration that LysMcre-mediated deletion has been reported to be insufficient in macrophages (Greenblatt et al., 2010) and CNS-microglia (Cho et al., 2008). Cho et al. were able to show that the LysMcre only deleted in approximately 4 % of the CNS-resident microglia in 8-week-old adult naïve mice, whereas the deletion efficiency in primary cultured microglia reached almost 40%. This discrepancy is due to the high activation status of primary cultured microglia an it can be speculated that deletion in CNS-resident microglia will be higher after EAE induction, because of the induced activation of microglia in the CNS. It will be interesting to look at the activation status of microglia in MOG_{35-55} immunized LysMcre $Cyld^{FL/FL}$ mice by looking at the extent of the matrix metalloproteinase MMP-15 down-regulation as shown by Toft-Hansen et al. (Toft-Hansen et al., 2004). It can not be excluded that the observed differences in EAE score between the LysMcre $Cyld^{FL/FL}$ and the littermate control mice is due to changes in the activation status of microglia caused by sCYLD overexpression. Sorting activated microglia from fully immunized mice of both groups and checking for sCYLD and FL-CYLD expression by qRT-PCR is among the first experiments, which need to be performed. MMP-, cytokine and chemokine expression by microglia should also be assessed by the same method. The activation status of microglia can be assessed by surface staining for the activation markers MHC class II and CD86 with subsequent FACS analysis. Immunohistochemical staining of brain and spinal cord cryosections, looking at T cell infiltration and myelin destruction, will also contribute to our understanding.

As to the macrophages, deletion efficiency has to be tested to exclude that the absence of a detectable phenotype is due to insufficient deletion. Even low levels of residual FL-CYLD could mask a potential phenotype and it has to be considered that the LysMcre might not be suitable for analyzing the impact of sCYLD on macrophage function. There is another Cre transgene (CD11b cre), which has been shown to delete in 50% of peritoneal macrophages and as much as 25% of cultured microglia (Boillee et al., 2006). Nevertheless, they did not show the deletion efficiency for microglia *in vivo*. It may be

worthwhile, to investigate the macrophage phenotype in CYLD$^{ex7/8}$ mice, even though it will not be a cell-type specific overexpression.

5.2 Bcl-3 overexpression in dendritic cells

As mentioned before, similar to what was found in B cells (Hovelmeyer et al., 2007), DCs in CYLD$^{ex7/8}$ mice expressed high levels of nuclear Bcl-3. Therefore, we decided to investigate whether Bcl-3 overexpression in DCs is sufficient to induce the hyperactive phenotype. For that purpose CD11c-Cre mice (Caton et al., 2007) were crossed to the ROSA-CAGs-STOP-Bcl-3-EGFP strain and BMDCs were generated and analyzed. Bone marrow derived dendritic cells overexpressed Bcl-3, as could be shown by immunoblotting. There was no detectable upregulation of surface activation markers (CD86, MHC class II), increase in cytokine secretion (IL-6) or enhanced capacity to stimulate T cells *in vitro* compared to control dendritic cells. *Ex vivo* isolated splenic dendritic cells did also not show a significant difference to control cells (data not shown). Taken together, these results suggest, that the CYLD$^{ex7/8}$ phenotype cannot solely be explained by Bcl-3 overexpression. Even though efficiency of the CD11c-Cre mediated recombination reached approximately 80 % in the CD11c$^+$ BMDC population (as monitored by EGFP expression), no visible phenotype could be observed. It does not seem worthwhile to sort EGFP$^+$ CD11c$^+$ cells to see whether there will be a phenotype, except maybe for repeating the co-culture experiment with the 2D2 TCR transgenic T cells in the presence of MOG_{35-55} peptide (Fig.31). In that specific experiment it could be important to have a pure EGFP$^+$ DC population, because very few EGFP$^-$ DCs could be sufficient to trigger T cell proliferation, thereby masking a possible defect of the EGFP$^+$ DCs.

It has to be taken into consideration that Bcl-3 exerts its function by interacting with NF-κB subunits, which we found to be upregulated in DCs from CYLD$^{ex7/8}$ mice but not CD11c-Cre Bcl-3 mice. The subunit p50, which is upregulated in CYLD$^{ex7/8}$ DCs and has been shown to confer an activating role to Bcl-3 when forming a nuclear complex, was not upregulated in DCs from CD11c-Cre Bcl-3 mice.

The DC phenotype of the CYLD$^{ex7/8}$ mice, therefore, does not seem to be caused solely by overexpression of Bcl-3. We favor a model in which elevated sCYLD levels cause an increase in the expression NF-κB subunits, by interfering with negative regulation of NF-κB signaling maybe functioning as a dominant negative. Similar to what has been shown by Brasier et al. (Brasier

et al., 2001), we expect Bcl-3 induction by NF-κB signaling, so that Bcl-3 in concert with NF-κB subunits (we favor p50 homodimers) can activate target gene expression leading to the observed hyperactive phenotype.

5.3 T cell specific overexpression of Bcl-3

Even though Bcl-3 belongs to the family of IκB (inhibitor of κB) it is distinct from other IκB proteins because it does not sequester NF-κB complexes in the cytoplasm. Instead, Bcl-3 is predominantly a nuclear protein and is involved in regulating nuclear NF-κB activities. Even though overexpression of Bcl-3 did not seem to affect thymocyte development (Caamano et al., 1996), it has been shown to play an important role in T cell survival after activation *in vivo* (Mitchell et al., 2001). Overexpression models exploring Bcl-3 function in T cells have so far included transgenic mice overexpressing Bcl-3 under the control of the proximal Lck promoter (Caamano et al., 1996) or the human CD2 promoter (Bassetti et al., 2009). Interestingly Bassetti et al. were not able to detect Bcl-3 overexpression neither on protein nor on mRNA levels when using the proximal or distal Lck promoter. In our model, we were able to use a conditional Bcl-3 overexpression mouse (provided by M. Wörns), which was crossed to the murine CD4-Cre transgene (Lee et al., 2001; Sawada et al., 1994). The offspring overexpressed Bcl-3 specifically in T cells under the control of an early murine T cell promoter. As soon as the first obtained litters aged (8-12 weeks), almost all mice developed severe diarrhea, which was often accompanied by a rectal prolapse. Endoscopic analysis of these mice revealed that they suffered from an inflammatory colitis-like phenotype. The endoscopic score of colitis severity was based on evaluation of colon translucency, presence of fibrin attached to the bowel wall, granular aspect of the mucosa, morphology of the vascular pattern, and the presence of loose stool.

Despite heterogeneous reports concerning the role of Th1, Th17 and Treg cells in inflammatory bowel disease as well as different models of colonic inflammation, it is still agreed upon that the different T cell subsets play major roles in colitis onset and development. Activated Th1 and Th17 cells have been reported to cause colon inflammation, but Th1 cells have also been reported to play a role in inducing IgM to IgA class switch B cells, which can then inhibit an immunogenic response to commensal gut microbes (Jiang et al., 2004; Kaser et al., 2010). Tregs on the other hand, have been shown to suppress and even cure colitis in several publications (Thompson and Powrie, 2004). Thymocytes and peripheral T cell populations were analyzed *ex vivo*,

to investigate whether Bcl-3 overexpression interfered with thymic T cell development or T cell differentiation. Similar to the results of Caamano et al. (Caamano et al., 1996), which showed that Bcl-3 overexpression driven by the proximal *lck*-promoter did not have an effect on thymocyte development, we could also not detect a difference in $CD4^+$ and $CD8^+$ thymocyte populations in the thymus. A phenotype we could observe repeatedly in all experiments was a reduction in $CD4^+$ T cell numbers in the periphery. Considering that CD4 and CD8 thymocyte numbers were normal, it seems as if $CD4^+$ cells undergo processes in the periphery, which lead to their deletion. CD4-Cre Bcl-3 mice also had significantly less effector/memory $CD4^+$ T cells in peripheral and mesenteric lymph nodes compared to control littermates. This finding together with a reduced total peripheral $CD4^+$ T cell population allows the hypothesis that $CD4^+$ T cells have a defect in their reaction to presented antigens, which impedes their proliferation and eventually leads to their death.

Analysis of T cell populations in the spleens, lymph nodes and mesenteric lymph nodes of CD4-Cre Bcl-3 mice revealed that the Th1 population was affected by Bcl-3 overexpression. Numbers of $CD4^+$ $IFN\gamma^+$ cells were significantly reduced in the peripheral lymphoid organs, whereas Th17 numbers remained unchanged. Th1 differentiation was shown to be unaffected in the absence of Bcl-3 (Corn et al., 2005), but there have been no reports about the impact of Bcl-3 overexpression on T cell differentiation. It will be interesting to analyze the impact of Bcl-3 overexpression on the expression of NF-κB signaling molecules, which play important roles in T cell differentiation (see introduction and for review (Banerjee et al., 2006)). So far, there have only been reports showing that overexpression of Bcl-3 prolongs the survival of naïve T cells *in vitro* (Bassetti et al., 2009).

Testing the *in vitro* differentiation potential of naïve $CD4^+$ T cells by stimulation with different sets of cytokines, revealed that naïve CD4 T cells from CD4-Cre Bcl-3 mice had a defect in the differentiation towards the Th1 and Th17 subsets, which are characterized by the expression of IFNγ and IL-17A respectively. We could further observe that Bcl-3-overexpressing CD4 T cells exhibited prolonged survival *in vitro* with and without addition of cytokines; a phenomenon similar to that observed by Mitchell et al. (Mitchell et al., 2001), who showed, that Bcl-3 improved the survival of activated T cells.

Another finding was that naïve Bcl-3 overexpressing $CD4^+$ T cells, which were transferred into lymphopenic RAG1 deficient mice, failed to proliferate *in vivo* and therefore did not cause colitis. *In vitro* proliferation assays supported this result, because naïve T cells from CD4-Cre Bcl-3 mice did almost not

proliferate in response to stimulation with anti-CD3 and/or anti-CD28. Bassetti et al. have shown in *in vivo* experiments, that T cells overexpressing Bcl-3 barely proliferated in response to antigen (Bassetti et al., 2009). The mice used in that study, however, do not have a reported inflammatory colitis phenotype. Which means that the reason for the severe colonic inflammation will still be a matter of investigation. Currently, three hypotheses prevail. The colitis can be caused by either one or a combination of the following:

- non-functional Tregs, which will be tested by performing *in vitro* Treg suppression assays. And later by a co-transfer experiment *in vivo*, in which wild type naïve CD4 T cells are co-transferred either with wild type or Bcl-3 overexpressing Tregs ($CD4^+CD25^+$ $FoxP3^+$) into lymphopenic or preferably irradiated wild type mice
- impaired T-B cell interactions in the gut-associated lymphoid tissues (GALT). It is known that T cells are required to induce an IgM to IgA class switch in B cells and that the IgA which does not only protect the host from commensal gut microbes but is also required for the acitivity of regulatory $CD4^+$ $CD25^+$ $CD45RB^{low}$ T cells, which can forestall or ameliorate the wasting and progression of the colitis symptoms (Jiang et al., 2004). We are currently in the process of analyzing IgA levels in sera (by ELISA) and GALT B cells (intracellular staining and quantitative real time PCR) of CD4-Cre Bcl-3 and control littermate mice
- impaired homing of memory T cells. For this we will analyze the expression of the integrin $\alpha4\beta7$ (which binds MadCAM) or the chemokine receptor CCR9 (which binds CCL25) and is selectively expressed in the small intestine (Cose, 2007). We will also have to investigate if memory T cells are increasingly homing to the GALT, especially because we found reduced numbers of effector/memory T cells in the periphery of CD4-Cre Bcl-3 mice compared to littermate controls.

Less likely, but yet other possible causes for the colitis phenotype are changes in the (mainly spleen-resident) $CD4^+$ $CD8^-$ $CD205^-$ $CD11b^+$ $CD11c^+$ myeloid dendritic cell population (Shortman and Liu, 2002) and/or changes in the function of the $CD8^+$ T cell populations. But since we have shown that dendritic cell-specific overexpression of Bcl-3 does not have functional consequences and since $CD8^+$ T cell dysfunctions have not been implicated in causing inflammatory gut diseases, $CD4^+$ T cells will remain the focus of our research.

6 Summary

CYLD is a deubiquitinating enzyme, which negatively regulates NF-κB signaling by removing Lys63-linked polyubiquitin chains from its substrates. In mice, there are two variants of CYLD: full-length CYLD (FL-CYLD) and its short splice variant sCYLD. sCYLD lacks the NEMO and TRAF2 binding sites and $CYLD^{ex7/8}$ mice, which have been generated in our laboratory, overexpress sCYLD in the absence of the full length transcript. In this thesis, we show that bone marrow-derived macrophages (BMDCs) overexpressing sCYLD display a hyperactive phenotype. They have increased levels of the inflammatory cytokines IL-6 and TNFα, have exaggerated stimulatory capacity and fail to induce tolerance in *in vivo* experiments. $CYLD^{ex7/8}$ BMDCs have increased levels of nuclear Bcl-3, which we could show to be directly induced by sCYLD expression. NF-κB signaling was markedly upregulated in $CYLD^{ex7/8}$ BMDCs.

Bcl-3 overexpressing BMDCs with normal CYLD expression, however, were not hyperactive, suggesting that Bcl-3 overexpression is not sufficient for causing the observed phenotype. Taken together we propose a model in which the exclusive overexpression of sCYLD with high nuclear levels of Bcl-3 in BMDCs is accompanied by an increased NF-κB activation, resulting in a hyperactive phenotype.

We further analyzed macrophages overexpressing sCYLD using the LysMcre $Cyld^{FL/FL}$ strain, but could not detect differences in activation marker expression, cytokine secretion or iNOS production. LysMcre $Cyld^{FL/FL}$ mice immunized with MOG_{35-55} peptide showed a more severe course of experimental autoimmune encephalomyelitis (EAE), which could not be explained by enhanced levels of MHC class II on CNS-resident macrophages and microglia or increased T cell infiltration.

Mice overexpressing Bcl-3 in T cells develop spontaneous colitis. They have less peripheral memory/effector T cells and less Th1 cells, whereas Th17 numbers are normal. Naïve T cells overexpressing Bcl-3 show defects in *in vitro* differentiation to the Th1 or Th17 fate. $CD4^+$ T cells overexpressing Bcl-3 show enhanced survival capacity in *in vitro* culture, but have a defect in proliferative capacity when stimulated *in vitro* or when adoptively transferred into lymphopenic hosts.

7 Zusammenfassung

CYLD ist eine Deubiquitinase, die durch das Entfernen von Lysin 63-gekoppelten poly-Ubiquitinketten von ihren Substraten den NF-κB Signalweg negativ reguliert. In Mäusen gibt es zwei bekannte Formen von CYLD: full-length CYLD (FL-CYLD) und die kürzere Spleiß-Variante short CYLD (sCYLD). In sCYLD fehlen die Bindestellen für NEMO und TRAF2. $CYLD^{ex7/8}$ Mäuse, die in unserem Labor hergestellt wurden, überexprimieren ausschließlich die sCYLD Variante. In dieser Arbeit zeigen wir, dass aus Knochenmark hergestellte dendritische Zellen (BMDCs) dieser Mäuse einen hyperaktiven Phänotyp haben. Sie weisen erhöhte Expression von Oberflächen-Aktivierungsmarkern auf und haben eine höhere Sekretion der inflammatorischen Zytokine IL-6 und TNFα. Außerdem zeigen sie eine erhöhte stimulatorische Aktivität und scheitern bei der Toleranz-Induktion in *in vivo* Experimenten. Dendritische Zellen von $CYLD^{ex7/8}$ Mäusen haben stärkere Bcl-3 Expression im Zellkern und der NF-κB Signalweg ist verstärkt aktiv. Wir konnten zeigen, dass Bcl-3 Expression von sCYLD direkt induziert werden kann.

Bcl-3 überexprimierende BMDCs mit normaler CYLD Expression zeigten jedoch keinen hyperaktiven Phänotyp. Daraus schließen wir, dass die Überexpression von Bcl-3 nicht ausreicht um den Phänotyp zu verursachen. Wir favorisieren ein Modell in dem erhöhte sCYLD Expression zur Bcl-3 Überexpression führt und im Zusammenhang mit höherer NF-κB Aktivierung im hyperaktiven Phänotyp resultiert.

Des Weiteren wurden Makrophagen von LysMcre $Cyld^{FL/FL}$ analysiert, die sCYLD nur in ebendiesen überexprimieren. Dort zeigte sich jedoch kein Phänotyp in der Expression von Aktivierungsmarkern, in der Zytokin Sekretion oder der iNOS Produktion. Lediglich MOG_{35-55}-immunisierte LysMcre $Cyld^{FL/FL}$ Mäuse zeigten einen verstärkten Krankheitsverlauf in einem Mausmodell für Multiple Sklerose. Dieses Phänomen konnte jedoch nicht mit veränderter MHC Klasse II Expression auf Makrophagen oder Mikroglia im zentralen Nervensystem (ZNS) erklärt werden. Es fand auch keine erhöhte Infiltration von Lymphozyten ins ZNS statt.

Mäuse die Bcl-3 in T Zellen überexprimieren (CD4 cre Bcl-3) erkranken spontan an Colitis. Sie haben weniger periphere Effektor- und Th1- T Zellen. Die Zahl der Th17 Zellen ist normal verglichen mit Kontrolltieren. Naive T Zellen von CD4-Cre Bcl-3 Mäusen zeigten Defekte bei der *in vitro*

Differenzierung zu Th1 und Th17 Zellen. $CD4^+$ T Zellen von CD4-Cre Bcl-3 Mäusen wiesen eine längere Überlebenskapazität *in vitro* auf, zeigten jedoch Defizite in der Zellproliferation nach Stimulation *in vitro*, sowie in einem adoptiven Zell-Transfer-Modell in lymphopenischen Mäuse.

8 References

Ahern, P.P., Izcue, A., Maloy, K.J., and Powrie, F. (2008). The interleukin-23 axis in intestinal inflammation. Immunol Rev *226*, 147-159.

Anthony, D.C., Miller, K.M., Fearn, S., Townsend, M.J., Opdenakker, G., Wells, G.M., Clements, J.M., Chandler, S., Gearing, A.J., and Perry, V.H. (1998). Matrix metalloproteinase expression in an experimentally-induced DTH model of multiple sclerosis in the rat CNS. J Neuroimmunol *87*, 62-72.

Baldwin, A.S., Jr. (1996). The NF-kappa B and I kappa B proteins: new discoveries and insights. Annu Rev Immunol *14*, 649-683.

Banchereau, J., Briere, F., Caux, C., Davoust, J., Lebecque, S., Liu, Y.J., Pulendran, B., and Palucka, K. (2000). Immunobiology of dendritic cells. Annu Rev Immunol *18*, 767-811.

Banchereau, J., and Steinman, R.M. (1998). Dendritic cells and the control of immunity. Nature *392*, 245-252.

Banerjee, A., Gugasyan, R., McMahon, M., and Gerondakis, S. (2006). Diverse Toll-like receptors utilize Tpl2 to activate extracellular signal-regulated kinase (ERK) in hemopoietic cells. Proc Natl Acad Sci U S A *103*, 3274-3279.

Barnes, M.J., and Powrie, F. (2009). Regulatory T cells reinforce intestinal homeostasis. Immunity *31*, 401-411.

Bassetti, M.F., White, J., Kappler, J.W., and Marrack, P. (2009). Transgenic Bcl-3 slows T cell proliferation. Int Immunol *21*, 339-348.

Belkaid, Y., and Tarbell, K. (2009). Regulatory T cells in the control of host-microorganism interactions (*). Annu Rev Immunol *27*, 551-589.

Bender, A., Bui, L.K., Feldman, M.A., Larsson, M., and Bhardwaj, N. (1995). Inactivated influenza virus, when presented on dendritic cells, elicits human CD8+ cytolytic T cell responses. J Exp Med *182*, 1663-1671.

Berger, T., Weerth, S., Kojima, K., Linington, C., Wekerle, H., and Lassmann, H. (1997). Experimental autoimmune encephalomyelitis: the antigen specificity of T lymphocytes determines the topography of lesions in the central and peripheral nervous system. Lab Invest *76*, 355-364.

Bettelli, E., Baeten, D., Jager, A., Sobel, R.A., and Kuchroo, V.K. (2006). Myelin oligodendrocyte glycoprotein-specific T and B cells cooperate to induce a Devic-like disease in mice. J Clin Invest *116*, 2393-2402.

Beyaert, R., Heyninck, K., and Van Huffel, S. (2000). A20 and A20-binding proteins as cellular inhibitors of nuclear factor-kappa B-dependent gene expression and apoptosis. Biochem Pharmacol *60*, 1143-1151.

Bhardwaj, N., Bender, A., Gonzalez, N., Bui, L.K., Garrett, M.C., and Steinman, R.M. (1994). Influenza virus-infected dendritic cells stimulate strong proliferative and cytolytic responses from human CD8+ T cells. J Clin Invest *94*, 797-807.

Bignell, G.R., Warren, W., Seal, S., Takahashi, M., Rapley, E., Barfoot, R., Green, H., Brown, C., Biggs, P.J., Lakhani, S.R.*, et al.* (2000). Identification of the familial cylindromatosis tumour-suppressor gene. Nat Genet *25*, 160-165.

Boillee, S., Yamanaka, K., Lobsiger, C.S., Copeland, N.G., Jenkins, N.A., Kassiotis, G., Kollias, G., and Cleveland, D.W. (2006). Onset and progression in inherited ALS determined by motor neurons and microglia. Science *312*, 1389-1392.

Boone, D.L., Turer, E.E., Lee, E.G., Ahmad, R.C., Wheeler, M.T., Tsui, C., Hurley, P., Chien, M., Chai, S., Hitotsumatsu, O.*, et al.* (2004). The ubiquitin-modifying enzyme A20 is required for termination of Toll-like receptor responses. Nat Immunol *5*, 1052-1060.

Bours, V., Franzoso, G., Azarenko, V., Park, S., Kanno, T., Brown, K., and Siebenlist, U. (1993). The oncoprotein Bcl-3 directly transactivates through kappa B motifs via association with DNA-binding p50B homodimers. Cell *72*, 729-739.

Brasier, A.R., Lu, M., Hai, T., Lu, Y., and Boldogh, I. (2001). NF-kappa B-inducible BCL-3 expression is an autoregulatory loop controlling nuclear p50/NF-kappa B1 residence. J Biol Chem *276*, 32080-32093.

Breckpot, K., Aerts-Toegaert, C., Heirman, C., Peeters, U., Beyaert, R., Aerts, J.L., and Thielemans, K. (2009). Attenuated expression of A20 markedly increases the efficacy of double-stranded RNA-activated dendritic cells as an anti-cancer vaccine. J Immunol *182*, 860-870.

Brummelkamp, T.R., Nijman, S.M., Dirac, A.M., and Bernards, R. (2003). Loss of the cylindromatosis tumour suppressor inhibits apoptosis by activating NF-kappaB. Nature *424*, 797-801.

Brunkow, M.E., Jeffery, E.W., Hjerrild, K.A., Paeper, B., Clark, L.B., Yasayko, S.A., Wilkinson, J.E., Galas, D., Ziegler, S.F., and Ramsdell, F. (2001). Disruption of a new forkhead/winged-helix protein, scurfin, results in the fatal lymphoproliferative disorder of the scurfy mouse. Nat Genet *27*, 68-73.

Burkly, L., Hession, C., Ogata, L., Reilly, C., Marconi, L.A., Olson, D., Tizard, R., Cate, R., and Lo, D. (1995). Expression of relB is required for the development of thymic medulla and dendritic cells. Nature *373*, 531-536.

Caamano, J.H., Perez, P., Lira, S.A., and Bravo, R. (1996). Constitutive expression of Bc1-3 in thymocytes increases the DNA binding of NF-kappaB1 (p50) homodimers in vivo. Mol Cell Biol *16*, 1342-1348.

Carmody, R.J., Ruan, Q., Palmer, S., Hilliard, B., and Chen, Y.H. (2007). Negative regulation of toll-like receptor signaling by NF-kappaB p50 ubiquitination blockade. Science *317*, 675-678.

Caton, M.L., Smith-Raska, M.R., and Reizis, B. (2007). Notch-RBP-J signaling controls the homeostasis of CD8- dendritic cells in the spleen. J Exp Med *204*, 1653-1664.

Cella, M., Scheidegger, D., Palmer-Lehmann, K., Lane, P., Lanzavecchia, A., and Alber, G. (1996). Ligation of CD40 on dendritic cells triggers production of high levels of interleukin-12 and enhances T cell stimulatory capacity: T-T help via APC activation. J Exp Med *184*, 747-752.

Chen, C.L., Singh, N., Yull, F.E., Strayhorn, D., Van Kaer, L., and Kerr, L.D. (2000). Lymphocytes lacking I kappa B-alpha develop normally, but have selective defects in proliferation and function. J Immunol *165*, 5418-5427.

Chen, Z.J. (2005). Ubiquitin signalling in the NF-kappaB pathway. Nat Cell Biol *7*, 758-765.

Cho, I.H., Hong, J., Suh, E.C., Kim, J.H., Lee, H., Lee, J.E., Lee, S., Kim, C.H., Kim, D.W., Jo, E.K.*, et al.* (2008). Role of microglial IKKbeta in kainic acid-induced hippocampal neuronal cell death. Brain *131*, 3019-3033.

Chung, D.R., Kasper, D.L., Panzo, R.J., Chitnis, T., Grusby, M.J., Sayegh, M.H., and Tzianabos, A.O. (2003). CD4+ T cells mediate abscess formation in intra-abdominal sepsis by an IL-17-dependent mechanism. J Immunol *170*, 1958-1963.

Clausen, B.E., Burkhardt, C., Reith, W., Renkawitz, R., and Forster, I. (1999). Conditional gene targeting in macrophages and granulocytes using LysMcre mice. Transgenic Res *8*, 265-277.

Corn, R.A., Hunter, C., Liou, H.C., Siebenlist, U., and Boothby, M.R. (2005). Opposing roles for RelB and Bcl-3 in regulation of T-box expressed in T cells, GATA-3, and Th effector differentiation. J Immunol *175*, 2102-2110.

Cose, S. (2007). T-cell migration: a naive paradigm? Immunology *120*, 1-7.

Courtois, G., and Gilmore, T.D. (2006). Mutations in the NF-kappaB signaling pathway: implications for human disease. Oncogene *25*, 6831-6843.

Crossen, P.E. (1989). Cytogenetic and molecular changes in chronic B-cell leukemia. Cancer Genet Cytogenet *43*, 143-150.

Das, J., Chen, C.H., Yang, L., Cohn, L., Ray, P., and Ray, A. (2001). A critical role for NF-kappa B in GATA3 expression and TH2 differentiation in allergic airway inflammation. Nat Immunol *2*, 45-50.

De Smedt, T., Smith, J., Baum, P., Fanslow, W., Butz, E., and Maliszewski, C. (2002). Ox40 costimulation enhances the development of T cell responses induced by dendritic cells in vivo. J Immunol *168*, 661-670.

DiPietro, L.A., Burdick, M., Low, Q.E., Kunkel, S.L., and Strieter, R.M. (1998). MIP-1alpha as a critical macrophage chemoattractant in murine wound repair. J Clin Invest *101*, 1693-1698.

Ferguson, B., Matyszak, M.K., Esiri, M.M., and Perry, V.H. (1997). Axonal damage in acute multiple sclerosis lesions. Brain *120 (Pt 3)*, 393-399.

Franzoso, G., Bours, V., Azarenko, V., Park, S., Tomita-Yamaguchi, M., Kanno, T., Brown, K., and Siebenlist, U. (1993). The oncoprotein Bcl-3 can facilitate NF-kappa B-mediated transactivation by removing inhibiting p50 homodimers from select kappa B sites. EMBO J *12*, 3893-3901.

Franzoso, G., Bours, V., Park, S., Tomita-Yamaguchi, M., Kelly, K., and Siebenlist, U. (1992). The candidate oncoprotein Bcl-3 is an antagonist of p50/NF-kappa B-mediated inhibition. Nature *359*, 339-342.

Franzoso, G., Carlson, L., Scharton-Kersten, T., Shores, E.W., Epstein, S., Grinberg, A., Tran, T., Shacter, E., Leonardi, A., Anver, M.*, et al.* (1997). Critical roles for the Bcl-3 oncoprotein in T cell-mediated immunity, splenic microarchitecture, and germinal center reactions. Immunity *6*, 479-490.

Fujita, T., Nolan, G.P., Liou, H.C., Scott, M.L., and Baltimore, D. (1993). The candidate proto-oncogene bcl-3 encodes a transcriptional coactivator that activates through NF-kappa B p50 homodimers. Genes Dev *7*, 1354-1363.

Gao, J., Huo, L., Sun, X., Liu, M., Li, D., Dong, J.T., and Zhou, J. (2008). The tumor suppressor CYLD regulates microtubule dynamics and plays a role in cell migration. J Biol Chem *283*, 8802-8809.

Ge, B., Li, O., Wilder, P., Rizzino, A., and McKeithan, T.W. (2003). NF-kappa B regulates BCL3 transcription in T lymphocytes through an intronic enhancer. J Immunol *171*, 4210-4218.

Gerondakis, S., Strasser, A., Metcalf, D., Grigoriadis, G., Scheerlinck, J.Y., and Grumont, R.J. (1996). Rel-deficient T cells exhibit defects in production of interleukin 3 and granulocyte-macrophage colony-stimulating factor. Proc Natl Acad Sci U S A *93*, 3405-3409.

Ghosh, S., May, M.J., and Kopp, E.B. (1998). NF-kappa B and Rel proteins: evolutionarily conserved mediators of immune responses. Annu Rev Immunol *16*, 225-260.

Goerdt, S., and Orfanos, C.E. (1999). Other functions, other genes: alternative activation of antigen-presenting cells. Immunity *10*, 137-142.

Gold, R., Linington, C., and Lassmann, H. (2006). Understanding pathogenesis and therapy of multiple sclerosis via animal models: 70 years of merits and culprits in experimental autoimmune encephalomyelitis research. Brain *129*, 1953-1971.

Gong, Y., Hart, E., Shchurin, A., and Hoover-Plow, J. (2008). Inflammatory macrophage migration requires MMP-9 activation by plasminogen in mice. J Clin Invest *118*, 3012-3024.

Greenblatt, M.B., Aliprantis, A., Hu, B., and Glimcher, L.H. (2010). Calcineurin regulates innate antifungal immunity in neutrophils. J Exp Med *207*, 923-931.

Happel, K.I., Dubin, P.J., Zheng, M., Ghilardi, N., Lockhart, C., Quinton, L.J., Odden, A.R., Shellito, J.E., Bagby, G.J., Nelson, S.*, et al.* (2005). Divergent roles of IL-23 and IL-12 in host defense against Klebsiella pneumoniae. J Exp Med *202*, 761-769.

Hatada, E.N., Nieters, A., Wulczyn, F.G., Naumann, M., Meyer, R., Nucifora, G., McKeithan, T.W., and Scheidereit, C. (1992). The ankyrin repeat domains of the NF-kappa B precursor p105 and the protooncogene bcl-3 act as specific inhibitors of NF-kappa B DNA binding. Proc Natl Acad Sci U S A *89*, 2489-2493.

Hawiger, D., Inaba, K., Dorsett, Y., Guo, M., Mahnke, K., Rivera, M., Ravetch, J.V., Steinman, R.M., and Nussenzweig, M.C. (2001). Dendritic cells induce peripheral T cell unresponsiveness under steady state conditions in vivo. J Exp Med *194*, 769-779.

Hayes, G.M., Woodroofe, M.N., and Cuzner, M.L. (1987). Microglia are the major cell type expressing MHC class II in human white matter. J Neurol Sci *80*, 25-37.

Hendriks, J.J., Teunissen, C.E., de Vries, H.E., and Dijkstra, C.D. (2005). Macrophages and neurodegeneration. Brain Res Brain Res Rev *48*, 185-195.

Heppner, F.L., Greter, M., Marino, D., Falsig, J., Raivich, G., Hovelmeyer, N., Waisman, A., Rulicke, T., Prinz, M., Priller, J.*, et al.* (2005). Experimental autoimmune encephalomyelitis repressed by microglial paralysis. Nat Med *11*, 146-152.

Hilliard, B.A., Mason, N., Xu, L., Sun, J., Lamhamedi-Cherradi, S.E., Liou, H.C., Hunter, C., and Chen, Y.H. (2002). Critical roles of c-Rel in autoimmune inflammation and helper T cell differentiation. J Clin Invest *110*, 843-850.

Hovelmeyer, N., Wunderlich, F.T., Massoumi, R., Jakobsen, C.G., Song, J., Worns, M.A., Merkwirth, C., Kovalenko, A., Aumailley, M., Strand, D.*, et al.*

(2007). Regulation of B cell homeostasis and activation by the tumor suppressor gene CYLD. J Exp Med *204*, 2615-2627.

Huang, W., Na, L., Fidel, P.L., and Schwarzenberger, P. (2004). Requirement of interleukin-17A for systemic anti-Candida albicans host defense in mice. J Infect Dis *190*, 624-631.

Hutti, J.E., Turk, B.E., Asara, J.M., Ma, A., Cantley, L.C., and Abbott, D.W. (2007). IkappaB kinase beta phosphorylates the K63 deubiquitinase A20 to cause feedback inhibition of the NF-kappaB pathway. Mol Cell Biol *27*, 7451-7461.

Inaba, K., Metlay, J.P., Crowley, M.T., and Steinman, R.M. (1990). Dendritic cells pulsed with protein antigens in vitro can prime antigen-specific, MHC-restricted T cells in situ. J Exp Med *172*, 631-640.

Jiang, H.Q., Thurnheer, M.C., Zuercher, A.W., Boiko, N.V., Bos, N.A., and Cebra, J.J. (2004). Interactions of commensal gut microbes with subsets of B- and T-cells in the murine host. Vaccine *22*, 805-811.

Jones, S.A. (2005). Directing transition from innate to acquired immunity: defining a role for IL-6. J Immunol *175*, 3463-3468.

Josefowicz, S.Z., and Rudensky, A. (2009). Control of regulatory T cell lineage commitment and maintenance. Immunity *30*, 616-625.

Kaser, A., Zeissig, S., and Blumberg, R.S. (2010). Inflammatory bowel disease. Annu Rev Immunol *28*, 573-621.

Kim, S., La Motte-Mohs, R.N., Rudolph, D., Zuniga-Pflucker, J.C., and Mak, T.W. (2003). The role of nuclear factor-kappaB essential modulator (NEMO) in B cell development and survival. Proc Natl Acad Sci U S A *100*, 1203-1208.

Kobayashi, T., Walsh, P.T., Walsh, M.C., Speirs, K.M., Chiffoleau, E., King, C.G., Hancock, W.W., Caamano, J.H., Hunter, C.A., Scott, P.*, et al.* (2003). TRAF6 is a critical factor for dendritic cell maturation and development. Immunity *19*, 353-363.

Koch, F., Stanzl, U., Jennewein, P., Janke, K., Heufler, C., Kampgen, E., Romani, N., and Schuler, G. (1996). High level IL-12 production by murine dendritic cells: upregulation via MHC class II and CD40 molecules and downregulation by IL-4 and IL-10. J Exp Med *184*, 741-746.

Koga, T., Lim, J.H., Jono, H., Ha, U.H., Xu, H., Ishinaga, H., Morino, S., Xu, X., Yan, C., Kai, H.*, et al.* (2008). Tumor suppressor cylindromatosis acts as a negative regulator for Streptococcus pneumoniae-induced NFAT signaling. J Biol Chem *283*, 12546-12554.

Kornek, B., Storch, M.K., Bauer, J., Djamshidian, A., Weissert, R., Wallstroem, E., Stefferl, A., Zimprich, F., Olsson, T., Linington, C.*, et al.*

(2001). Distribution of a calcium channel subunit in dystrophic axons in multiple sclerosis and experimental autoimmune encephalomyelitis. Brain *124*, 1114-1124.

Kovalenko, A., Chable-Bessia, C., Cantarella, G., Israel, A., Wallach, D., and Courtois, G. (2003). The tumour suppressor CYLD negatively regulates NF-kappaB signalling by deubiquitination. Nature *424*, 801-805.

Kuwata, H., Watanabe, Y., Miyoshi, H., Yamamoto, M., Kaisho, T., Takeda, K., and Akira, S. (2003). IL-10-inducible Bcl-3 negatively regulates LPS-induced TNF-alpha production in macrophages. Blood *102*, 4123-4129.

Lardon, F., Snoeck, H.W., Berneman, Z.N., Van Tendeloo, V.F., Nijs, G., Lenjou, M., Henckaerts, E., Boeckxtaens, C.J., Vandenabeele, P., Kestens, L.L.*, et al.* (1997). Generation of dendritic cells from bone marrow progenitors using GM-CSF, TNF-alpha, and additional cytokines: antagonistic effects of IL-4 and IFN-gamma and selective involvement of TNF-alpha receptor-1. Immunology *91*, 553-559.

Lee, E.G., Boone, D.L., Chai, S., Libby, S.L., Chien, M., Lodolce, J.P., and Ma, A. (2000). Failure to regulate TNF-induced NF-kappaB and cell death responses in A20-deficient mice. Science *289*, 2350-2354.

Lee, P.P., Fitzpatrick, D.R., Beard, C., Jessup, H.K., Lehar, S., Makar, K.W., Perez-Melgosa, M., Sweetser, M.T., Schlissel, M.S., Nguyen, S.*, et al.* (2001). A critical role for Dnmt1 and DNA methylation in T cell development, function, and survival. Immunity *15*, 763-774.

Li, Q., Lu, Q., Bottero, V., Estepa, G., Morrison, L., Mercurio, F., and Verma, I.M. (2005). Enhanced NF-kappaB activation and cellular function in macrophages lacking IkappaB kinase 1 (IKK1). Proc Natl Acad Sci U S A *102*, 12425-12430.

Lim, J.H., Stirling, B., Derry, J., Koga, T., Jono, H., Woo, C.H., Xu, H., Bourne, P., Ha, U.H., Ishinaga, H.*, et al.* (2007). Tumor suppressor CYLD regulates acute lung injury in lethal Streptococcus pneumoniae infections. Immunity *27*, 349-360.

Lutz, M.B., Kukutsch, N., Ogilvie, A.L., Rossner, S., Koch, F., Romani, N., and Schuler, G. (1999). An advanced culture method for generating large quantities of highly pure dendritic cells from mouse bone marrow. J Immunol Methods *223*, 77-92.

Massoumi, R., Chmielarska, K., Hennecke, K., Pfeifer, A., and Fassler, R. (2006). Cyld inhibits tumor cell proliferation by blocking Bcl-3-dependent NF-kappaB signaling. Cell *125*, 665-677.

Matsumoto, Y., Hara, N., Tanaka, R., and Fujiwara, M. (1986). Immunohistochemical analysis of the rat central nervous system during

experimental allergic encephalomyelitis, with special reference to Ia-positive cells with dendritic morphology. J Immunol *136*, 3668-3676.

McQualter, J.L., Darwiche, R., Ewing, C., Onuki, M., Kay, T.W., Hamilton, J.A., Reid, H.H., and Bernard, C.C. (2001). Granulocyte macrophage colony-stimulating factor: a new putative therapeutic target in multiple sclerosis. J Exp Med *194*, 873-882.

Mitchell, T.C., Hildeman, D., Kedl, R.M., Teague, T.K., Schaefer, B.C., White, J., Zhu, Y., Kappler, J., and Marrack, P. (2001). Immunological adjuvants promote activated T cell survival via induction of Bcl-3. Nat Immunol *2*, 397-402.

Moro, J.R., Iwata, M., and von Andriano, U.H. (2008). Vitamin effects on the immune system: vitamins A and D take centre stage. Nat Rev Immunol *8*, 685-698.

Morrissey, P.J., Charrier, K., Braddy, S., Liggitt, D., and Watson, J.D. (1993). CD4+ T cells that express high levels of CD45RB induce wasting disease when transferred into congenic severe combined immunodeficient mice. Disease development is prevented by cotransfer of purified CD4+ T cells. J Exp Med *178*, 237-244.

Moser, M., and Murphy, K.M. (2000). Dendritic cell regulation of TH1-TH2 development. Nat Immunol *1*, 199-205.

Muhlbauer, M., Chilton, P.M., Mitchell, T.C., and Jobin, C. (2008). Impaired Bcl3 up-regulation leads to enhanced lipopolysaccharide-induced interleukin (IL)-23P19 gene expression in IL-10(-/-) mice. J Biol Chem *283*, 14182-14189.

Mullis, K.B., and Faloona, F.A. (1987). Specific synthesis of DNA in vitro via a polymerase-catalyzed chain reaction. Methods Enzymol *155*, 335-350.

Murray, H.W. (1988). Interferon-gamma, the activated macrophage, and host defense against microbial challenge. Ann Intern Med *108*, 595-608.

Nolan, G.P., Fujita, T., Bhatia, K., Huppi, C., Liou, H.C., Scott, M.L., and Baltimore, D. (1993). The bcl-3 proto-oncogene encodes a nuclear I kappa B-like molecule that preferentially interacts with NF-kappa B p50 and p52 in a phosphorylation-dependent manner. Mol Cell Biol *13*, 3557-3566.

North, R.J. (1978). The concept of the activated macrophage. J Immunol *121*, 806-809.

Ohno, H., Takimoto, G., and McKeithan, T.W. (1990). The candidate proto-oncogene bcl-3 is related to genes implicated in cell lineage determination and cell cycle control. Cell *60*, 991-997.

Podolsky, D.K., Lobb, R., King, N., Benjamin, C.D., Pepinsky, B., Sehgal, P., and deBeaumont, M. (1993). Attenuation of colitis in the cotton-top tamarin by anti-alpha 4 integrin monoclonal antibody. J Clin Invest *92*, 372-380.

Powrie, F., Leach, M.W., Mauze, S., Caddle, L.B., and Coffman, R.L. (1993). Phenotypically distinct subsets of CD4+ T cells induce or protect from chronic intestinal inflammation in C. B-17 scid mice. Int Immunol *5*, 1461-1471.

Preischl, E.E., Pendl, G.G., Elbe, A., Serfling, E., Harrer, N.E., Stingl, G., and Baumruker, T. (1996). Induction of the TNF-alpha promoter in the murine dendritic cell line 18 and the murine mast cell line CPII is differently regulated. J Immunol *157*, 2645-2653.

Redford, E.J., Smith, K.J., Gregson, N.A., Davies, M., Hughes, P., Gearing, A.J., Miller, K., and Hughes, R.A. (1997). A combined inhibitor of matrix metalloproteinase activity and tumour necrosis factor-alpha processing attenuates experimental autoimmune neuritis. Brain *120 (Pt 10)*, 1895-1905.

Regamey, A., Hohl, D., Liu, J.W., Roger, T., Kogerman, P., Toftgard, R., and Huber, M. (2003). The tumor suppressor CYLD interacts with TRIP and regulates negatively nuclear factor kappaB activation by tumor necrosis factor. J Exp Med *198*, 1959-1964.

Reiley, W., Zhang, M., and Sun, S.C. (2004). Negative regulation of JNK signaling by the tumor suppressor CYLD. J Biol Chem *279*, 55161-55167.

Reiley, W.W., Jin, W., Lee, A.J., Wright, A., Wu, X., Tewalt, E.F., Leonard, T.O., Norbury, C.C., Fitzpatrick, L., Zhang, M.*, et al.* (2007). Deubiquitinating enzyme CYLD negatively regulates the ubiquitin-dependent kinase Tak1 and prevents abnormal T cell responses. J Exp Med *204*, 1475-1485.

Reiley, W.W., Zhang, M., Jin, W., Losiewicz, M., Donohue, K.B., Norbury, C.C., and Sun, S.C. (2006). Regulation of T cell development by the deubiquitinating enzyme CYLD. Nat Immunol *7*, 411-417.

Reis e Sousa, C., Hieny, S., Scharton-Kersten, T., Jankovic, D., Charest, H., Germain, R.N., and Sher, A. (1997). In vivo microbial stimulation induces rapid CD40 ligand-independent production of interleukin 12 by dendritic cells and their redistribution to T cell areas. J Exp Med *186*, 1819-1829.

Saiki, R.K., Scharf, S., Faloona, F., Mullis, K.B., Horn, G.T., Erlich, H.A., and Arnheim, N. (1985). Enzymatic amplification of beta-globin genomic sequences and restriction site analysis for diagnosis of sickle cell anemia. Science *230*, 1350-1354.

Saito, K., Kigawa, T., Koshiba, S., Sato, K., Matsuo, Y., Sakamoto, A., Takagi, T., Shirouzu, M., Yabuki, T., Nunokawa, E.*, et al.* (2004). The CAP-Gly domain of CYLD associates with the proline-rich sequence in NEMO/IKKgamma. Structure *12*, 1719-1728.

Sawada, S., Scarborough, J.D., Killeen, N., and Littman, D.R. (1994). A lineage-specific transcriptional silencer regulates CD4 gene expression during T lymphocyte development. Cell *77*, 917-929.

Schmidt-Supprian, M., Tian, J., Grant, E.P., Pasparakis, M., Maehr, R., Ovaa, H., Ploegh, H.L., Coyle, A.J., and Rajewsky, K. (2004). Differential dependence of CD4+CD25+ regulatory and natural killer-like T cells on signals leading to NF-kappaB activation. Proc Natl Acad Sci U S A *101*, 4566-4571.

Schulze-Luehrmann, J., and Ghosh, S. (2006). Antigen-receptor signaling to nuclear factor kappa B. Immunity *25*, 701-715.

Schwarz, E.M., Krimpenfort, P., Berns, A., and Verma, I.M. (1997). Immunological defects in mice with a targeted disruption in Bcl-3. Genes Dev *11*, 187-197.

Senftleben, U., Cao, Y., Xiao, G., Greten, F.R., Krahn, G., Bonizzi, G., Chen, Y., Hu, Y., Fong, A., Sun, S.C.*, et al.* (2001). Activation by IKKalpha of a second, evolutionary conserved, NF-kappa B signaling pathway. Science *293*, 1495-1499.

Shortman, K., and Liu, Y.J. (2002). Mouse and human dendritic cell subtypes. Nat Rev Immunol *2*, 151-161.

Song, X.T., Evel-Kabler, K., Shen, L., Rollins, L., Huang, X.F., and Chen, S.Y. (2008). A20 is an antigen presentation attenuator, and its inhibition overcomes regulatory T cell-mediated suppression. Nat Med *14*, 258-265.

Speirs, K., Lieberman, L., Caamano, J., Hunter, C.A., and Scott, P. (2004). Cutting edge: NF-kappa B2 is a negative regulator of dendritic cell function. J Immunol *172*, 752-756.

Srokowski, C.C., Masri, J., Hovelmeyer, N., Krembel, A.K., Tertilt, C., Strand, D., Mahnke, K., Massoumi, R., Waisman, A., and Schild, H. (2009). Naturally occurring short splice variant of CYLD positively regulates dendritic cell function. Blood *113*, 5891-5895.

Stanley, E.R. (1985). The macrophage colony-stimulating factor, CSF-1. Methods Enzymol *116*, 564-587.

Stegmeier, F., Sowa, M.E., Nalepa, G., Gygi, S.P., Harper, J.W., and Elledge, S.J. (2007). The tumor suppressor CYLD regulates entry into mitosis. Proc Natl Acad Sci U S A *104*, 8869-8874.

Steinman, R.M., Hawiger, D., and Nussenzweig, M.C. (2003). Tolerogenic dendritic cells. Annu Rev Immunol *21*, 685-711.

Steinman, R.M., and Inaba, K. (1999). Myeloid dendritic cells. J Leukoc Biol *66*, 205-208.

Sternberg, N., and Hamilton, D. (1981). Bacteriophage P1 site-specific recombination. I. Recombination between loxP sites. J Mol Biol *150*, 467-486.
Sun, S.C. (2008). Deubiquitylation and regulation of the immune response. Nat Rev Immunol *8*, 501-511.

Thompson, C., and Powrie, F. (2004). Regulatory T cells. Curr Opin Pharmacol *4*, 408-414.

Toft-Hansen, H., Nuttall, R.K., Edwards, D.R., and Owens, T. (2004). Key metalloproteinases are expressed by specific cell types in experimental autoimmune encephalomyelitis. J Immunol *173*, 5209-5218.

Trompouki, E., Hatzivassiliou, E., Tsichritzis, T., Farmer, H., Ashworth, A., and Mosialos, G. (2003). CYLD is a deubiquitinating enzyme that negatively regulates NF-kappaB activation by TNFR family members. Nature *424*, 793-796.

Vallabhapurapu, S., and Karin, M. (2009). Regulation and function of NF-kappaB transcription factors in the immune system. Annu Rev Immunol *27*, 693-733.

Watanabe, N., Iwamura, T., Shinoda, T., and Fujita, T. (1997). Regulation of NFKB1 proteins by the candidate oncoprotein BCL-3: generation of NF-kappaB homodimers from the cytoplasmic pool of p50-p105 and nuclear translocation. EMBO J *16*, 3609-3620.

Waterfield, M.R., Zhang, M., Norman, L.P., and Sun, S.C. (2003). NF-kappaB1/p105 regulates lipopolysaccharide-stimulated MAP kinase signaling by governing the stability and function of the Tpl2 kinase. Mol Cell *11*, 685-694.

Weaver, C.T., and Hatton, R.D. (2009). Interplay between the TH17 and TReg cell lineages: a (co-)evolutionary perspective. Nat Rev Immunol *9*, 883-889.

Weih, F., and Caamano, J. (2003). Regulation of secondary lymphoid organ development by the nuclear factor-kappaB signal transduction pathway. Immunol Rev *195*, 91-105.

Weih, F., Carrasco, D., Durham, S.K., Barton, D.S., Rizzo, C.A., Ryseck, R.P., Lira, S.A., and Bravo, R. (1995). Multiorgan inflammation and hematopoietic abnormalities in mice with a targeted disruption of RelB, a member of the NF-kappa B/Rel family. Cell *80*, 331-340.

Wertz, I. E., O'Rourke, K. M., Zhou, H., Eby, M., Aravind, L., Seshagiri, S., Wu, P., Wiesmann, C., Baker, R., Boone, D. L., Ma, A., Koonin, E. V., Dixit, V. M. (2004). De-ubiquitination and ubiquitin ligase domains of A20 downregulate NF-kappaB signalling. Nature, 430, 694-9.

Wright, A., Reiley, W.W., Chang, M., Jin, W., Lee, A.J., Zhang, M., and Sun, S.C. (2007). Regulation of early wave of germ cell apoptosis and spermatogenesis by deubiquitinating enzyme CYLD. Dev Cell *13*, 705-716.

Wu, L., D'Amico, A., Winkel, K.D., Suter, M., Lo, D., and Shortman, K. (1998). RelB is essential for the development of myeloid-related CD8alpha- dendritic cells but not of lymphoid-related CD8alpha+ dendritic cells. Immunity *9*, 839-847.

Wulczyn, F.G., Naumann, M., and Scheidereit, C. (1992). Candidate proto-oncogene bcl-3 encodes a subunit-specific inhibitor of transcription factor NF-kappa B. Nature *358*, 597-599.

Xiao, G., Harhaj, E.W., and Sun, S.C. (2001). NF-kappaB-inducing kinase regulates the processing of NF-kappaB2 p100. Mol Cell *7*, 401-409.

Xiao, S., Jin, H., Korn, T., Liu, S.M., Oukka, M., Lim, B., and Kuchroo, V.K. (2008). Retinoic acid increases Foxp3+ regulatory T cells and inhibits development of Th17 cells by enhancing TGF-beta-driven Smad3 signaling and inhibiting IL-6 and IL-23 receptor expression. J Immunol *181*, 2277-2284.

Yoshida, H., Jono, H., Kai, H., and Li, J.D. (2005). The tumor suppressor cylindromatosis (CYLD) acts as a negative regulator for toll-like receptor 2 signaling via negative cross-talk with TRAF6 AND TRAF7. J Biol Chem *280*, 41111-41121.

Yoshimura, S., Bondeson, J., Foxwell, B.M., Brennan, F.M., and Feldmann, M. (2001). Effective antigen presentation by dendritic cells is NF-kappaB dependent: coordinate regulation of MHC, co-stimulatory molecules and cytokines. Int Immunol *13*, 675-683.

Zanetti, M., Castiglioni, P., Schoenberger, S., and Gerloni, M. (2003). The role of relB in regulating the adaptive immune response. Ann N Y Acad Sci *987*, 249-257.

Zhou, L., Chong, M.M., and Littman, D.R. (2009). Plasticity of CD4+ T cell lineage differentiation. Immunity *30*, 646-655.

Zou, G.M., and Hu, W.Y. (2005). LIGHT regulates CD86 expression on dendritic cells through NF-kappaB, but not JNK/AP-1 signal transduction pathway. J Cell Physiol *205*, 437-443.

9 Acknowledgements

10 Erklärung

Ich versichere, dass ich die von mir vorgelegte Dissertation selbständig angefertigt, die benutzten Quellen und Hilfsmittel vollständig angegeben und die Stellen der Arbeit – einschließlich Tabellen, Karten und Abbildungen -, die anderen Werken im Wortlaut oder dem Sinn nach entnommen sind, in jedem Einzelfall als Entlehnung kenntlich gemacht habe; dass diese Dissertation noch keiner anderen Fakultät oder Universität zur Prüfung vorgelegen hat; dass sie - abgesehen von unten angegebenen Teilpublikationen - noch nicht veröffentlicht worden ist sowie, dass ich eine solche Veröffentlichung vor Abschluss des Promotionsverfahrens nicht vornehmen werde.
Die Bestimmungen dieser Promotionsordnung sind mir bekannt.

Mainz, im September 2010

Joumana Masri

11 Curriculum Vitae

12 Publications

*C.C. Srokowski, *J. Masri, N. Hövelmeyer, AK Krembel, C. Tertilt, D. Strand, K. Mahnke, R. Massoumi, † A. Waisman, † HJ. Schild
Naturally occurring short splice variant of CYLD positively regulates dendritic cell function
Blood, Jun 2009; 113(23): 5891-5895

M Bros, N. Dexheimer, V. Besche, J. Masri, S. Trojandt, N. Hövelmeyer, S. Reissig, R. Massoumi, S. Grabbe, A. Waisman and AB Reske-Kunz
Mutated CYLD affects the functional state of dendritic cells
European Journal of Immunology, accepted manuscript online: 28 Jul 2010